# HIGH FREQUENCY SCATTERING BY A RESISTIVE STRIP

by

Martin I. Herman

and

John L. Volakis

Radiation Laboratory
Department of Electrical Engineering and Computer Science
The University of Michigan
Ann Arbor, Michigan 48109

July 1986

This work was performed under Contract No. L6XN-395803-913 with Rockwell International-NAAO

*Abstract*-An asymptotic solution is presented for the diffraction of a resistive strip which is useful in the simulation of thin dielectric layers. Up to third order diffraction terms are derived which include the surface wave field effects in a uniform manner.

The derivation of the higher order terms is based on the Extended Spectral Ray Method. A new first order diffraction coefficient is also given.

# Table of Contents

# 1 Introduction

A resistive strip,shown in figure 1, is an adequate model for studying the scattering by thin dielectric slabs and coatings of finite length which are widely used for radar cross section reduction. Because the strip is amenable to an analytic solution, several authors [Bowman 1967, Senior 1979a, b, Tiberio et. al. 1982] have investigated its scattering behavior. In all of these investigations the goal has been to obtain a high frequency solution for the multiply diffracted fields which can be added to the first order contribution [Senior 1952, Maliuzhinets 1958, Tiberio 1982] for predicting the total scattered field by the strip. However, a uniform asymptotic evaluation of the multiply diffracted field which is valid everywhere has yet to appear. Therefore, the scope of this report is to present such a solution.

The difficulty in obtaining a valid solution for the multiply diffracted fields is primarily due to the non-ray optical behavior of the field which illuminates the second edge after diffraction from the first. This occurs for incidence angles near edge-on and can be quite dominant in the backscatter and forward directions. Because of the non-ray optical behavior of the interacting fields in these situations, the concept of slope diffraction [Kouyoumjian 1975 and Buyukdura 1984] is not applicable. Senior's [1979a] approach to evaluate the higher order contributions involved a heuristic modification of a known (Fialkovskiy [1966]) uniform solution for the perfectly conducting strip. However, this was found inadequate and was just used as a guideline in arriving at simpler integral expressions for the edge-on backscattered field. Tiberio et. al.[1982] presented a valid high frequency

solution for the diffraction by an impedance strip which included the effect of the surface wave pole but was restricted to the edge-on incidence. Their approach in treating the non-ray optical fields involved the use of the Extended Spectral Ray Method(ESRM) (Tiberio and Kouyoumjian 1982, and 1984) which has been found quite successful, and its principles will also be employed in our analysis. The ESRM can be considered as an extension of the Uniform Geometrical Theory of Diffraction (UTD)(Kouyoumjian and Pathak [1974]) and is related to the spectral theory of diffraction introduced by Rahmat-Samii and Mittra [1977].

In our high frequency analysis of the diffraction by a resistive strip, particular attention will be given on the uniform evaluation of the surface wave fields and their effect on the diffraction pattern. With this in mind, section II presents a uniform first order diffraction coefficient using a method introduced by Clemmow[1966] (see also Senior 1981) and expounded upon by Volakis and Herman[1986]. In section III, the ESRM is employed to find explicit simple expressions for the second order diffracted field in a parallel manner to that used by Tiberio et. al. [1985] in their analysis of a perfectly conducting double wedge. A similar evaluation is performed for the triply diffracted field (section IV).

The sum of the fields up to third order were then used for the computation of scattering patterns by strips which may or may not support surface waves. We found remarkable agreement with moment method data for strip widths even down to an $\frac{1}{8}$ of a wavelength for backscattering and $.5\lambda$ for forward scattering.

## 2 A Uniform Diffraction Coefficient for an Impedance and a Resistive Half Plane

Assuming an E-polarized plane wave normally incident [1] on an impedance half plane shown in figure 2,

$$E_z^i = e^{jk(x\cos\phi_o + y\sin\phi_o)} \tag{1}$$

we find from Senior[1952] that an integral representation of the scattered field is

$$E^s = -\frac{j}{2\pi}\int_C \frac{1}{\cos\alpha+\cos\phi_o}\left\{1 \mp \frac{y}{|y|}\eta\sqrt{(1+\cos\alpha)(1+\cos\phi_o)}\right\} \cdot K_+(\alpha)K_+(\phi_o)e^{-jk\rho\cos(\alpha-\phi)}d\alpha; \qquad y \gtrless 0 \tag{2}$$

where C is depicted in figure 3, $\phi_o$ is the incident angle, $\phi$ is the observation angle, $\eta$ is the normalized impedance and $K_+(\alpha)$ is the split function, defined by

$$K_+(\alpha) = 2^{\frac{3}{2}}\sqrt{\frac{2}{\eta}}\sin\frac{\alpha}{2}\left\{\frac{\Psi_\pi(\frac{3\pi}{2}-\alpha-\theta)\Psi_\pi(\frac{\pi}{2}-\alpha+\theta)}{\Psi_\pi^2(\frac{\pi}{2})}\right\}^2 \Big/\left\{\left(1+\sqrt{2}\cos\left(\frac{\frac{\pi}{2}-\alpha+\theta}{2}\right)\right)\left(1+\sqrt{2}\cos\left(\frac{\frac{3\pi}{2}-\alpha-\theta}{2}\right)\right)\right\} \tag{3}$$

$$\Psi_\pi(z) \approx \begin{cases} 1-0.0139z^2 & |z| \text{ small} \\ 1.05302\left\{\cos\frac{1}{4}(z-j(ln2)\right\}^{\frac{1}{2}} exp\left\{\frac{jz}{2\pi}e^{jz}\right\} & \mathrm{Im}(z) \text{ large} \end{cases} \tag{4}$$

The above is a highly accurate approximation of the Maliuzhinets function[1958] $\Psi_\pi(z)$ given by Volakis and Senior[1985].

In order to perform a uniform asymptotic evaluation of (2) it is necessary to consider the effect of the geometrical optics and surface wave poles as they ap-

[1] throughout this report an $e^{j\omega t}$ time convention is assumed and suppressed

proach the saddle point at $\alpha = \phi$. Clearly the geometrical optics (g.o.) poles are located at $\alpha = \pi - \phi_o$ and $\pi + \phi_o$, while the surface wave pole at $\alpha = -\theta$ corresponds to the zero of the term $1+\sqrt{2}\cos[(\frac{3\pi}{2}-\alpha-\theta)/2]$ appearing in the expression for $K_+(\alpha)$. The object of the uniform evaluation is to maintain total field continuity for all pattern angles $\phi$. For the perfectly conducting case (all poles lie on the real axis) a uniform evaluation referred to as UTD(Uniform Theory of Diffraction (Kouyoumjian and Pathak [1974]) involved a modified Pauli-Clemmow (Pathak and Kouyoumjian [1970]) evaluation of the integral by retaining the first non-zero term of the pertinent Maclaurin series expansion of the integrand. Thus, it is restricted to cases where the pole crosses the saddle point as $\phi$ is varied and therefore not applicable to the present situation where a complex pole exists.

Our approach for evaluating (2) follows the one described in Volakis and Herman [1986](see Appendix A). It involves first the subtraction and addition (to the integral) of certain auxiliary functions, each containing one of the singularities of the integrand. The auxiliary functions can be usually integrated exactly and the residue of the pertinent singularity is equal to that obtained with the original integrand. Thus, the new expression can be subdivided into singular and non-singular parts. The non-singular parts are evaluated asymptotically in a non-uniform manner while the singular ones correspond to the added auxiliary functions which are integrated exactly and will therefore be uniform.

Appropriate auxiliary functions for the integral at hand are

$$G_{pi}(\alpha,\phi) = \sec\left(\frac{\alpha - \alpha_{pi} \pm \pi}{2}\right); \qquad i = 1,2,3 \tag{5}$$

which are clearly singular at $\alpha = \alpha_{pi}$, where $\alpha_{p1} = \pi - \phi_o$, $\alpha_{p2} = \pi + \phi_o$, and

$\alpha_{p3} = -\theta$ correspond to the poles of the integrand in (2). Proceeding as discussed above, we can express the uniform diffracted field by an impedance half plane as

$$E_z^d(\phi, \phi_o; \eta) = E_z^{dNU}(\phi, \phi_o; \eta) + E_z^{dGO}(\phi, \phi_o; \eta) + E_z^{dSW}(\phi, \phi_o; \eta) \qquad (6)$$

In the above, $E_z^{dNU}$ denotes the non-uniform diffracted field by the impedance half plane, $E_z^{dGO}$ represents the contribution of the g.o. poles to the diffracted field and $E_z^{dSW}$ denotes a similar contribution caused by the existence of the surface wave pole. They are given by

$$\begin{aligned} E_z^{dNU} &= j\sqrt{\frac{2\pi}{k\rho}}\left\{t_o(\phi)\sec\frac{\beta^+}{2} + t_1(\phi)\sec\frac{\beta^-}{2}\right\} \\ &\quad \cdot K_+(\phi)e^{-j\frac{\pi}{4}}e^{-jk\rho}, \end{aligned} \qquad (7)$$

$$\begin{aligned} E_z^{dGO} &= \left[j\sqrt{\frac{2\pi}{k\rho}}\left\{-t_o(\alpha_{p1})K_+(\alpha_{p1})\sec\frac{\beta^+}{2}\right.\right. \\ &\quad \left.-t_1(\alpha_{p2})K_+(\alpha_{p2})\sec\frac{\beta^-}{2}\right\} \\ &\quad \mp t_o(\alpha_{p1})K_+(\alpha_{p1})4\sqrt{\pi}F_c[\pm\sqrt{2k\rho}\cos\frac{\beta^+}{2}] \\ &\quad \left.\mp t_1(\alpha_{p2})K_+(\alpha_{p2})4\sqrt{\pi}F_c[\pm\sqrt{2k\rho}\cos\frac{\beta^-}{2}]\right]e^{-j\frac{\pi}{4}}e^{-jk\rho}, \end{aligned} \qquad (8)$$

$$\begin{aligned} E_z^{dSW} &= -K_{+u}(\alpha_{p3})\left\{t_{o_2}(\alpha_{p3})\sec(\frac{-\theta+\phi_o}{2}) + t_{1_3}(\alpha_{p3})\sec(\frac{-\theta-\phi_o}{2})\right\} \\ &\quad \cdot\left[j\sqrt{\frac{2\pi}{k\rho}}\sec(\frac{\mp\pi\pm\phi+\theta}{2})\right. \\ &\quad \left.\mp 4\sqrt{\pi}F_c[\pm\sqrt{2k\rho}\cos(\frac{\pm\phi\mp\pi+\theta}{2})]\right]e^{-j\frac{\pi}{4}}e^{-jk\rho}; \qquad y \gtrless 0, \end{aligned} \qquad (9)$$

where

$$\beta^{\pm} = \phi \pm \phi_o, \tag{10}$$

$$t_0(\alpha) = \frac{-j}{2\pi}\left[\frac{1}{4\sin\frac{\alpha}{2}\sin\frac{\phi_o}{2}} - \frac{\eta}{2}\right] K_+(\phi_o), \tag{11}$$

$$t_1(\alpha) = \frac{-j}{2\pi}\left[-\frac{1}{4\sin\frac{\alpha}{2}\sin\frac{\phi_o}{2}} - \frac{\eta}{2}\right] K_+(\phi_o), \tag{12}$$

$$t_2(\alpha) = \frac{-j}{2\pi}\left[\frac{1}{4\sin\frac{\alpha}{2}\sin\frac{\phi_o}{2}} + \frac{\eta}{2}\right] K_+(\phi_o), \tag{13}$$

$$t_3(\alpha) = \frac{-j}{2\pi}\left[-\frac{1}{4\sin\frac{\alpha}{2}\sin\frac{\phi_o}{2}} + \frac{\eta}{2}\right] K_+(\phi_o), \tag{14}$$

$$K_{+c}(\pm\alpha) = \frac{K_+(\pm\alpha)}{\sin(\frac{\pm\alpha}{2})}, \tag{15}$$

$$K_{+u}(\alpha) = \left\{1 + \sqrt{2}\cos[(\frac{3\pi}{2} - \alpha - \theta)/2]\right\} K_+(\alpha), \tag{16}$$

and

$$F_c(\pm x) = e^{jx^2}\int_{\pm x}^{\infty} e^{-j\tau^2} d\tau \tag{17}$$

is the Clemmow [1966] transition function satisfying the identity

$$F_c(-x) = \sqrt{x}e^{-j\frac{\pi}{4}}e^{jx^2} - F_c(x), \tag{18}$$

essential for maintaining total field continuity. In (17), the minus sign is chosen when $\frac{\pi}{4} < \arg(x) < \frac{5\pi}{4}$ , otherwise the positive sign is used. To illustrate how continuity is maintained, figure 4 shows the position of the surface wave pole in relation to the closed contour and the corresponding argument of $F_C$. Contour C is detoured to close the path of integration in the steepest descents method of integration. This path (steepest descent path) is described by the Gudermann

function and the location where it crosses the real $\alpha$ axis is determined by the observation angle $\phi$. When the closed contour C and 1 (the SDP) captures the surface wave pole, we find in (17) that arg(x)> $\frac{\pi}{4}$ and therefore the negative sign is chosen. Thus, (18) must be invoked to recover the residue contribution of the surface wave pole. When the pole lies directly on the steepest descent path (contour 2) the corresponding phase of the argument of $F_c$ is exactly $\frac{\pi}{4}$. Finally when the surface wave pole is not captured by the closed contour (curve 3) the phase of the argument of $F_c$ is less than $\frac{\pi}{4}$ requiring the choice of the positive sign in (17).

As mentioned above,when the $\pm$ sign within the transition function changes, we can apply the identity given by equation (18) to recover the residue contributions of the poles. Such a result is, of course, easily checked by calculating this residue contribution directly from the integral. Applying (18) to the transition functions appearing in (8), we find that the geometrical optics pole residue contributions are

$$-4\pi j t_o(\alpha_{p1}) K_+(\alpha_{p1}) e^{jk\rho\cos\beta^+} \tag{19}$$

$$-4\pi j t_1(\alpha_{p2}) K_+(\alpha_{p2}) e^{jk\rho\cos\beta^-}. \tag{20}$$

In addition, from (9) we obtain the surface wave pole residue contribution to be

$$4\pi j t_o(\alpha_{p3}) K_{+u}(\alpha_{p3}) \sec\left(\frac{-\theta+\phi_o}{2}\right) e^{-jk\rho\cos(\theta+\phi)} \quad y>0 \tag{21}$$

$$4\pi j t_2(\alpha_{p3}) K_{+u}(\alpha_{p3}) \sec\left(\frac{-\theta-\phi_o}{2}\right) e^{-jk\rho\cos(\theta-\phi)} \quad y<0. \tag{22}$$

Clearly (21) and (22) represent (attenuating) plane waves traveling on the upper or lower face of the half plane, respectively.

It is important when considering the general class of surface waves to distinguish between the contributions due to the residue of the surface wave pole and that due to surface wave diffraction. The first is generally referred to as the surface wave field. However, even if the surface wave field is absent (the surface wave pole is not captured by the closed contour), the diffracted field ( termed surface ray field ) given by (9), must still be included for a complete uniform representation of the total field.

Equations (6)-(9) give the uniform diffracted field from an impedance half plane in terms of the Clemmow transition function. We can easily rewrite our result using the transition function introduced by Kouyoumjian and Pathak [1974] in the context of UTD by employing the relation,

$$F_{KP}(x^2) = \pm 2jxF_C(\pm x). \tag{23}$$

The diffracted field can now be expressed as

$$E^d = D(\phi, \phi_o; \eta)\frac{e^{-jk\rho}}{\sqrt{\rho}} \tag{24}$$

with

$$D(\phi, \phi_o; \eta) = D^{dNU}(\phi, \phi_o; \eta) + D^{dGO}(\phi, \phi_o; \eta) + D^{dSW}(\phi, \phi_o; \eta) \tag{25}$$

being the uniform diffraction coefficient. From (7)-(9) and (23) we find that

$$D^{dNU} = j\sqrt{\frac{2\pi}{k}}K_+(\phi)\left\{t_o(\phi)\sec\frac{\beta^+}{2} + t_1(\phi)\sec\frac{\beta^-}{2}\right\}e^{-j\frac{\pi}{4}} \tag{26}$$

$$\begin{aligned} D^{dGO} = {} & -j\sqrt{\frac{2\pi}{k}}\left\{t_o(\alpha_{p1})K_+(\alpha_{p1})\sec\frac{\beta^+}{2}\left(1 - F_{KP}[2k\rho\cos^2\left(\frac{\beta^+}{2}\right)]\right)\right. \\ & \left. + t_1(\alpha_{p2})K_+(\alpha_{p2})\sec\frac{\beta^-}{2}\left(1 - F_{KP}[2k\rho\cos^2\left(\frac{\beta^-}{2}\right)]\right)\right\}e^{-j\frac{\pi}{4}} \end{aligned} \tag{27}$$

$$\begin{aligned} D^{dSW} = {} & -j\sqrt{\frac{2\pi}{k}}K_{+u}(\alpha_{p3})\sec\left(\frac{\mp\pi \pm \phi + \theta}{2}\right) \\ & \left\{\left(t_{0_2}(\alpha_{p3})\sec\left(\frac{-\theta + \phi_o}{2}\right) + t_{1_3}(\alpha_{p3})\sec\left(\frac{-\theta - \phi_o}{2}\right)\right)\right. \\ & \left.\cdot\left(1 - F_{KP}[2k\rho\cos^2\left(\frac{\pm\phi \mp \pi + \theta}{2}\right)]\right)\right\}e^{-j\frac{\pi}{4}} \qquad y \gtrless 0 \end{aligned} \tag{28}$$

The above diffraction coefficient for the impedance half plane includes the contribution of both electric and magnetic currents. In order to obtain a corresponding diffraction coefficient for a resistive half plane, one needs to only keep those terms associated with the electric currents. This is easily done by keeping the first term of $t_n(\alpha)$ in (11)-(14).

Examples of bistatic patterns illustrating the effects of surface waves from an impedance half plane are shown in figures 5 and 6. An E-polarized wave is normally incident upon the half plane and observed at a distance of $1.6\lambda$ from the edge. The impedance half plane in figure 5 is inductive; therefore, no surface waves exist [Bucci and Franceschetti 1976] but surface ray fields are present,

although usually small. This is easily seen by observing that the total field tends to zero as the observation angle approaches the shadowed side of the half plane. For figure 6 the angle of incidence and observation distance are the same as those in figure 5; however, the half plane consists of a capacitive material which may (it does in this example) support surface waves. The total field on the shadowed side of the half plane is now quite significant due to the surface wave field. It is clear from the prior example that the most significant effects of the surface wave, when it exists, occur near grazing observations. This is especially important when accounting for the sources of higher order diffraction mechanisms as will be encountered in the next section.

# 3 Second Order Diffraction

The second order diffracted field is that which is diffracted from edge $Q_2(Q_1)$ after diffraction from $Q_1(Q_2)$. As shown in figure 7 there are four mechanisms associated with this phenomenon. In evaluating their contribution we must also consider the existance of possible surface waves in addition to the ray field components. A traditional approach would have been to repeatedly employ the uniform edge diffraction coefficient in (7)-(9) or in (25)-(28) with the incident field being the one diffracted from the previous edge. However,such a procedure requires that all incident fields be ray-optical , a condition which is obviously not satisfied when the argument of the transition function is small. For the second order mechanisms this occurs for near grazing incidence ($\phi_o$ near 180°). In that case the second edge will be in the transition region of the first and thus one must

resort to an alternative procedure for evaluating the second order fields.

As discussed earlier, our evaluation of the second order fields will be based on the principles of the ESRM [Extended Spectral Ray Method]. The procedure to be followed is similar to that employed by Tiberio et. al.[1985] for evaluating the second order diffraction by a perfectly conducting wedge. In short, the incident field to the second edge (see equation 29) is interpreted as a sum (integral) of inhomogeneous plane waves. Each one of these plane waves can then be treated individually. This implies that its far zone contribution to double diffraction can be accounted for by simply multiplying its spectral strength with the non-uniform diffraction coefficient using complex angles of incidence. The total doubly diffracted field is subsequently found by summing (integrating) the contributions of all inhomogeneous plane waves. However,in the case of the resistive strip, when performing the integration it is necessary to also consider the effect of the surface wave pole which adds substantially to the complexity of the problem.

The exact integral representation of the field incident to edge $Q_2$ after diffraction from $Q_1$ is given by

$$E_1 = \frac{-j}{2\pi} \int_{S(0)} \frac{\sin\frac{\alpha}{2}}{\cos\alpha + \cos\phi_o} K_{+c}(\alpha) K_+(\phi_o) e^{-jk\rho\cos(\alpha)} d\alpha \qquad (29)$$

At the second edge we may invoke reciprocity and have a plane wave incident at an angle $\phi_2$ (see figure 8) and diffracted at a complex angle $-\alpha$. A negative instead of a positive $\alpha$ was chosen here to prevent the false occurence of a double surface wave pole later in the integrand. Equation (29) is evaluated

non-uniformily to yield

$$E_2 = \frac{j}{2\pi}\sqrt{\frac{2\pi}{k\rho}}e^{j\frac{\pi}{4}}e^{-jk\rho}\frac{\sin(\alpha/2)}{\cos\alpha+\cos\phi_2}K_{+c}(-\alpha)K_+(\phi_2). \tag{30}$$

The integrand of (29) can now be multiplied by (30) to give the doubly diffracted field from edge $Q_1$ to $Q_2$ and then to the observer. We obtain

$$\begin{aligned} E^d_{21}(\phi_2,\phi_0) &= -\frac{\sqrt{2\pi}}{4\pi^2}\frac{e^{j\pi/4}e^{-jk\rho}}{\sqrt{k\rho}}\int_{S(\phi)}\frac{-\sin^2(\frac{\alpha}{2})K_{+c}(\alpha)K_{+c}(-\alpha)}{[\cos\alpha+\cos\phi_o][\cos\alpha+\cos\phi_2]} \\ &\quad \cdot K_+(\phi_o)K_+(\phi_2)e^{-jk\rho\cos(\alpha-\phi)}d\alpha, \end{aligned} \tag{31}$$

where the integral can be evaluated asymptotically via the steepest descents method (SDP). Before proceeding to do so, it is convenient to subdivide the integrand to a sum of simpler components. Straightforward use of trigonometric identities gives

$$\begin{aligned} E^d_{21}(\phi_2,\phi_0) &= \frac{\sqrt{2\pi}}{64\pi^2}\frac{K_+(\phi_o)K_+(\phi_2)}{\cos\frac{\phi_o}{2}\cos\frac{\phi_2}{2}}\frac{e^{j\frac{\pi}{4}}e^{-jk\rho}}{\sqrt{k\rho}}\int_{S(\phi)}\frac{1}{\cos^2\frac{\alpha}{2}} \\ &\quad \cdot\Big[\sec(\frac{\alpha+\phi_o}{2})\sec(\frac{\alpha+\phi_2}{2})K_{+c}(\alpha)K_{+c}(-\alpha)\sin^2\frac{\alpha}{2} \\ &\quad +\sec(\frac{\alpha+\phi_o}{2})\sec(\frac{\alpha-\phi_2}{2})K_{+c}(\alpha)K_{+c}(-\alpha)\sin^2\frac{\alpha}{2} \\ &\quad +\sec(\frac{\alpha-\phi_o}{2})\sec(\frac{\alpha+\phi_2}{2})K_{+c}(\alpha)K_{+c}(-\alpha)\sin^2\frac{\alpha}{2} \\ &\quad +\sec(\frac{\alpha-\phi_o}{2})\sec(\frac{\alpha-\phi_2}{2})K_{+c}(\alpha)K_{+c}(-\alpha)\sin^2\frac{\alpha}{2}\Big] \\ &\quad \cdot e^{-jka\cos(\alpha-\phi)}d\alpha \end{aligned} \tag{32}$$

Each one of the four terms composing the integrand in (32) is clearly associated with three poles located at $\alpha_{p1}=\pi\pm\phi_o$, $\alpha_{p2}=\pi\pm\phi_2$, and $\alpha_{p3}=-\theta$ (surface wave

pole). Furthermore, we recognize that the first non-vanishing term associated with the SDP evaluation of (32) is the same for all integrand terms. Thus one needs only to evaluate the integral for one of the integrand terms and then multiply by 4. Using the results given in Appendix B we obtain that

$$E_{21}^{d}(\phi_2,\phi_0) \approx +j\frac{K_+(\phi_o)K_+(\phi_2)}{8\pi^{\frac{3}{2}}}K_{+c}^2(\alpha=0)a_3\frac{e^{-jkw}e^{-jk\rho}}{\sqrt{k\rho}}\sqrt{\frac{\pi}{kw}}\quad e^{-jkw\cos\phi_2} \cdot[A\{1-F_{KP}(kwa_1)\}+B\{1-F_{KP}(kwa_2)\}+C\{1-F_{KP}(kwa_3)\}] \tag{33}$$

where

$$a_1 = 2\cos^2\frac{\phi_o}{2} \tag{34}$$

$$a_2 = 2\cos^2\frac{\phi_2}{2} \tag{35}$$

$$a_3 = 2\sin^2\frac{\theta}{2} \tag{36}$$

$$A = \frac{-1}{(a_2-a_1)(a_3-a_1)} \tag{37}$$

$$B = \frac{-1}{(a_1-a_2)(a_3-a_2)} \tag{38}$$

$$C = \frac{-1}{(a_1-a_3)(a_2-a_3)} \tag{39}$$

Equation (33) is the second term and first non-zero one of the Maclaurin series expansion. The final solution for the doubly diffracted field in (33) contains a factor of one-half to account for the grazing incidence at the second edge.

As a check of this bistatic solution for the double diffraction from a strip, we evaluate the case corresponding to a perfectly conducting strip ($\eta \to 0$). As $\eta$

goes to zero we find that

$$a_3 \rightarrow \infty^2, \tag{40}$$

$$K_{+c}(\alpha = 0) \rightarrow \sqrt{2}, \tag{41}$$

and

$$K_{+}(\alpha) \rightarrow \sqrt{2}\sin(\alpha/2). \tag{42}$$

Substituting these values in (33) gives

$$E^d_{21pc}(\phi_2, \phi_0) \approx j\frac{4\sin\frac{\phi_o}{2}\sin\frac{\phi_2}{2}}{8\pi^{\frac{3}{2}}}(\infty^2)\frac{e^{-jkw}e^{-jk\rho}}{\sqrt{k\rho}}\sqrt{\frac{\pi}{kw}}\left\{-\frac{1}{(a_2-a_1)\infty^2}\{1-F_{KP}(kwa_1)\}\right.$$
$$\left.-\frac{1}{(a_1-a_2)\infty^2}\{1-F_{KP}(kwa_2)\}-\frac{1}{\infty^4}\{1-F_{KP}(kwa_3)\}\right\} \tag{43}$$

$$\approx j\frac{\sin\frac{\phi o}{2}\sin\frac{\phi 2}{2}}{2(a_2-a_1)\pi\sqrt{kw}}\frac{e^{-jkw}e^{-jk\rho}}{\sqrt{k\rho}}\{F_{KP}(kwa_1)-F_{KP}(kwa_2)\} \tag{44}$$

At edge-on incidence we have $\phi_o \rightarrow \pi, (a_1 \rightarrow 0)$ and $\phi_2 \rightarrow \pi - \phi$ (i.e. only two mechanisms exist), implying,

$$E^d_{21pc}(\pi-\phi,\pi) \approx \frac{-j\cos\frac{\phi}{2}}{2\pi\sin^2\frac{\phi}{2}\sqrt{kw}}e^{-jkw}\frac{e^{-jk\rho}}{\sqrt{k\rho}}F_{KP}(2kw\sin^2\frac{\phi}{2}) \tag{45}$$

This is the same second order result as derived by Tiberio et. al. [1979] for the perfectly conducting strip.

# 4 Third Order Diffraction

As shown in figure 9 there are eight third order diffraction mechanisms to be considered. Four emanate from edge $Q_1$ and each gives an equal contribution

to the diffracted field. The other four emanate from edge $Q_2$ and likewise are of equal strength. Each mechanism involves first a diffraction from $Q_1(Q_2)$ to $Q_2(Q_1)$ and then a subsequent diffraction from $Q_2(Q_1)$ to $Q_1(Q_2)$ and back to the observer( not necessarily backscattering). In accordance with the ESRM, an integral representaion for the triply diffracted field from $Q_1$ is

$$E^d_{121} = \frac{-j}{2\pi}\int_{S(0)} \frac{-\sin\frac{\alpha}{2}}{\cos\alpha + \cos\phi} E^d_{21}(\alpha,\phi_o) K_{+c}(-\alpha) K_+(\phi) e^{-jk\rho\cos(\alpha)} d\alpha \qquad (46)$$

Equation (46) can again be considered as a sum of inhomogeneous plane waves incident to edge $Q_2$ at a complex angle -$\alpha$. In the case of third order diffraction each one of these must first diffract from $Q_2$ to $Q_1$ before returning to the observer (because of reciprocity the observation angle is now $\phi_o$). Clearly, this scenario corresponds to that of a second order diffraction with plane wave incidence and far zone diffraction computed in the previous section. Using the result in (33),equation (46) becomes,

$$\begin{aligned} E^d_{121}(\phi,\phi_o) \;=\; & \frac{j}{2\pi}\int_{S(0)} \\ & \left\{ \frac{\sin\frac{\alpha}{2}}{4\cos\frac{\alpha}{2}\cos\frac{\phi}{2}} \left[ \sec\left(\frac{\alpha+\phi_o}{2}\right) + \sec\left(\frac{\alpha-\phi_o}{2}\right) \right] K_{+c}(-\alpha) K_+(\phi) \right. \\ & \cdot -jK_+(\phi_o) K_+(\alpha) K^2_{+c}(\alpha=0) a_3 \frac{e^{-j2kw - jk\rho\cos(\alpha)}}{4\pi kw\sqrt{k\rho}} \\ & \cdot \left[ \frac{1}{(a_2-a_1)(a_3-a_1)} \{1 - F_{KP}(kwa_1)\} + \frac{1}{(a_1-a_2)(a_3-a_2)} \{1 - F_{KP}(kwa_2)\} \right. \\ & \left. \left. \cdot \frac{1}{(a_1-a_3)(a_2-a_3)} \{1 - F_{KP}(kwa_3)\} \right] \right\} d\alpha \end{aligned} \qquad (47)$$

This integral is evaluated via the modified Pauli-Clemmow steepest descents

method to yield

$$
\begin{aligned}
E^d_{121}(\phi,\phi_o) &= j\frac{\sqrt{2}}{16(k\pi)^{\frac{3}{2}}w}e^{j3\pi/4}e^{-j2kw}K^4_{+c}(\alpha=0)a_3^2K_+(\phi_o)K_+(\phi) \\
&\cdot\left[\frac{1}{(2-a_1)(a_3-a_1)}\{1-F_{KP}(kwa_1)\}+\frac{1}{(a_1-2)(a_3-2)}\{1-F_{KP}(kw2)\}\right. \\
&\left.+\frac{1}{(a_1-a_3)(2-a_3)}\{1-F_{KP}(kwa_3)\}\right] \\
&\cdot\frac{1}{(a_3-a_4)}\{F_{KP}(kwa_3)-F_{KP}(kwa_4)\}\frac{e^{-jk\rho}}{\sqrt{\rho}} \qquad (48)
\end{aligned}
$$

where

$$
a_4 = 2\cos^2\frac{\phi}{2}. \qquad (49)
$$

The details of the evaluation are given in Appendix C.

Equation 48 includes the multiplicative factor of 4 (for the four diffraction mechanism per edge) and one fourth to account for the double grazing effect.

As a check of this bistatic third order diffraction term we evaluate it for the perfectly conducting case as was done for the double diffraction term.Letting $\eta \rightarrow 0$ gives

$$E^d_{121_{pc}}(\phi,\phi_o) \approx j\sqrt{\frac{2\pi}{kw}}\frac{e^{j3\pi/4}e^{-j2kw}}{16\pi^2 k\sqrt{w}}4\cdot 2\infty^4 \sin\frac{\phi_o}{2}\sin\frac{\phi}{2}$$
$$\cdot\left[\frac{1}{(2-a_1)\infty^2}\{1-F_{KP}(kwa_1)\}+\frac{1}{(a_1-2)\infty^2}\{1-F_{KP}(kw2)\}+\frac{1}{\infty^4}\{1-1\}\right]$$
$$\cdot\frac{1}{\infty^2}\{F_{KP}(kwa_3)-F_{KP}(kwa_4)\}\frac{e^{-jk\rho}}{\sqrt{\rho}} \quad (50)$$
$$\approx \frac{je^{j3\pi/4}e^{-j2kw}\sin\frac{\phi_o}{2}\sin\frac{\phi}{2}}{\sqrt{2}(k\pi)^{3/2}w(2-a_1)}$$
$$\cdot(F_{KP}(2kw)-F_{KP}(kwa_1))(F_{KP}(kwa_3)-F_{KP}(kwa_4))\frac{e^{-jk\rho}}{\sqrt{\rho}} \quad (51)$$

If we further let $a_1 = 0, \phi_o = \pi$ (edge-on incidence)

$$E^d_{121_{pc}}(\phi,\pi) \approx \frac{je^{j3\pi/4}e^{-j2kw}\sin\frac{\phi}{2}}{2\sqrt{2}kw\pi^{3/2}}(1-F_{KP}(2kw\cos^2\frac{\phi}{2}))\frac{e^{-jk\rho}}{\sqrt{k\rho}} \quad (52)$$
$$\approx \frac{-je^{-j\pi/4}e^{-j2kw}\sin\frac{\phi}{2}}{2\sqrt{2}kw\pi^{3/2}}(1-F_{KP}(2kw\cos^2\frac{\phi}{2}))\frac{e^{-jk\rho}}{\sqrt{k\rho}}, \quad (53)$$

which is the same third order term derived by Tiberio [1979] for the perfectly conducting strip.

## 5 Numerical Results

The sum of the fields due to the first, second and third order diffraction was found to yield a good approximation of the total (bistatic) diffracted field by the strip. In a series of patterns to be presented, the far zone field will be compared with corresponding data via the moment method. Our goal in these comparisons is not only to validate the accuracy of our high frequency solution,

but to also examine its inherent limitations as the strip width becomes small. Also of interest is the verification of our original claim that the resistive strip is capable of simulating thin dielectric layers.

Figures 11 to 22 present a variety of backscattering patterns for strip widths ranging from $2\lambda$ down to $\lambda/8$, with four figures corresponding to each strip width. Two of these four figures refer to the case where $|\theta| = 2$ and the other two to the case of $|\theta| = .25$ (see figure 10). Clearly, for the last choice of $\theta$,the surface wave pole is near the saddle point and may also be near one of the geometrical optics poles. Therefore, this situation corresponds to a more severe testing of our solution. Finally, we recognize that of the two figures associated with a specific $|\theta|$ and strip width, one contains curves with capacitive impedances and the other with inductive impedances. For the last case, no surface waves exist and thus all higher order fields are simply due to surface ray diffraction. However, when the impedance is capacitive, $\mathrm{Im}(\theta) > 0$, the surface wave pole ($-\theta$) may be captured during the detouring of the C contour to the steepest descent path. When this occurs the higher order diffracted fields become dominant as can be verified by examining the corresponding patterns in the $0^o$ to $20^o$ region. We further verified the continuity of our solution when the surface wave pole is just crossing the SDP contour. In any case, it is clear that all backscatter patterns obtained via our high frequency solution are in complete agreement with the moment method results for all values of $\theta$, and for strip widths down to $\lambda/8$.

Next we examine the capability of a resistive strip to accurately model a thin

dielectric slab. For such a model, the resistivity of the strip is chosen to be

$$R = \frac{-jZ_o}{(\epsilon_r - 1)k\tau} \tag{54}$$

where $\tau$ is the thickness of the slab and $k\tau$ must be maintained very small. We selected, $\epsilon_r = 4(1 - j\tan\delta), \tan\delta = .1$(loss tangent), $\tau = \frac{\lambda}{40}$ and a strip width of $5\lambda$ to correspond to the strip used in Richmond[1985] (moment method solution). It is shown in figure 23 that our high frequency solution compared exactly with that given by Richmond. As expected, the resisitve strip corresponding to the dielectric slab will always support a surface wave field which is seen to be quite dominant for backscatter angles less than $45^o$ .

To further examine the validity of our solution for the smaller strip widths, figure 24 presents the edge-on backscattering echo width as a function of the width of the strip(w). The comparison with the moment method data (Richmond [1985]) is excellent.

We now turn our attention to the bistatic case. Again a series of patterns are presented in figures 25 to 40 with $\phi_o$(incidence angle) = $150^o$ or $175^o$ and strip widths ranging from $2\lambda$ down to $\lambda/4$. Furthermore, the curves on each figure correspond to various impedance (or $\theta$) values which follows the same format discussed for the backscatter patterns (see figures 11 to 22). The high frequency solution again compares very well with the moment method data except near forward scattering when the strip width is below $\lambda/4$. This is probably due to the need for additional higher order terms in our solution and also to errors associated with single precision arithmetic when performing the subtraction of infinities.

# 6 Self-Consistent Formulation

R.C. Rudduck[1975] and Nan Wang [1976] introduced the self-consistent approach to account for the infinite number of multiple interactions for geometrical optics diffraction from polygonal cylinders. This concept is used here to account for the multiple interactions of the surface waves. The main assumptions to be made are that the surface waves do exist and dominate higher order diffraction. This approach will, of course, be more valid for wider strips.

We define four equivalent surface wave/ray fields impinging upon the edges of the strip (figure 42). The backscatter field is then defined as the superposition of the primary diffraction from the edges (figure 41) and that contributed by the surface waves/ray(s) evaluated via the self-consistent formulation. The equivalent surface waves are formed by using the reflection and transmission coefficients defined by Maliuzhinets [1958] and are incident at the edges of the strip at the Brewster's angle ($\theta$). By a simple matrix solution the equivalent surface waves are defined.

$$\begin{bmatrix} 1 & 0 & -C^+ & -C^- \\ 0 & 1 & -C^- & -C^+ \\ -C^+ & -C^- & 1 & 0 \\ -C^- & -C^+ & 0 & 1 \end{bmatrix} \begin{bmatrix} C_1 \\ C_2 \\ C_3 \\ C_4 \end{bmatrix} = \begin{bmatrix} D(0, \pi - \phi_o, \rho = a)e^{-jkz} \\ D(2\pi, \pi - \phi_o, \rho = a)e^{-jkz} \\ D(0, \phi_o, \rho = a) \\ D(2\pi, \phi_o, \rho = a) \end{bmatrix} \tag{55}$$

$$\text{S.W. Contribution} = \sum_{i=1}^{4} C_i D(\phi, \phi_o, \rho = \infty)e^{jkz_i}$$

where $x_i$ is the phase factor referred to edge $Q_1$,$D(\phi, \phi_o, \rho)$ is the edge diffraction coefficient, and $C^+$ and $C^-$ are the reflection and transmission coefficients using the Brewster's angle, respectively.

This solution is used to analyze the same $5\lambda$ resistive strip used in the previous section figure 23 and as senn in figure 43 it matches the moment method results except near edge-on incidence. This is not surprising since this is a non-ray optical situation.

# 7 Conclusion

Explicit high frequency expressions were given for the diffraction by a resistive strip. These included up to third order terms (primary,secondary and tertiary mechanisms) and compared very well with numerical data. Particularly, our solution was found remarkably accurate in the backscatter case down to strip widths of $\lambda/8$ and down to $\lambda/2$ near the forward scatter region.

The derivation of the second and third order diffracted fields was based on the principles of the Extended Spectral Ray Method (ESRM) and included the surface wave field effects in a uniform manner. A new uniform first order diffraction coefficient was also derived which remained valid at the surface wave boundary. This coefficient was initially employed in a self-consistent manner (along with reciprocity) for the diffraction analysis of the strip. The (expected) failure of this approach then prompted us to consider a rigorous derivation of the higher order terms via the ERSM, again in conjunction with reciprocity.

## References


[1] Bowman, J.J. (1967), High-frequency backscattering from an absorbing infinite strip with arbitrary face impedances, *Can. J. Phys.*, 45(7), 2409-2430

[2] Bucci,O.M. and G. Franceschetti (1976) , Electromagnetic scattering by a half-plane with two face impedances, *Radio Sci.*,11(1), 49-59

[3] Buyukdura, O.M.(1984), Radiation From Sources and Scatterers Near The Edge Of A Perfectly Conducting Wedge, Ph.D. dissertation, The Ohio State University

[4] Clemmow,P.C. (1966), The Plane Wave Spectrum Representation of Electromagnetic Fields, Pergamon, New York

[5] Fialkovskiy, A.T. (1966), Diffraction of planar electromagnetic waves by a slot and a strip, *Radio Eng. Electron.*, 11, 150-157

[6] Kouyoumjian, R.G. (1975), The geometrical theory of diffraction and its applications , in Numerical and Asymptotic Techniques in Electromagnetics, R. Mittra, Ed, New York, Springer-Verlag

[7] Kouyoumjian, R.G., and P.H. Pathak (1974), A uniform geometrical theory of diffraction for an edge in a perfectly conducting surface, *Proc. IEEE*, 62(11), 1448-1461

[8] Maliuzhinets, G. D. (1958), Excitation, reflection and emission of surface waves from a wedge with given face impedances, *Sov. Phys. Dokl.*, Engl. Transl., 3, 752-755

[9] Pathak, P.H. and R.G. Kouyoumjian (1970), The dyadic diffraction coefficient for a perfectly conducting wedge, Sci. Rep. 5, ElectroScience Lab., Dep. of Electr. Eng., Ohio State Univ., Columbus, Ohio

[10] Rahmat-Samii, Y. and R. Mittra (1977), A spectral domain interpretation of high-frequency diffraction phenomena, *IEEE Trans. Antennas Propag.*, AP-25, 676-687

[11] Richmond, J.H. (1985), Scattering by thin dielectric strips, *IEEE Trans. Antennas Propag.*, AP-33, 64-68

[12] Rudduck, R.C. (1975), Application of wedge difrraction and wave interaction methods to antenna theory, OSU short course notes for GTD and Numerical Techniques, vol. 1, September 1975

[13] Senior, T.B.A. (1952), Diffraction by a semi-infinite metallic sheet, *Proc. Roy. Soc.* (London), A 213(1115), 436-458

[14] Senior, T.B.A. (1979a), Backscattering from resistive sheets, *IEEE Trans. Antennas Propag.*, AP-27, 808-813

[15] Senior, T.B.A. (1979b), Scattering by resistive strips, *Radio Sci.*,14(5), 911-924

[16] Senior, T.B.A. (1981), The current induced in a resistive half plane, *Radio Sci.*, 16(6), 1248-1254

[17] Tiberio, R. and R.G. Kouyoumjian (1979), A uniform GTD solution for the diffraction by strips at grazing incidence, *Radio Sci.*, 14(6), 933-941

[18] Tiberio, R. et. al. (1982), Scattering by a strip with two face impedances at edge-on incidence, *Radio Sci*, 17(5), 1199-1210

[19] Tiberio, R. and R.G. Kouyoumjian (1984), Calculation of high-frequency diffraction by two nearby edges illuminated at grazing incidence, *IEEE Trans. Antennas Propag.*, AP-32, 1186-1196

[20] Tiberio, R. et. al. , High-Frequency diffraction by a double wedge, AP Symposium June 1985 Vancouver, Canada

[21] Volakis, J. L. (1986), *IEEE Trans. Antennas Propag.*, AP-34, 172-180

[22] Volakis, J. L. and M. I. Herman (1986), A uniform asymptotic evaluation of integrals, to be published *Proc. IEEE*

[23] Volakis, J. L. and T.B.A. Senior (1985), Simple expressions for a function occurring in diffraction theory, *IEEE Trans. Antennas Propag.*,AP-33, 678-680

[24] Wang, N. (1976), Self-consistent GTD formulation for conducting cylinders with arbitrary convex cross section, *IEEE Trans. Antennas Propag.*, AP-24, 463-468

Note that for each Appendix the equation sequence is reset to 1.

# Appendix A

# A UNIFORM ASYMPTOTIC EVALUATION OF INTEGRALS

by

John L. Volakis and Martin I. Herman
Radiation Laboratory
Department of Electrical Engineering and Computer Science
The University of Michigan
Ann Arbor, Michigan 48109

## Abstract

Previous uniform asymptotic evaluations of integrals have been restricted to cases where the integrand singularities are close to the saddle point(s). A method is presented here which allows such uniform evaluations with integrand singularities anywhere near the steepest descent path.

## I. Introduction

Often in electromagnetic scattering or diffraction problems the integral of the form

$$I(\phi) = \int_C g(\alpha,\phi)e^{\kappa f(\alpha,\phi)}\, d\alpha = \int_C \frac{p(\alpha,\phi)}{q(\alpha,\phi)}\, e^{\kappa f(\alpha,\phi)}\, d\alpha \qquad (1)$$

is encountered at the final steps of the analysis. The evaluation of this integral via the steepest descent method for large real $\kappa$ involves the deformation of C to a steepest descent path (SDP) through the saddle point(s) defined by $f'(\alpha_s,\phi) = 0$. In so doing, the evaluation of (1) is decomposed to contributions obtained from the SDP integral(s) and those associated with the residues of all poles (real or complex) that were captured during the contour deformation process (assuming no branch cuts exist).

When evaluating the SDP integral(s), one must carefully consider the presence of any poles near the SDP such that $I(\phi)$ remains bounded and continuous when the pole crosses the SDP as $\phi$ is varied (the variable $\phi$ here represents the pattern angle). Such evaluations are usually referred to as uniform and have been the subject of several investigations [1,2,3]. However, none of the previous formulations are applicable to situations involving several complex integrand poles which may cross the SDP anywhere in the complex plane. Therefore, the purpose of this letter is to introduce a technique which can be used for obtaining uniform evaluations of integrals involving integrands which may contain several distinct singularities in the complex plane.

The procedure involves the regularization of the integrand over the SDP by the subtraction and addition of certain auxiliary integrals

(one for each singularity) whose integrands satisfy a condition so that the desired uniformity is achieved. The resulting integrals with or without singularities can then be evaluated asymptotically. This procedure is a generalization of a method applied by Clemmow [4] and Senior [5] to integrals with specific $f(\alpha,\phi)$ when considering a single pole.

## II. Formulation

In proceeding with the uniform evaluation of (1) we assume that the integral exists as $\kappa \to \infty$. For the sake of simplicity, this section will also be restricted to the case that $q(\alpha,\phi)$ is associated with a single zero at $\alpha = \alpha_p$ and the SDP crosses a single first order saddle point at $\alpha = \alpha_s$. Generalizations to several integrand poles and saddle points are given in the next section.

On the basis of the above assumptions, (1) can be written as

$$I(\phi) = 2\pi j R_p(\phi) + A_p(\phi) \int_{C_{SDP}} G_p(\alpha,\phi) e^{\kappa f(\alpha,\phi)}\, d\alpha + \int_{C_{SDP}} K(\alpha,\phi) e^{\kappa f(\alpha,\phi)} d\alpha \tag{2}$$

with

$$K(\alpha,\phi) = g(\alpha,\phi) - A_p(\phi) G_p(\alpha,\phi) \quad , \tag{3}$$

where

$$R_p(\phi) = \begin{cases} \dfrac{p(\alpha_p,\phi)}{q'(\alpha_p,\phi)} e^{\kappa f(\alpha_p,\phi)} & \text{pole enclosed by } C\text{-}C_{SDP} \\ 0 & \text{otherwise} \end{cases} \tag{4}$$

is the residue of the enclosed pole and $A_p(\phi)G_p(\alpha,\phi)$ is an unknown product of functions which has been added and subtracted to $g(\alpha,\phi)$. Note also that $q'(\alpha_p,\phi) = (d/d\alpha)q(\alpha,\phi)\big|_{\alpha=\alpha_p}$.

If we, however, require

$$G_p(\alpha,\phi) = \frac{1}{q_p(\alpha,\phi)} \tag{5}$$

to have a pole at $\alpha = \alpha_p$ (there is no restriction for additional poles provided they are not close to the SDP) and choose

$$A_p(\phi) = \lim_{\alpha \to \alpha_p} \left[\frac{g(\alpha,\phi)}{G_p(\alpha,\phi)}\right] = p(\alpha_p,\phi)\,\frac{q'_p(\alpha_p,\phi)}{q'(\alpha_p,\phi)} \quad , \tag{6}$$

then $K(\alpha,\phi)$ becomes free of singularities and thus the asymptotic evaluation of the pertinent (second) integral in (2) is known to be continuous and can be found in [6] up to $O(1/\kappa^3)$. Our task has then reduced to finding an appropriate $G_p(\alpha,\phi)$ which accounts for the discontinuity of $R_p(\phi)$.

Since $G_p(\alpha,\phi)$ has a single pole near the SDP, we have that for large $\kappa$ [1,2]

$$I(\phi) = 2\pi\, jR_p(\phi) + \sqrt{\frac{-2\pi}{\kappa f''(\alpha_s,\phi)}}\, e^{\kappa f(\alpha_s,\phi)} \left[A_p(\phi)G_p(\alpha_s,\phi)F_{KP}(\pm\kappa b_p^2) + K(\alpha_s,\phi)\right] + O(1/\kappa) \tag{7}$$

with the upper sign for $-3\pi/4 < \arg(b_p) < \pi/4$ and lower sign for $\pi/4 < \arg(b_p) < 5\pi/4$, where

$$b_p = \sqrt{j[f(\alpha_s,\phi) - f(\alpha_p,\phi)]} \quad . \tag{8}$$

The function $F_{KP}(\pm z^2)$ is given by

$$F_{KP}(\pm z^2) = \pm 2jz\, e^{jz^2} \int_{\pm z}^{\infty} e^{-jt^2}\, dt \tag{9}$$

and thus satisfies the identity

$$F_{KP}(-z^2) = -2jz\sqrt{\pi}\, e^{-j\pi/4}\, e^{jz^2} + F_{KP}(z^2) \quad . \tag{10}$$

Furthermore, the transition points associated with $b_p$ correspond to the crossing of $C_{SDP}$ by the pole (the particular order of correspondence may vary).

By employing (4) and (10) in (7), it is found that $I(\phi)$ as given in (7) is continuous (uniform) only if

$$\frac{q_p'(\alpha_p,\phi)}{q_p(\alpha_s,\phi)} = e^{-j(\phi_s-\pi/4)}\left|\sqrt{\frac{f''(\alpha_s,\phi)}{2}}\right|\frac{1}{b_p} \tag{11}$$

where $\phi_s$ is the angle formed by the real axis of the $\alpha$-plane and the direction of the $C_{SDP}$ at the saddle point [6]. For example, if $f(\alpha,\phi) = -j\cos(\phi - \alpha)$ then $\alpha_s = \phi$, $\phi_s = \pi/4$, $b_p = \sqrt{2}\cos[(\phi - \alpha_p - \pi)/2]$ and an appropriate choice for $G_p(\alpha,\phi)$ is $G_p(\alpha,\phi) = G_p(\alpha) = \sec[(\alpha - \alpha_p - \pi)/2]$. Therefore, for this example the integration of the singular integrand as given in (7) is exact and the accuracy of $I(\phi)$ is only limited by the asymptotic expansion of the integral associated with $K(\alpha,\phi)$.

When $\alpha_p$ is far from the SDP, then $F_{KP}(z)\tilde{}1$ with $-3\pi/4 < \arg(z) < \pi/4$, and (7) reduces to the usual non-uniform asymptotic form. To avoid any complication with any other poles of $G_p(\alpha,\phi)$, one should always return to this non-uniform form especially when dealing with multiple saddle points as discussed in the next section.

## III. Generalization to Multiple Poles and Saddle Points

When the integrand of (1) contains N distinct poles, $\alpha_p$, which may cross or be near the SDP, the formulation given above can be generalized to give

$$I(\phi) = 2\pi j \sum_{p=1}^{N} R_p(\phi) + \sqrt{\frac{-2\pi}{\kappa f''(\alpha_s,\phi)}}\, e^{\kappa f(\alpha_s,\phi)} \left[ K_A(\alpha_s,\phi) \right.$$

$$\left. + \sum_{p=1}^{N} A_p(\phi) G_p(\alpha_s,\phi) F_{KP}(\pm \kappa b_p^2) \right] + O\left(\frac{1}{\kappa}\right) \quad (12)$$

where

$$K_A(\alpha,\phi) = g(\alpha,\phi) - \sum_{p=1}^{N} A_p(\phi) G_p(\alpha,\phi) \quad (13)$$

and $R_p(\phi)$ with $A_p(\phi)$ are defined in (4) and (6), respectively. In addition, each of the functions $G_p(\alpha,\phi)$ must have a pole at $\alpha = \alpha_p$ and be chosen to satisfy (11).

The above uniform evaluation of integrals can be also generalized to cases where $C_{SDP}$ may be associated with more than one saddle point. This is accomplished by simply treating each saddle point individually and only in conjunction with those poles which may cross or be near the SDP.

References


1. L. B. Felsen and N. Marcuvitz, Radiation and Scattering of Waves, Prentice-Hall, 1973, pp. 399-410.

2. P. C. Clemmow, "A Method for the Exact Solution of a Class of Two Dimensional Diffraction Problems," Proc. Roy. Soc., 205A, 1951, pp. 286-308.

3. C. Gennarelli and L. Palumbo, "A Uniform Asymptotic Expansion of Typical Diffraction Integrals with Many Coalescing Simple Pole Singularities and a First-Order Saddle Point", IEEE Trans. Antennas Propagat., Vol. AP-32, Oct. 1984, pp. 1122-1124.

4. P. C. Clemmow, The Plane Wave Spectrum Representation of Electromagnetic Fields, Pergamon Press, 1966, pp. 56-58.

5. T.B.A. Senior, "The Current Induced in a Resistive Half Plane," Radio Sci., Vol. 16, Nov.-Dec. 1981, pp. 1249-1254.

6. R. H. Schafer and R. G. Kouyoumjian, "Higher Order Terms in the Saddle Point Approximation," Proc. IEEE, Vol. 55, August 1967, pp. 1496-1497.

# Appendix B

The integral representation of the diffracted field from the first to the second edge of the resistive strip is given by

$$u_1 = \frac{-j}{2\pi}\int_{S(0)} \frac{\sin\frac{\alpha}{2}}{\cos\alpha + \cos\phi_o} K_{+c}(\alpha) K_+(\phi_o) e^{-jk\rho\cos(\alpha)} d\alpha \qquad (1)$$

where

$w$ width of the strip($/\lambda$)

$K_+(\pm\alpha)$ split fuction

$$K_{+c}(\pm\alpha) = \frac{K_+(\pm\alpha)}{\sin(\frac{\pm\alpha}{2})}$$

$$K_{+u}(\alpha) = \left\{1 + \sqrt{2}\cos[(\frac{3\pi}{2} - \alpha - \theta)/2]\right\} K_+(\alpha)$$

$\phi_o$ incident angle at edge 1

$\phi_2$ launching angle at edge 2

Equation (1) can be considered as an integral sum of inhomogeneous plane waves incident upon the second edge at an angle of -$\alpha$. The negative sign prevents the occurrence of a double surface wave pole in the later calculations. The far zone diffracted field from the second edge due a plane wave incidence at $-\alpha$ is

$$u_2 = \frac{-j}{2\pi}\sqrt{\frac{2\pi}{k\rho}} e^{j\frac{\pi}{4}} e^{-jk\rho} \frac{\sin(-\alpha/2)}{\cos\alpha + \cos\phi_2} K_{+c}(-\alpha) K_+(\phi_2) \qquad (2)$$

where $\phi_2$ is the angle of incidence and $-\alpha$ is the angle of diffraction. By invoking reciprocity along with the above interpretation of (1), we can express the doubly diffracted field as

$$u_{21}^{d} = -\frac{\sqrt{2\pi}}{4\pi^2}\frac{e^{j\pi/4}e^{-jk\rho}}{\sqrt{k\rho}}\int_{S(\phi)}\frac{-\sin^2(\frac{\alpha}{2})K_{+c}(\alpha)K_{+c}(-\alpha)}{[\cos\alpha+\cos\phi_o][\cos\alpha+\cos\phi_2]} \cdot K_+(\phi_o)K_+(\phi_2)e^{-jkw\cos(\alpha-\phi)}d\alpha \tag{3}$$

or,

$$u_{21}^{d} = \frac{\sqrt{2\pi}}{64\pi^2}\frac{K_+(\phi_o)K_+(\phi_2)}{\cos\frac{\phi_o}{2}\cos\frac{\phi_2}{2}}\frac{e^{j\frac{\pi}{4}}e^{-jk\rho}}{\sqrt{k\rho}} \int_{S(\phi)}\left\{\left[\sec(\frac{\alpha+\phi_o}{2})+\sec(\frac{\alpha-\phi_o}{2})\right]\left[\sec(\frac{\alpha+\phi_2}{2})+\sec(\frac{\alpha-\phi_2}{2})\right]\right\} \cdot\sin^2(\frac{\alpha}{2})\frac{K_{+c}(\alpha)K_{+c}(-\alpha)}{\cos^2\frac{\alpha}{2}}e^{-jkw\cos(\alpha-\phi)}d\alpha \tag{4}$$

where the poles of (4) are

$$\text{g.o.}: \alpha_{p1} = \pi \pm \phi_o \tag{5}$$

$$\alpha_{p2} = \pi \pm \phi_2 \tag{6}$$

$$\text{s.w.}: \alpha_{p3} = -\theta \tag{7}$$

Expanding the trigonometeric terms in (4), $u_{21}^{d}$ becomes

$$
\begin{aligned}
u_{21}^{d} = & \frac{\sqrt{2\pi}}{64\pi^2} \frac{K_+(\phi_o)K_+(\phi_2)}{\cos\frac{\phi_o}{2}\cos\frac{\phi_2}{2}} \frac{e^{j\frac{\pi}{4}}e^{-jk\rho}}{\sqrt{k\rho}} \int_{S(0)} \frac{1}{\cos^2\frac{\alpha}{2}} \\
& \cdot \Big[\sec(\frac{\alpha+\phi_o}{2})\sec(\frac{\alpha+\phi_2}{2})K_{+c}(\alpha)K_{+c}(-\alpha)\sin^2\frac{\alpha}{2} \\
& + \sec(\frac{\alpha+\phi_o}{2})\sec(\frac{\alpha-\phi_2}{2})K_{+c}(\alpha)K_{+c}(-\alpha)\sin^2\frac{\alpha}{2} \\
& + \sec(\frac{\alpha-\phi_o}{2})\sec(\frac{\alpha+\phi_2}{2})K_{+c}(\alpha)K_{+c}(-\alpha)\sin^2\frac{\alpha}{2} \\
& + \sec(\frac{\alpha-\phi_o}{2})\sec(\frac{\alpha-\phi_2}{2})K_{+c}(\alpha)K_{+c}(-\alpha)\sin^2\frac{\alpha}{2}\Big] \\
& \cdot e^{-jkw\cos(\alpha)}d\alpha
\end{aligned} \tag{8}
$$

consisting of four terms each producing the same result when evaluated via the modified Pauli-Clemmow steepest descents approach. Therefore, it is only necessary to perform this evaluation for one of them and multiply the result by four. The details of the modified Pauli-Clemmow approach used to evaluate the integral asymptotically are given below.

The steepest descent path is mapped to the real axis via the transformation $f(\alpha) = f(\alpha_s) - \mu^2$, where $\alpha_s$ is the saddle point. From this relationship we obtain the relations

$$f(\alpha) = -j\cos(\alpha) \tag{9}$$

$$\sin\frac{\alpha}{2} = \sqrt{\frac{j}{2}}\mu \tag{10}$$

$$\frac{d\alpha}{d\mu} = \frac{\sqrt{2j}}{\sqrt{1-\frac{j}{2}\mu^2}} \tag{11}$$

$$e^{-jk\rho\cos(\alpha)} = e^{-jk\rho}e^{-k\rho\mu^2} \tag{12}$$

Mapping one of the integral terms in (8) unto the real axis we have

$$I(kw) = e^{kwf(\alpha_s)} \int_{-\infty}^{\infty} F(\alpha) \frac{d\alpha}{d\mu} e^{-kw\mu^2} d\mu \tag{13}$$

where

$$F(\alpha) = \oint^{0} \frac{\sin^2 \frac{\alpha}{2} K_{+c}(\alpha) K_{+c}(-\alpha)}{\cos^2 \frac{\alpha}{2}} \sec(\frac{\alpha + \phi_o}{2}) \sec(\frac{\alpha + \phi_2}{2}) \tag{14}$$

and

$$D = \frac{\sqrt{2\pi}}{64\pi^2} \frac{K_+(-k\cos\phi_o) K_+(-k\cos\phi_2)}{\cos\frac{\phi_o}{2} \cos\frac{\phi_2}{2}} \frac{e^{j\frac{\pi}{4}} e^{-jk\rho}}{\sqrt{k\rho}} \tag{15}$$

Noting that $\alpha_{pi}$ are the poles of F($\alpha$)

$$\begin{aligned} f(\alpha) - f(\alpha_{p1}) &= f(\alpha_s) - \mu^2 - f(\alpha_{p1}) \\ &= -j(1 + \cos\phi_o) - \mu^2 \\ &= -(\mu^2 + ja_1) \qquad a_1 = 2\cos^2\frac{\phi_o}{2} \end{aligned} \tag{16}$$

$$\begin{aligned} f(\alpha) - f(\alpha_{p2}) &= f(\alpha_s) - \mu^2 - f(\alpha_{p2}) \\ &= -j(1 + \cos\phi_2) - \mu^2 \\ &= -(\mu^2 + ja_2) \qquad a_2 = 2\cos^2\frac{\phi_2}{2} \end{aligned} \tag{17}$$

$$\begin{aligned} f(\alpha) - f(\alpha_{p3}) &= f(\alpha_s) - \mu^2 - f(\alpha_{p3}) \\ &= -j(1 - \cos\theta) - \mu^2 \\ &= -(\mu^2 + ja_3) \qquad a_3 = 2\sin^2\frac{\theta}{2} \end{aligned} \tag{18}$$

I($kw$) can be written as

$$I(kw) = e^{-jkw}\int_{-\infty}^{\infty}\frac{\mathcal{F}(\mu)e^{-kw\mu^2}}{(\mu^2+ja_1)(\mu^2+ja_2)(\mu^2+ja_3)}d\mu \tag{19}$$

where

$$\mathcal{F}(\mu) = -F(\alpha)\frac{d\alpha}{d\mu}(\mu^2+ja_1)(\mu^2+ja_2)(\mu^2+ja_3) \tag{20}$$

is a regular function. Thus it can be represented by a Maclaurin series expansion

$$\mathcal{F}(\mu) = \sum_{m=o}^{\infty} A_m\mu^m. \tag{21}$$

substituting in (19) yields

$$I(kw) = e^{-jkw}\sum_{m=0}^{\infty} A_m\int_{-\infty}^{\infty}\frac{\mu^m e^{-kw\mu^2}}{(\mu^2+ja_1)(\mu^2+ja_2)(\mu^2+ja_3)}d\mu \tag{22}$$

Clearly the integral in (22) vanishes for odd m and we further note the $A_o$=0. Thus, the first non-vanishing term of the Maclaurin series expansion corresponds to m=2. To evaluate the integral in (22) for m=2, we first employ the partial fraction expansion

$$\frac{1}{(\mu^2+ja_1)(\mu^2+ja_2)(\mu^2+ja_3)} = \frac{A}{(\mu^2+ja_1)}+\frac{B}{(\mu^2+ja_2)}+\frac{C}{(\mu^2+ja_3)} \tag{23}$$

where

$$A = \frac{1}{(-ja_1+ja_2)(-ja_1+ja_3)} = \frac{-1}{(a_2-a_1)(a_3-a_1)} \tag{24}$$

$$B = \frac{1}{(-ja_2 + ja_1)(-ja_2 + ja_3)} = \frac{-1}{(a_1 - a_2)(a_3 - a_2)} \tag{25}$$

$$C = \frac{1}{(-ja_3 + ja_1)(-ja_3 + ja_2)} = \frac{-1}{(a_1 - a_3)(a_2 - a_3)} \tag{26}$$

In addition, noting that

$$\int_{-\infty}^{\infty} \frac{e^{-kw\mu^2}}{\mu^2 + ja} d\mu = \sqrt{\frac{\pi}{kw}} \frac{F_{KP}(kwa)}{ja} \tag{27}$$

$$\int_{-\infty}^{\infty} \frac{\mu^2 e^{-kw\mu^2}}{\mu^2 + ja} d\mu = \sqrt{\frac{\pi}{kw}} \{1 - F_{KP}(kwa)\} \tag{28}$$

it is found that

$$u_{21}^d = -e^{-jkw} A_2 \sqrt{\frac{\pi}{kw}} \cdot [A\{1 - F_{KP}(kwa_1)\} + B\{1 - F_{KP}(kwa_2)\} + C\{1 - F_{KP}(kwa_3)\}] \tag{29}$$

where

$$A_2 = \frac{1}{2} \mathcal{F}''(\mu)|_{\mu=0} = \frac{1}{2} \frac{\partial^2 \mathcal{F}_1(\alpha)}{\partial \alpha^2} \left(\frac{d\alpha}{d\mu}\right)^3 . \tag{30}$$

Since

$$\mathcal{F}_1(\alpha) = F(\alpha)(f(\alpha) - f(\alpha_{p1}))(f(\alpha) - f(\alpha_{p2}))(f(\alpha) - f(\alpha_{p3})) \tag{31}$$

$$= -D \sin^2 \frac{\alpha}{2} \sec\left(\frac{\alpha - \phi_o}{2}\right) \sec\left(\frac{\alpha - \phi_2}{2}\right) \frac{K_{+c}(\alpha) K_{+c}(-\alpha)}{\cos^2 \frac{\alpha}{2}} \cdot (j \cos \phi_o + j \cos \alpha)(j \cos \phi_2 + j \cos \alpha)(-j \cos \theta + j \cos \alpha) \tag{32}$$

we find that (note that $\mu$=0 maps to $\alpha = \alpha_s = 0$)

$$\mathcal{F}_1(\alpha_s) = jD\frac{\alpha^2}{4}\sec\frac{\phi_o}{2}\sec\frac{\phi_2}{2}K_{+c}^2(\alpha=0)(2\cos^2\frac{\phi_o}{2})(2\cos^2\frac{\phi_2}{2})(2\sin^2\frac{\theta}{2}) \tag{33}$$

$$= jD2\alpha^2\cos\frac{\phi_o}{2}\cos\frac{\phi_2}{2}K_{+c}^2(\alpha=0)\sin^2\frac{\theta}{2} \tag{34}$$

$$\mathcal{F}_1'(\alpha_s) = j4D\alpha\cos\frac{\phi_o}{2}\cos\frac{\phi_2}{2}K_{+c}^2(\alpha=0)\sin^2\frac{\theta}{2} \tag{35}$$

$$\frac{\partial^2\mathcal{F}_1(\alpha_s)}{\partial\alpha^2} = j4D\cos\frac{\phi_o}{2}\cos\frac{\phi_2}{2}K_{+c}^2(\alpha=0)\sin^2\frac{\theta}{2} \tag{36}$$

$$\frac{\partial^2\mathcal{F}_1(\alpha_s)}{\partial\alpha^2} = j2D\cos\frac{\phi_o}{2}\cos\frac{\phi_2}{2}K_{+c}^2(\alpha=0)a_3 \tag{37}$$

$$\frac{d\alpha}{d\mu}|_{\mu=0} = \sqrt{2j} \tag{38}$$

$$\left(\frac{d\alpha}{d\mu}\right)^3|_{\mu=0} = 2^{\frac{3}{2}}e^{j\frac{3\pi}{4}} \tag{39}$$

Using (31) to (39) gives

$$A_2 = D\frac{1}{2}[j2\cos\frac{\phi_o}{2}\cos\frac{\phi_2}{2}K_{+c}^2(\alpha=0)a_3]2^{\frac{3}{2}}e^{j\frac{3\pi}{4}} \tag{40}$$

Substituting this in (29) and multiplying by 4 yields the doubly diffracted field

$$u_{21}^d = +j\frac{K_+(\phi_o)K_+(\phi_2)}{8\pi^{\frac{3}{2}}}K_{+c}^2(\alpha=0)a_3\frac{e^{-jkw}e^{-jk\rho}}{\sqrt{k\rho}}\sqrt{\frac{\pi}{kw}}$$
$$\cdot[A\{1-F_{KP}(kwa_1)\}+B\{1-F_{KP}(kwa_2)\}+C\{1-F_{KP}(kwa_3)\}] \tag{41}$$

A factor of one-half has been included to account for the grazing incidence of the singly diffracted wave upon the second edge.

# Appendix C

The approach for deriving the third order diffracted field uses the Extended Spectral Ray Method which was utilized in the derivation of the double diffraction coefficient. The double diffraction coefficient (see Appendix B) is

$$u_{21}^{d}(\phi_2,\phi_o) = +j\frac{K_+(\phi_o)K_+(\phi_2)}{4\pi^{\frac{3}{2}}}K_{+c}^{2}(\alpha=0)a_3\frac{e^{-jkw}e^{-jk\rho}}{\sqrt{k\rho}}\sqrt{\frac{\pi}{kw}}$$
$$\cdot[A\{1-F_{KP}(kwa_1)\}+B\{1-F_{KP}(kwa_2)\}+C\{1-F_{KP}(kwa_3)\}] \quad (1)$$

where

$w$ width of the strip$(/\lambda)$

$K_+(\pm\alpha)$ split fuction

$$K_{+c}(\pm\alpha) = \frac{K_+(\pm\alpha)}{\sin(\frac{\pm\alpha}{2})}$$

$$K_{+u}(\alpha) = \left\{1+\sqrt{2}\cos[(\frac{3\pi}{2}-\alpha-\theta)/2]\right\}K_+(\alpha)$$

$\phi_o$ incident angle at edge 1

$\phi_2$ launching angle at edge 2

$$A = \frac{-1}{(a_2-a_1)(a_3-a_1)}$$
$$B = \frac{-1}{(a_1-a_2)(a_3-a_2)}$$
$$C = \frac{-1}{(a_1-a_3)(a_2-a_3)}$$

and

$$a_1 = 2\cos^2\frac{\phi_o}{2} \quad (2)$$

$$a_2 = 2\cos^2\frac{\phi_2}{2} \tag{3}$$

$$a_3 = 2\sin^2\frac{\theta}{2} \tag{4}$$

The triply diffracted field may then be represented

$$u^d_{121} = \frac{-j}{2\pi}\int_{S(0)} \frac{-\sin\frac{\alpha}{2}}{\cos\alpha+\cos\phi} u^d_{21}(\alpha,\phi_o)K_{+c}(-\alpha)K_+(-k\cos\phi)e^{-jk\rho\cos(\alpha)}d\alpha. \tag{5}$$

This integral can be interpreted as a sum of inhomogeneous plane waves diffracting from the second edge and incident upon the first at a complex angle of $-\alpha$. The negative sign is used to prevent the occurrence of a double surface wave pole later in the calculations. Using the identity

$$\frac{1}{\cos\alpha+\cos\phi_o} = \frac{1}{4\cos\frac{\alpha}{2}\cos\frac{\phi_o}{2}}\left[\sec(\frac{\alpha+\phi_o}{2})+\sec(\frac{\alpha-\phi_o}{2})\right] \tag{6}$$

in (~~46~~ 5), we obtain

$$\begin{aligned} u^d_{121} = \frac{j}{2\pi}\int_{S(0)} \Bigg\{ & \frac{\sin\frac{\alpha}{2}}{4\cos\frac{\alpha}{2}\cos\frac{\phi}{2}}\left[\sec(\frac{\alpha+\phi_o}{2})+\sec(\frac{\alpha-\phi_o}{2})\right]K_{+c}(-\alpha)K_+(\phi) \\ & \cdot -jK_+(\phi_o)K_+(\alpha)K^2_{+c}(\alpha=0)a_3\frac{e^{-j2kw-jk\rho\cos(\alpha)}}{4\pi kw\sqrt{k\rho}} \\ & \cdot\Bigg[\frac{1}{(a_2-a_1)(a_3-a_1)}\{1-F_{KP}(kwa_1)\}+\frac{1}{(a_1-a_2)(a_3-a_2)}\{1-F_{KP}(kwa_2)\} \\ & \cdot\frac{1}{(a_1-a_3)(a_2-a_3)}\{1-F_{KP}(kwa_3)\}\Bigg]\Bigg\}d\alpha. \end{aligned} \tag{7}$$

which can be evaluated via the modified Pauli-Clemmow steepest descents method.

The steepest descent path is mapped to the real axis via the transformation $f(\alpha) = f(\alpha_s) - \mu^2$, where $\alpha_s$ is the saddle point. From this relationship we obtain

relations similar to those given in appendix B (9)-(12). The triply diffracted term in (7) can then be written as

$$u^d_{121} = e^{kwf(\alpha_s)} \int_{-\infty}^{\infty} F(\alpha) \frac{d\alpha}{d\mu} e^{-kw\mu^2} d\mu \tag{8}$$

~~(9)~~

Noting that $\alpha_{pi}$ are the poles of $F(\alpha)$

$$\begin{aligned} f(\alpha) - f(\alpha_{p3}) &= f(\alpha_s) - \mu^2 - f(\alpha_{p3}) \\ &= -j(1 - \cos\theta) - \mu^2 \\ &= -(\mu^2 + ja_3) \qquad a_3 = 2\sin^2\frac{\theta}{2} \end{aligned} \tag{10}$$

$$\begin{aligned} f(\alpha) - f(\alpha_{p4}) &= f(\alpha_s) - \mu^2 - f(\alpha_{p4}) \\ &= -j(1 + \cos\phi) - \mu^2 \\ &= -(\mu^2 + ja_4) \qquad a_4 = 2\cos^2\frac{\phi}{2} \end{aligned} \tag{11}$$

$u^d_{121}$ can be expressed as

$$u^d_{121} = e^{-jkw} \int_{-\infty}^{\infty} \frac{\mathcal{F}(\mu) e^{-kw\mu^2}}{(\mu^2 + ja_3)(\mu^2 + ja_4)} d\mu \tag{12}$$

where

$$\mathcal{F}(\mu) = F(\alpha) \frac{d\alpha}{d\mu} (\mu^2 + ja_3)(\mu^2 + ja_4) \tag{13}$$

is a regular function. Thus it can be represented by a Maclaurin series expansion

$$\mathcal{F}(\mu) = \sum_{m=o}^{\infty} A_m \mu^m. \tag{14}$$

which when substituted in (11) yields

$$u_{121}^d = e^{-jkw} \sum_{m=0}^{\infty} A_m \int_{-\infty}^{\infty} \frac{\mu^m e^{-kw\mu^2}}{(\mu^2 + ja_3)(\mu^2 + ja_4)} d\mu \tag{15}$$

Clearly the integral in (14) vanishes for odd m and we further note the $A_o$=0. Thus, the first non-vanishing term of the Maclaurin series expansion corresponds to m=2. To evaluate the integral in (14) for m=2, we first employ a partial fraction expansion. In addition, noting that

$$\int_{-\infty}^{\infty} \frac{e^{-kw\mu^2}}{\mu^2 + ja} d\mu = \sqrt{\frac{\pi}{kw}} \frac{F_{KP}(kwa)}{ja} \tag{16}$$

$$\int_{-\infty}^{\infty} \frac{\mu^2 e^{-kw\mu^2}}{\mu^2 + ja} d\mu = \sqrt{\frac{\pi}{kw}} \{1 - F_{KP}(kwa)\} \tag{17}$$

it is found that

$$u_{121}^d = e^{kwf(\alpha_s)} A_2 \int_{-\infty}^{\infty} \frac{\mu^2 e^{-k\mu^2} d\mu}{(\mu^2 + ja_4)(\mu^2 + ja_3)} \tag{18}$$

$$= \tilde{e}^{jkw} A_2 \frac{1}{j(a_3 - a_4)} \left[ \int_{-\infty}^{\infty} \frac{\mu^2 e^{-k\mu^2} d\mu}{(\mu^2 + ja_4)} - \int_{-\infty}^{\infty} \frac{\mu^2 e^{-k\mu^2} d\mu}{(\mu^2 + ja_3)} \right] \tag{19}$$

$$= \tilde{e}^{jkw} A_2 \frac{1}{j(a_3 - a_4)} \left[ \sqrt{\frac{\pi}{kw}} \{1 - F_{KP}(kwa_4)\} - \sqrt{\frac{\pi}{kw}} \{1 - F_{KP}(kwa_3)\} \right] \tag{20}$$

$$= \tilde{e}^{jkw} A_2 \frac{1}{j(a_3 - a_4)} \sqrt{\frac{\pi}{kw}} \{F_{KP}(kwa_3) - F_{KP}(kwa_4)\} \tag{21}$$

where

$$A_2 = \frac{1}{2}\mathcal{F}''(\mu)|_{\mu=0} = \frac{1}{2}\frac{\partial^2 \mathcal{F}_1(\alpha)}{\partial \alpha^2}\left(\frac{d\alpha}{d\mu}\right)^3. \tag{22}$$

Since

$$\begin{aligned}
\mathcal{F}_1(\alpha) \approx\ & \frac{-\alpha^2 K_{+c}^4(\alpha=0)2\cos^2\frac{\phi}{2}a_3^2}{4\cdot 16\pi^2 k\sqrt{w}\cos^2\frac{\phi}{2}}K_+(\phi_o)K_+(\phi)e^{-jkw} \\
& \cdot\left[\frac{1}{(2-a_1)(a_3-a_1)}\{1-F_{KP}(kwa_1)\} + \frac{1}{(a_1-2)(a_3-2)}\{1-F_{KP}(kwa_2)\}\right. \\
& \left. + \frac{1}{(a_1-a_3)(2-a_3)}\{1-F_{KP}(kwa_3)\}\right] \qquad (23) \\
\mathcal{F}_1''(\alpha) \approx\ & \frac{-K_{+c}^4(\alpha=0)a_3^2}{16\pi^2 k\sqrt{w}}K_+(\phi_o)K_+(\phi)e^{-jkw} \\
& \cdot\left[\frac{1}{(2-a_1)(a_3-a_1)}\{1-F_{KP}(kwa_1)\}\right. \\
& + \frac{1}{(a_1-2)(a_3-2)}\{1-F_{KP}(kw2)\} \\
& \left. + \frac{1}{(a_1-a_3)(2-a_3)}\{1-F_{KP}(kwa_3)\}\right]. \qquad (24)
\end{aligned}$$

Also

$$\frac{d\alpha}{d\mu}|_{\mu=0} = \sqrt{2j} \tag{25}$$

$$\left(\frac{d\alpha}{d\mu}\right)^3|_{\mu=0} = 2^{\frac{3}{2}}e^{j\frac{3\pi}{4}} \tag{26}$$

Using (21) to (25) to solve for $A_2$ and substituting the result into (20) gives

$$
\begin{aligned}
u_{121}^{d} \;=\; & \sqrt{2}e^{j3\pi/4}e^{-jkw}\left(\frac{-K_{+c}^{4}(\alpha=0)a_3^2}{16\pi^2 k\sqrt{w}}\,K_+(\phi_o)K_+(\phi)e^{-jkw}\right. \\
& \cdot\left[\frac{1}{(2-a_1)(a_3-a_1)}\{1-F_{KP}(kwa_1)\}\right. \\
& \left.\left.+\,\frac{1}{(a_1-2)(a_3-2)}\{1-F_{KP}(kwa_2)\}+\frac{1}{(a_1-a_3)(2-a_3)}\{1-F_{KP}(kwa_3)\}\right]\right) \\
& \cdot\frac{1}{j(a_3-a_4)}\sqrt{\frac{\pi}{kw}}\left\{F_{KP}(kwa_{3)}-F_{KP}(kwa_4)\right\}\frac{e^{-jk\rho}}{\sqrt{\rho}} \qquad (27)
\end{aligned}
$$

Rewriting (26)

$$
\begin{aligned}
u_{121}^{d} \;=\; & j\frac{\sqrt{2}}{16(kw)^{\frac{3}{2}}w}e^{j3\pi/4}e^{-j2kw}K_{+c}^{4}(\alpha=0)a_3^2K_+(\phi_o)K_+(\phi) \\
& \cdot\left[\frac{1}{(2-a_1)(a_3-a_1)}\{1-F_{KP}(kwa_1)\}+\frac{1}{(a_1-2)(a_3-2)}\{1-F_{KP}(kw2)\}\right. \\
& \left.+\,\frac{1}{(a_1-a_3)(2-a_3)}\{1-F_{KP}(kwa_3)\}\right] \\
& \cdot\frac{1}{(a_3-a_4)}\{F_{KP}(kwa_3)-F_{KP}(kwa_4)\}\frac{e^{-jk\rho}}{\sqrt{\rho}} \qquad (28)
\end{aligned}
$$

Equation (27) is the complete triply diffracted field.It contains the factors of 4 for four mechanisms per edge times one-fourth to account for two cases of grazing incidence upon the edges (note that (1)of this appendix was multiplied by a factor of two to prevent any double counting of grazing incidence effects).

MISSING
PAGE

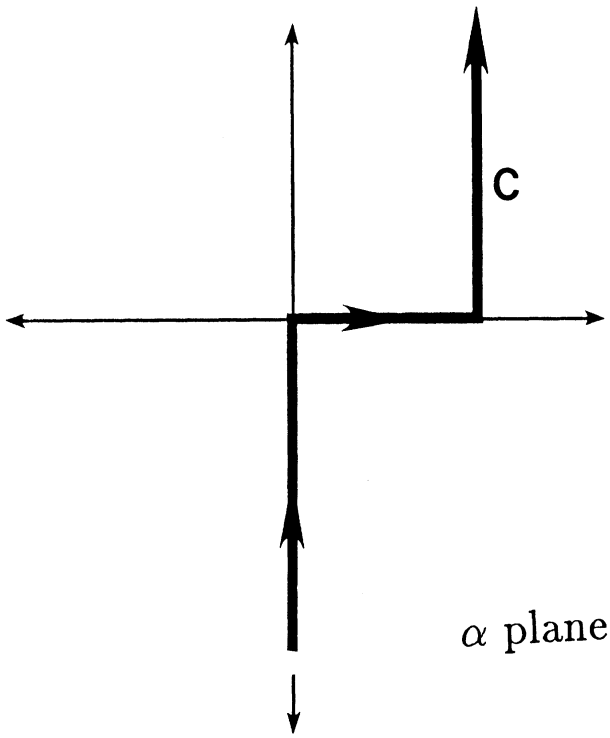


Fig. 3. Topology of the integral representation of the edge diffracted field.

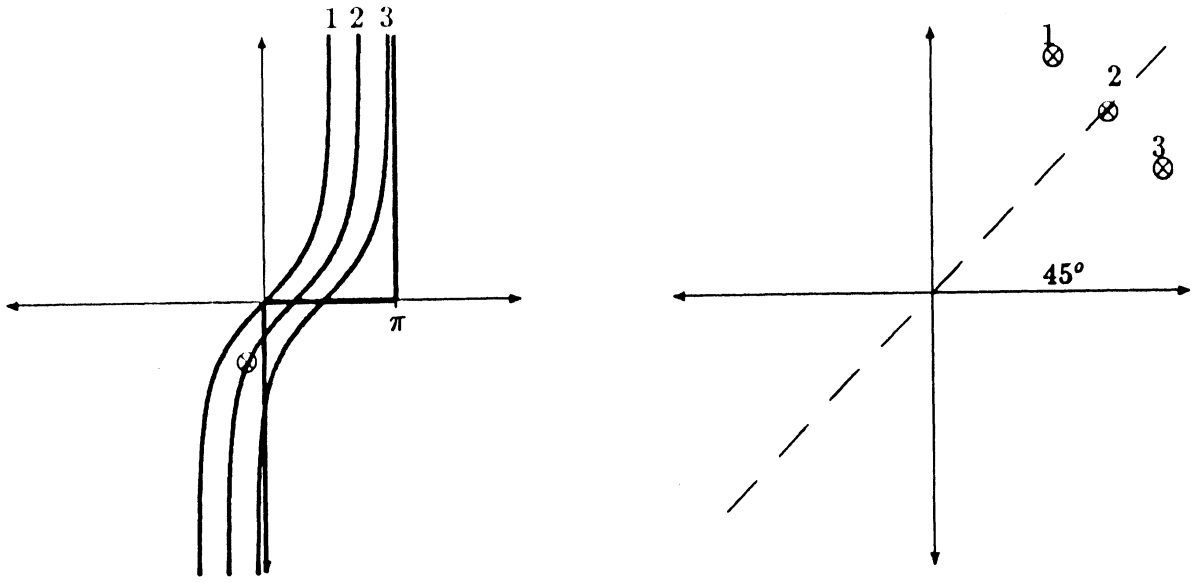


$\alpha$ plane

Surface Wave Continuity
(phase of the argument of $F_c$)

Fig. 4. Continuity of the surface wave field and the corresponding argument in the Clemmow transition function.

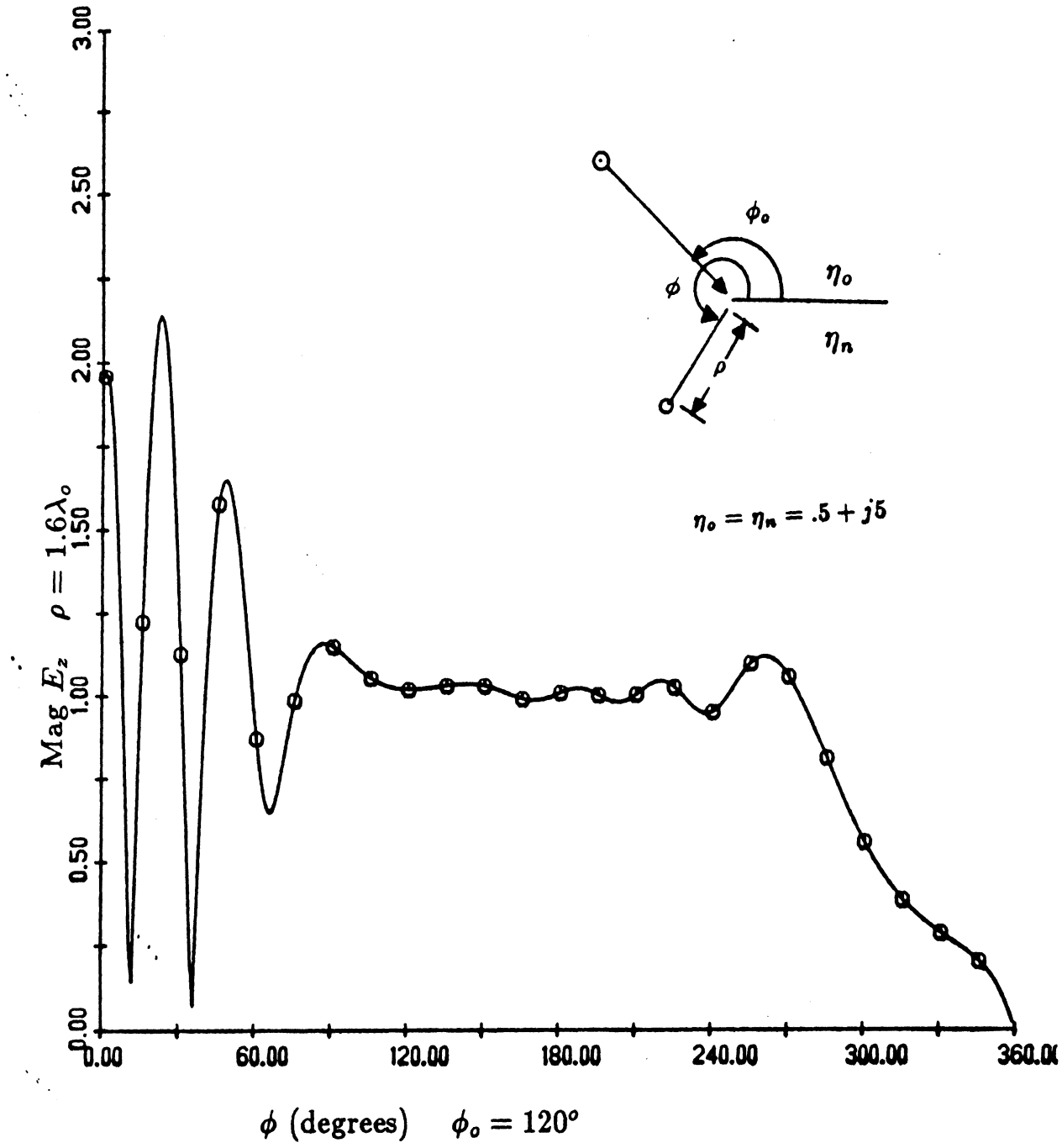


Fig. 5. Pattern of the total electric field due to a plane wave source incident on an impedance half plane ($\eta = .5 + j5$) at $\phi_o$=120°.

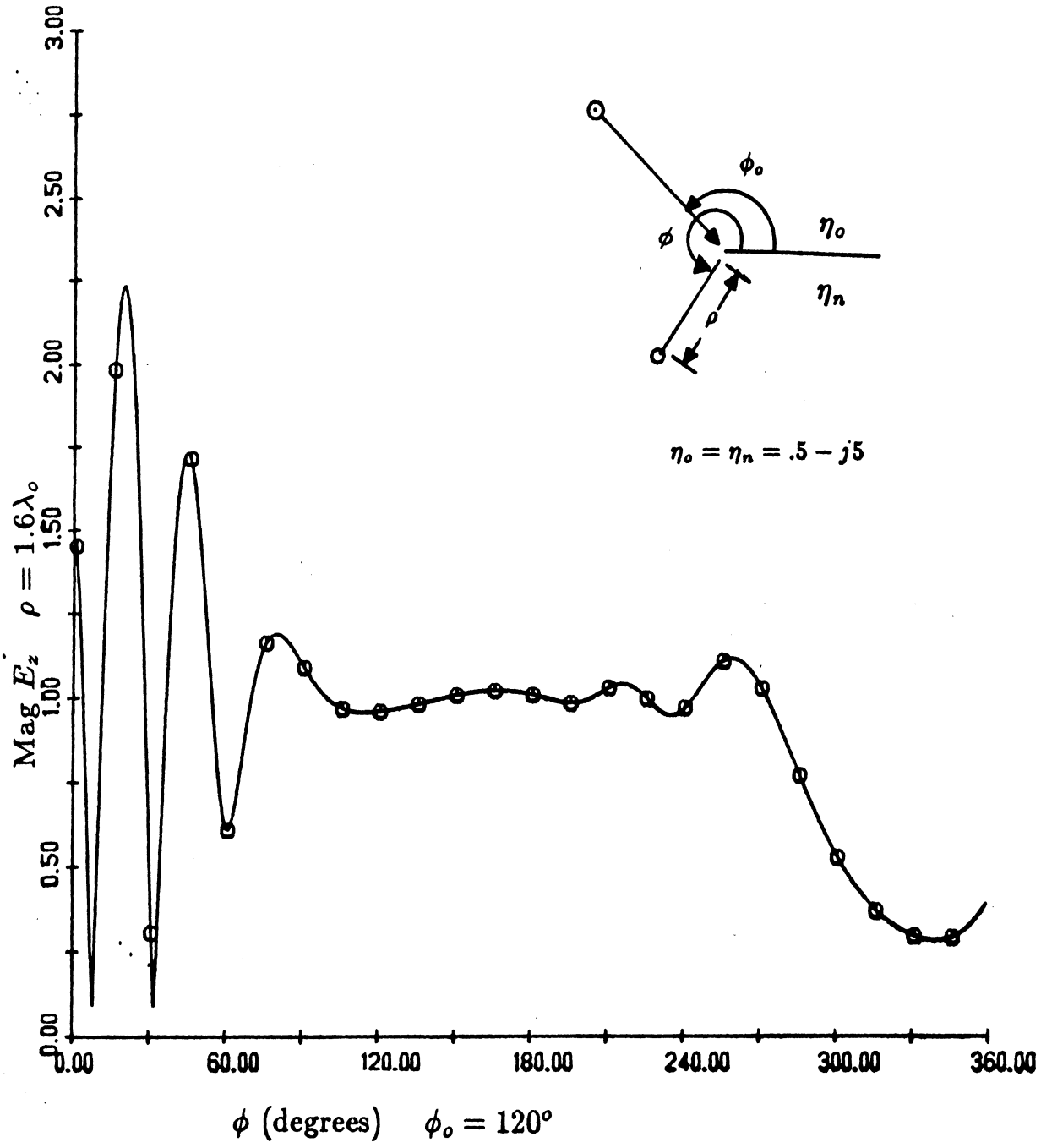


Fig. 6. Pattern of the total electric field due to a plane wave source incident on an impedance half plane ($\eta = .5 - j5$) at $\phi_o$=120°.

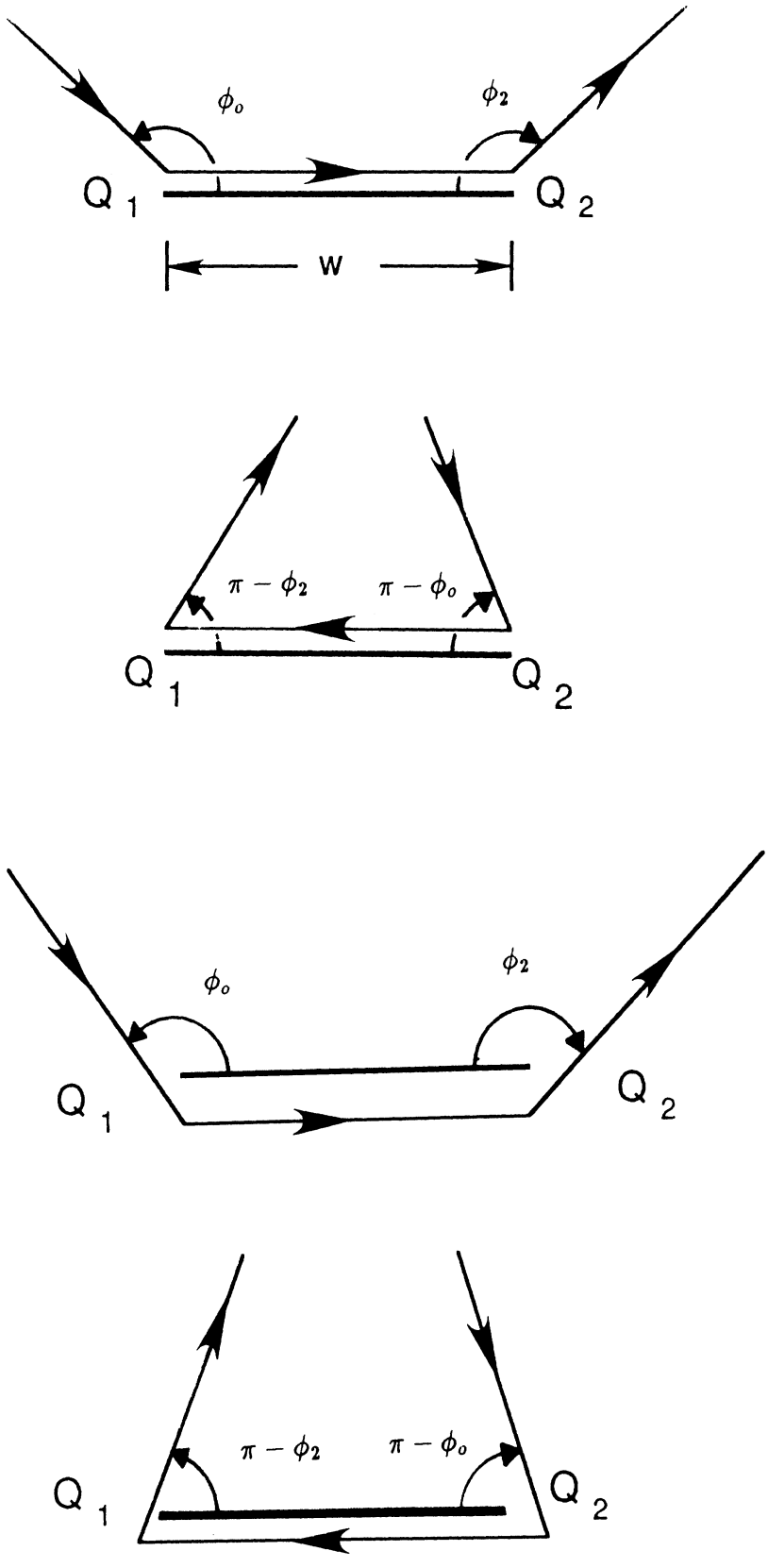


Fig. 7. Illustration of double diffraction ray mechanisms of a strip.

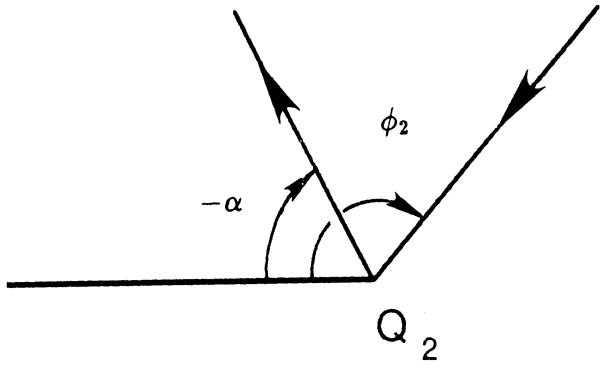


Fig. 8. Plane wave field incidence and diffraction at a complex angle $-\alpha$ on edge $Q_2$.

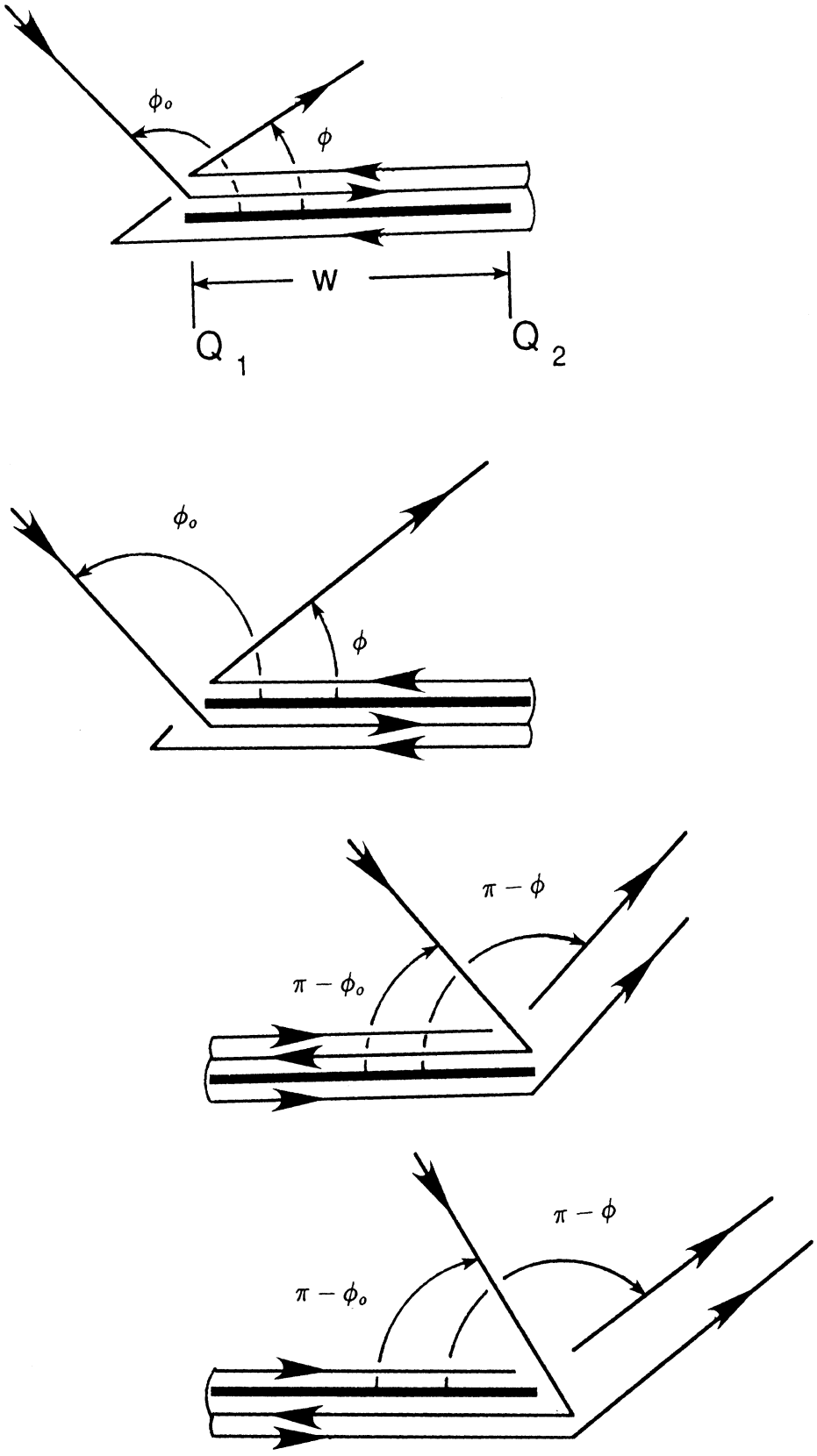


Fig. 9. Illustration of triply diffracted ray mechanisms of a strip.

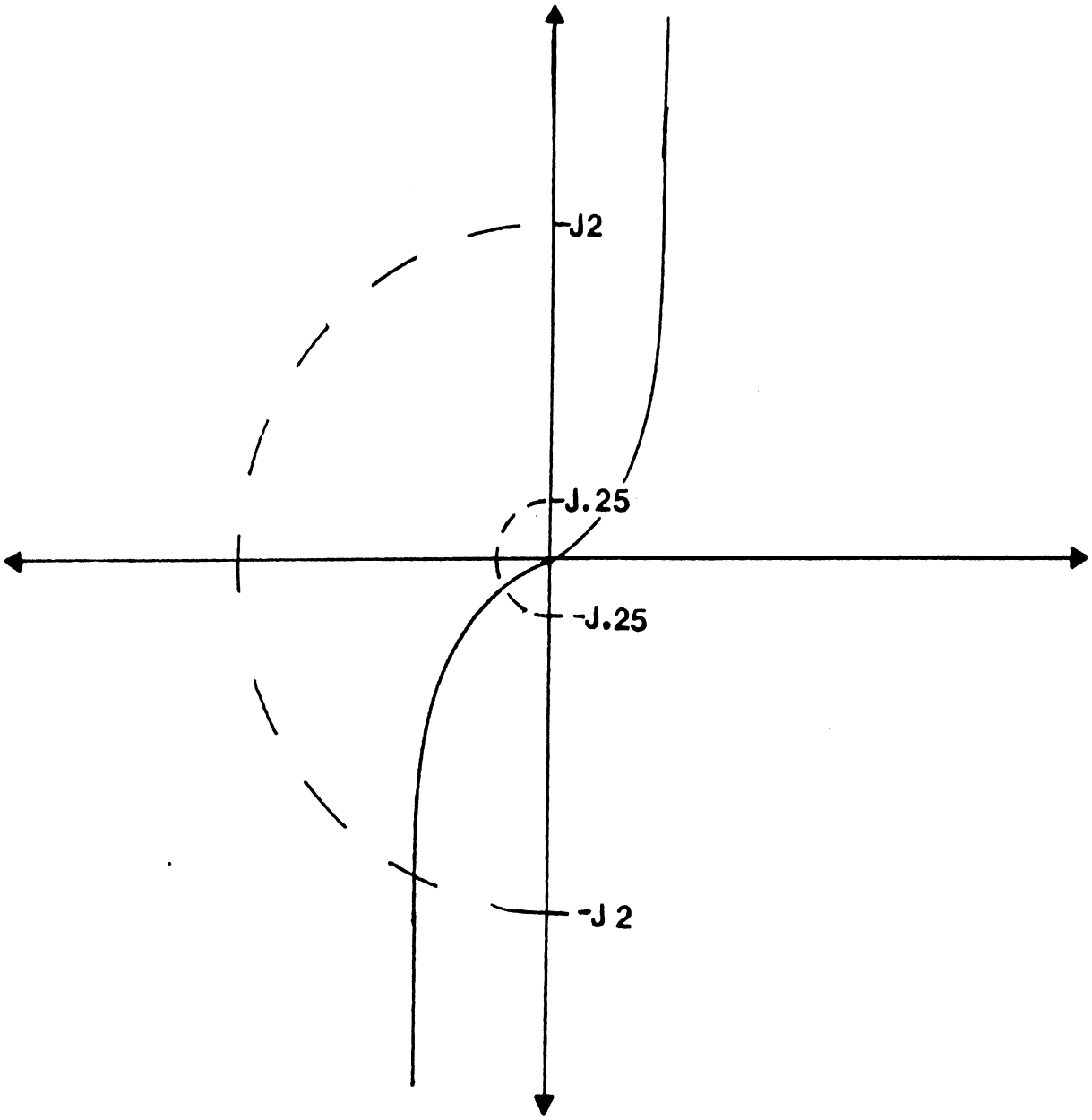


Fig. 10. Path of constant surface wave pole magnitudes (.25 and 2)
in relation to the steepest descent path
(a Gudermann function).

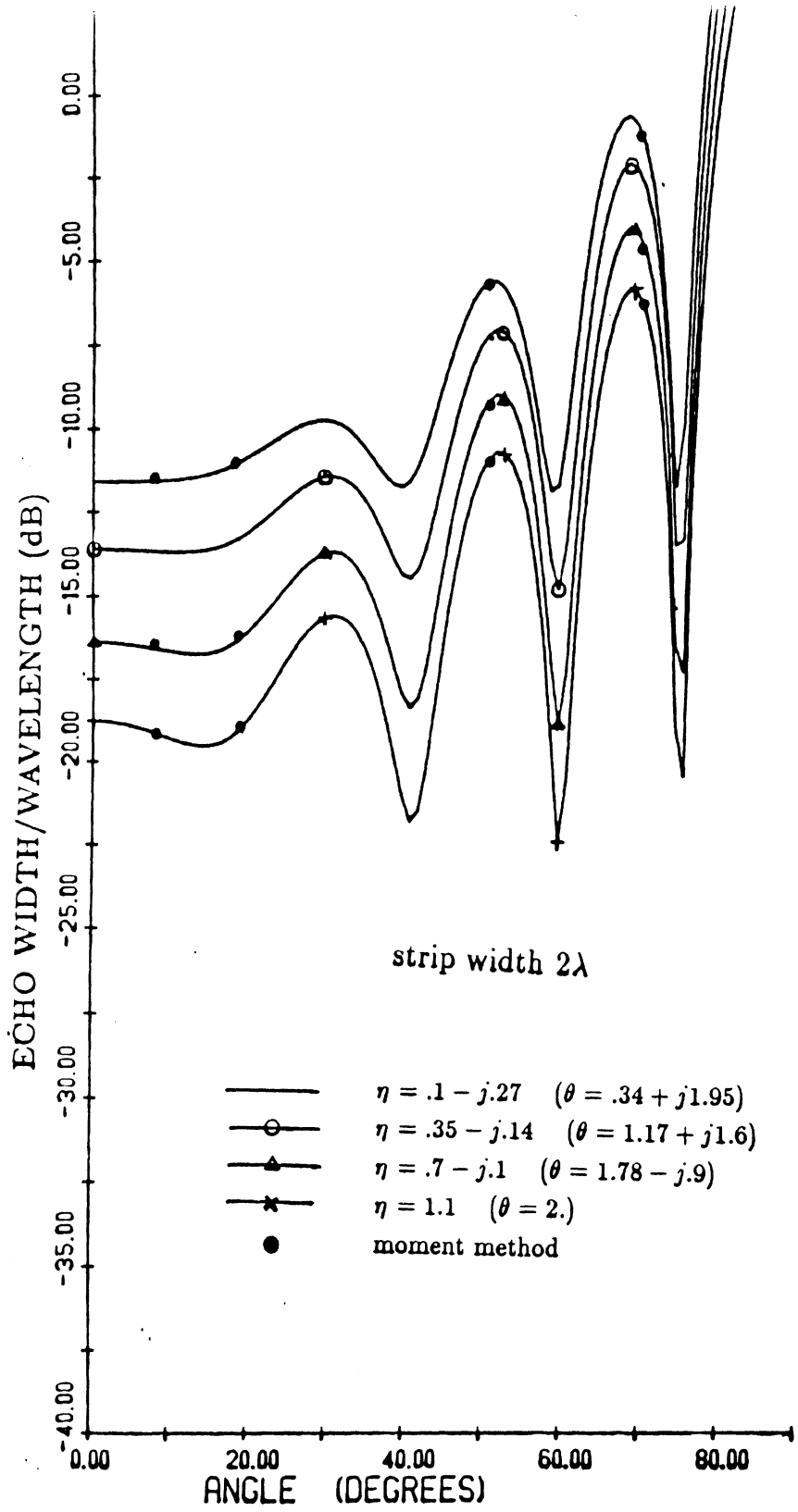


Fig. 11. Comparison of the solution for backscattering with moment method data from a $2\lambda$ wide resistive strip with $\eta = .1 - j.27, .35 - j.14, .7 - j.1$, and 1.1(constant surface wave pole magnitude $\sim 2$), E-polarization.

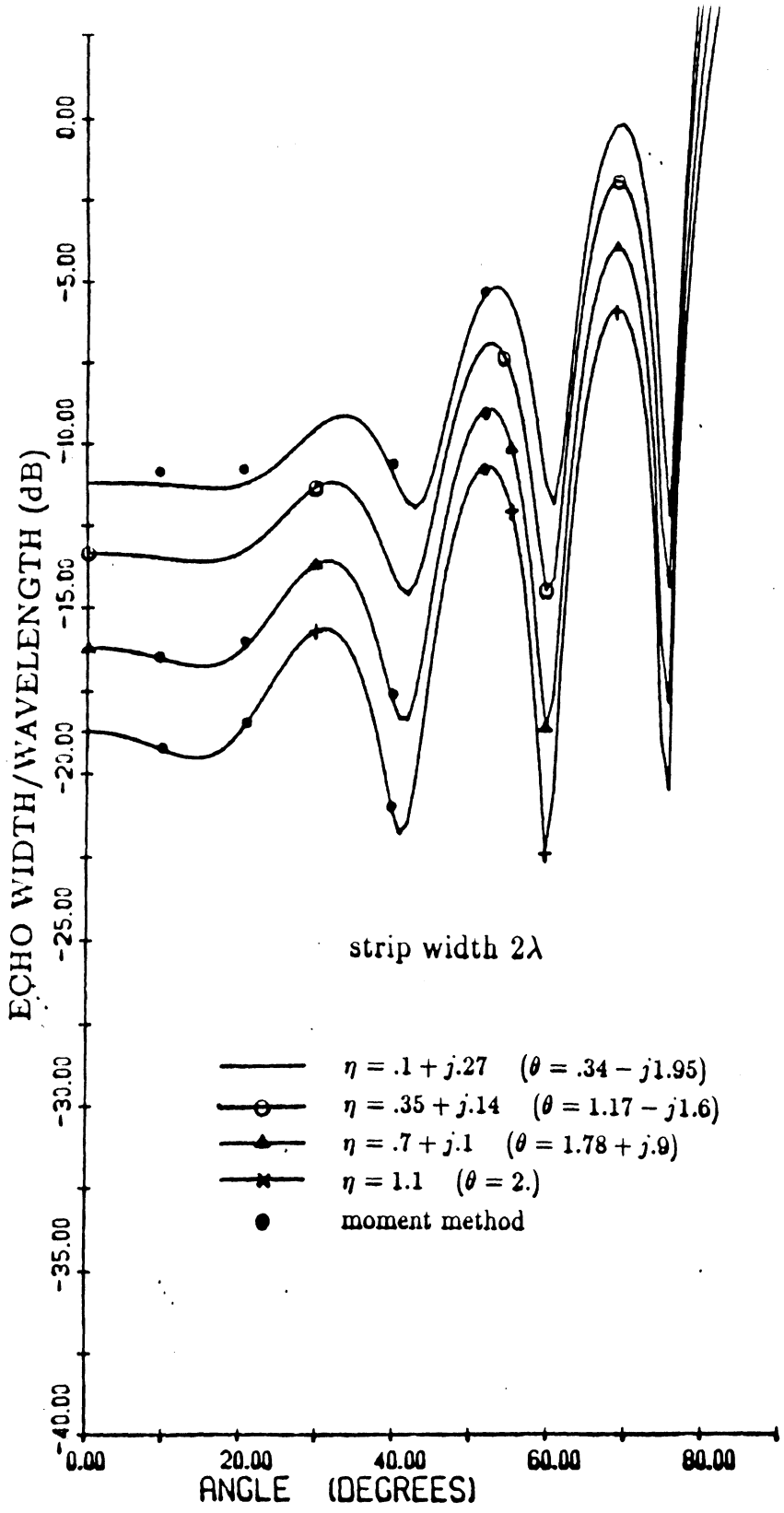


Fig. 12. Comparison of the solution for backscattering with moment method data from a $2\lambda$ wide resistive strip with $\eta = .1 + j.27, .35 + j.14, .7 + j.1$, and 1.1(constant surface wave pole magnitude $\sim 2$), E-polarization.

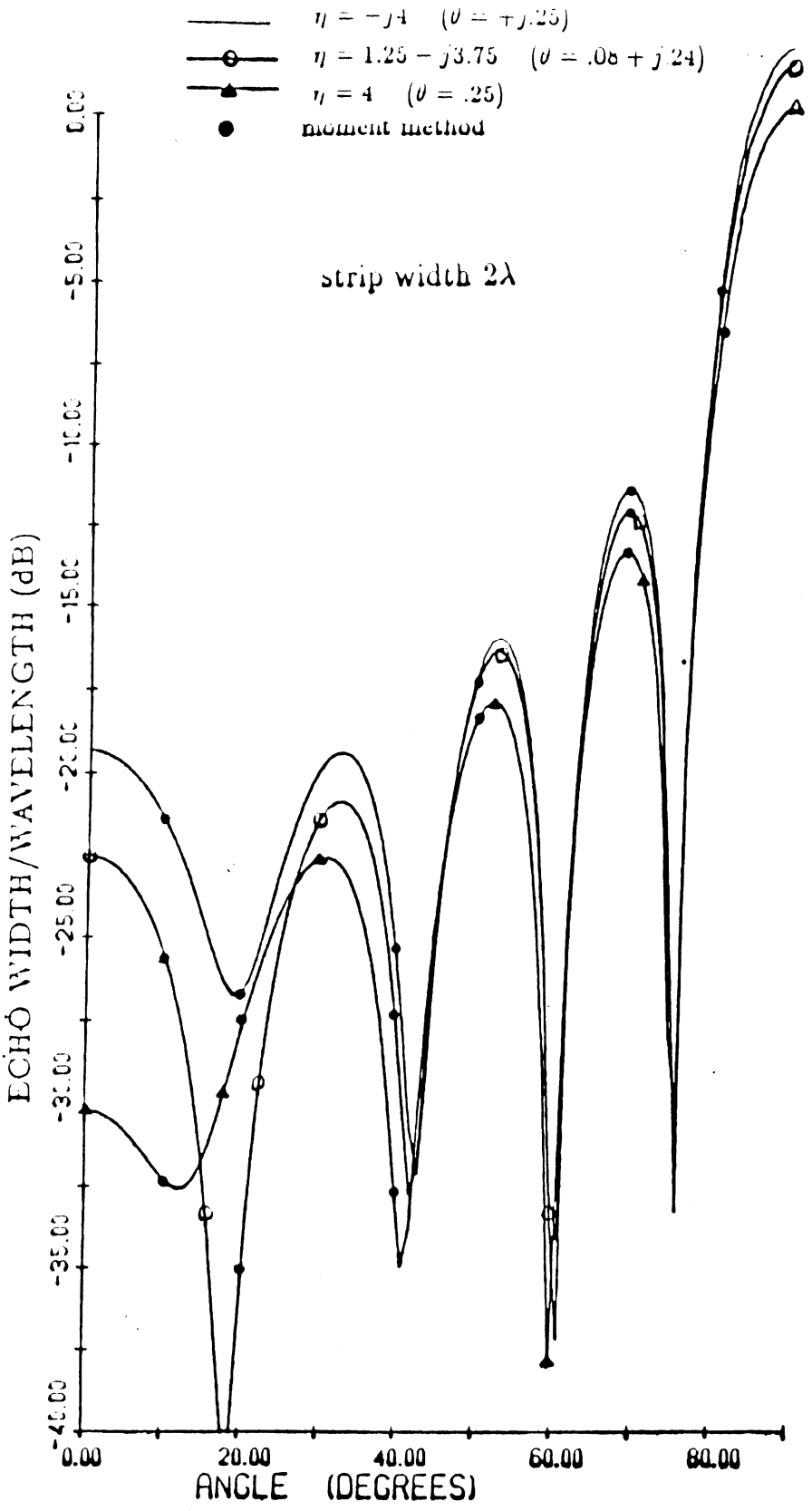


Fig. 13. Comparison of the solution for backscattering with moment method data from a $2\lambda$ wide resistive strip with $\eta = -j4, 1.25 - j3.75$, and 4(constant surface wave pole magnitude $\sim .25$), E-polarization.

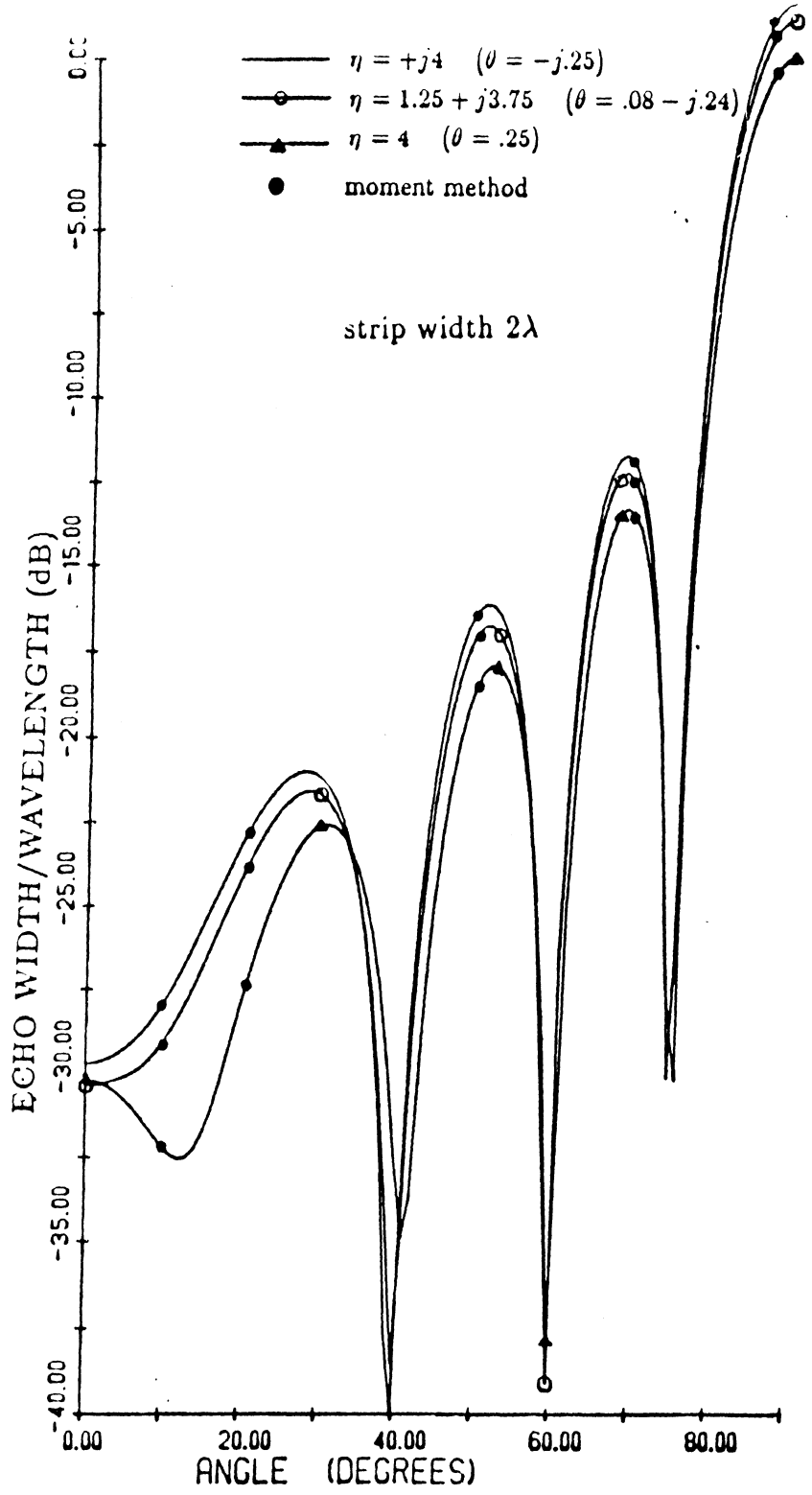


Fig. 14. Comparison of the solution for backscattering with moment method data from a $2\lambda$ wide resistive strip with $\eta = j4, 1.25 + j3.75$, and 4(constant surface wave pole magnitude $\sim .25$), E-polarization.

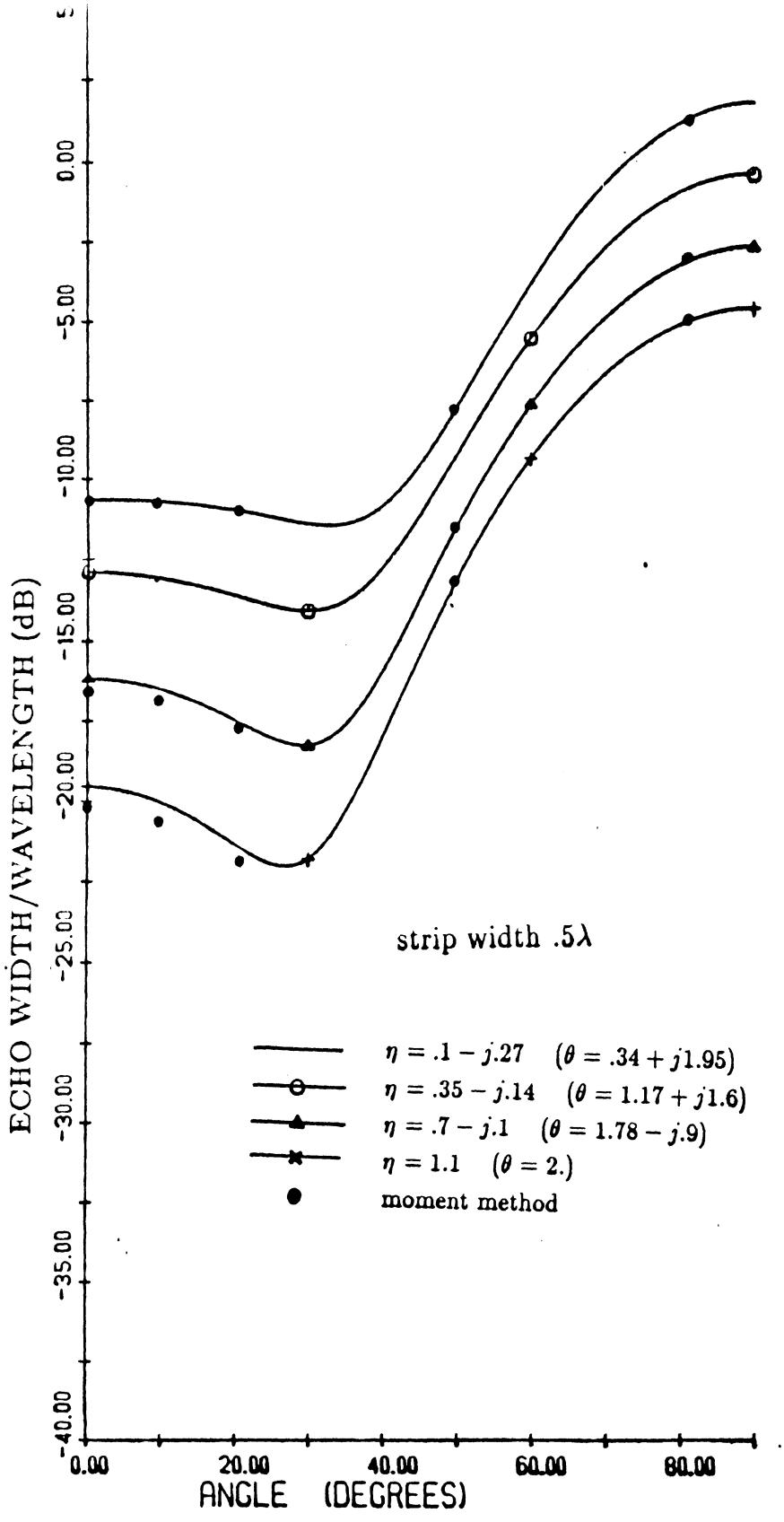


Fig. 15. Comparison of the solution for backscattering with moment method data from a .5λ wide resistive strip with $\eta = .1 - j.27, .35 - j.14, .7 - j.1$, and 1.1(constant surface wave pole magnitude $\sim 2$), E-polarization.

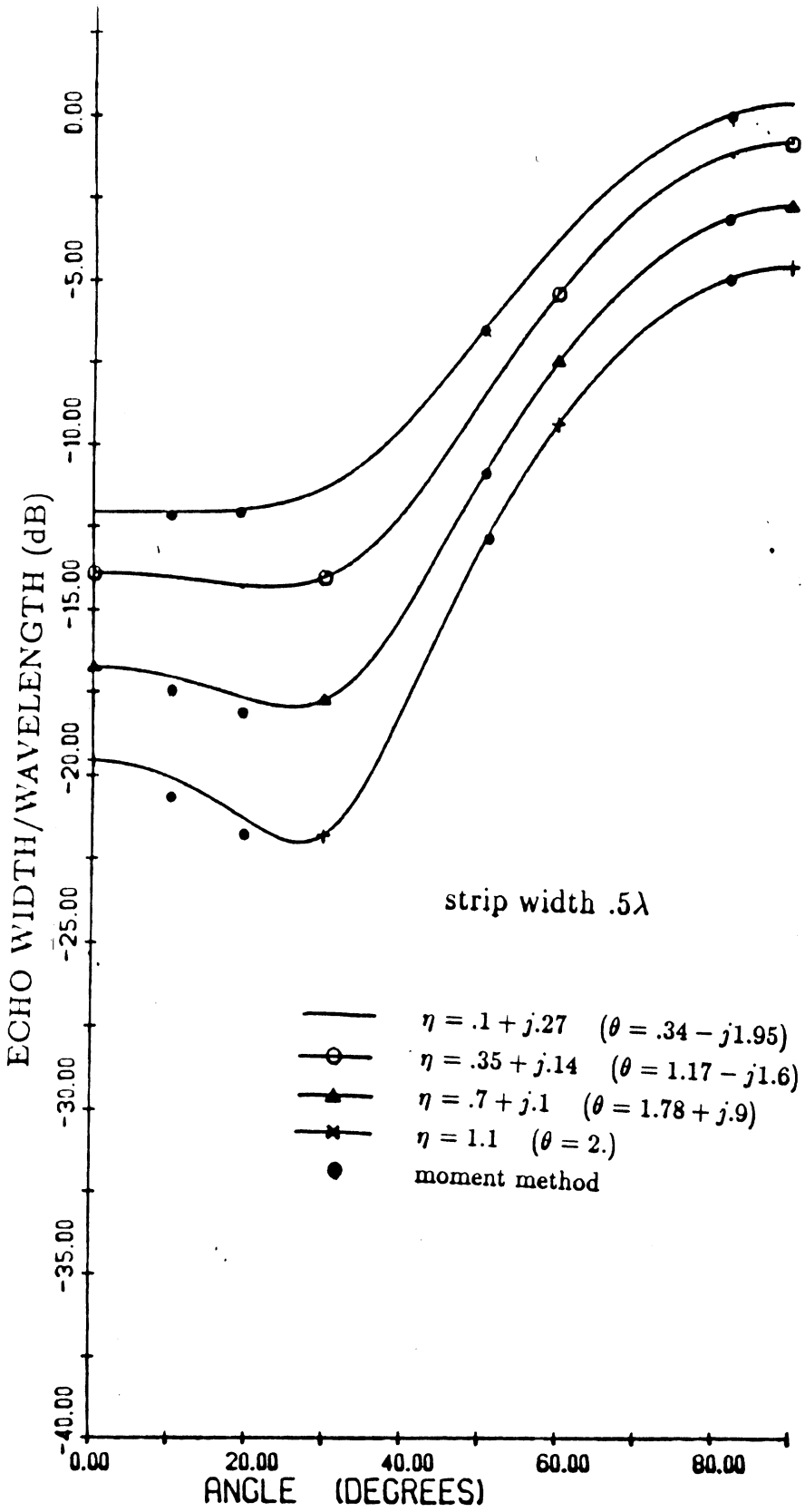


Fig. 16. Comparison of the solution for backscattering with moment method data from a .5λ wide resistive strip with $\eta = .1 + j.27, .35 + j.14, .7 + j.1$, and 1.1(constant surface wave pole magnitude $\sim 2$), E-polarization.

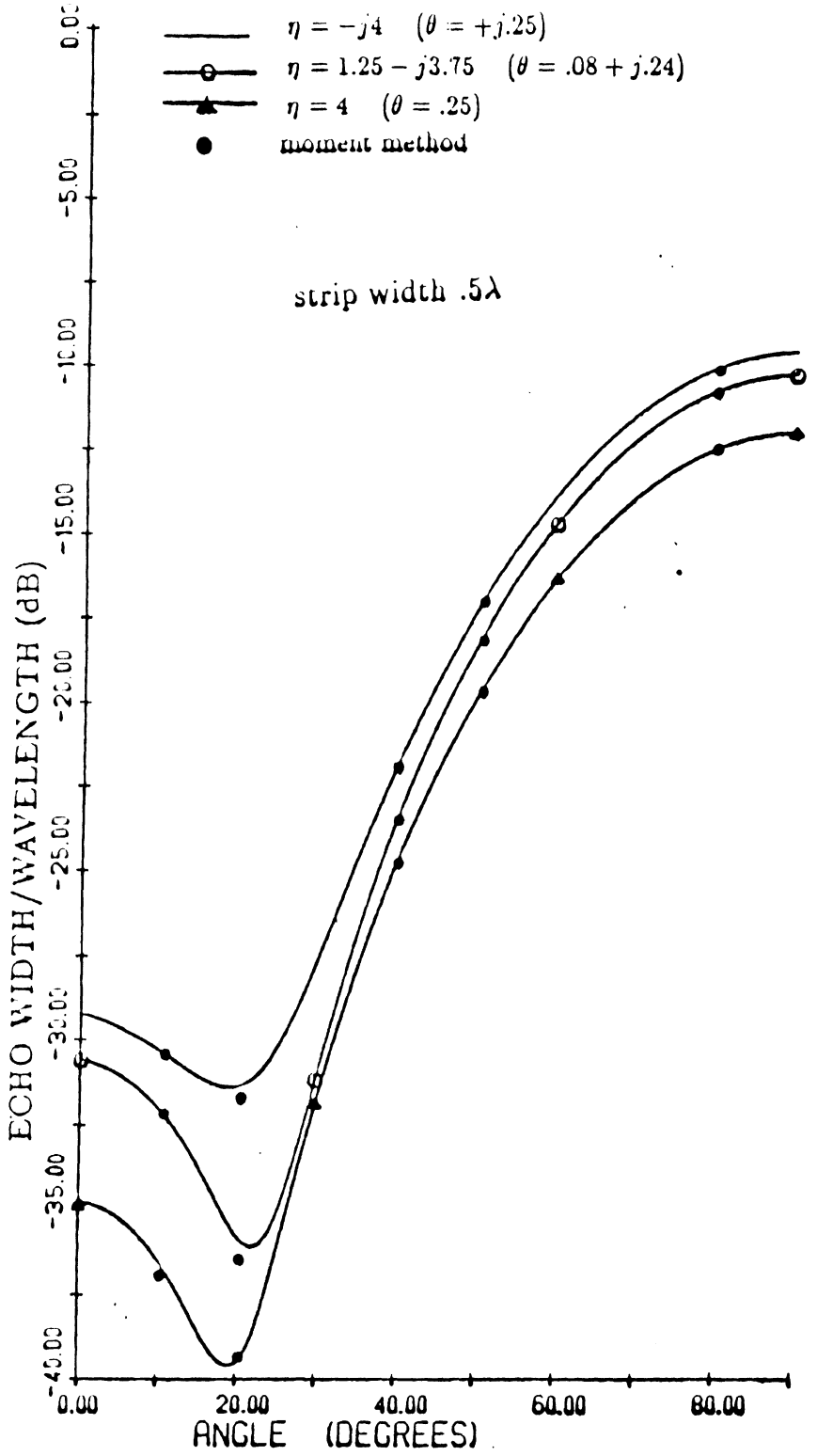


Fig. 17. Comparison of the solution for backscattering with moment method data from a .5λ wide resistive strip with $\eta = -j4, 1.25 - j3.75$, and 4(constant surface wave pole magnitude ~ .25), E-polarization.

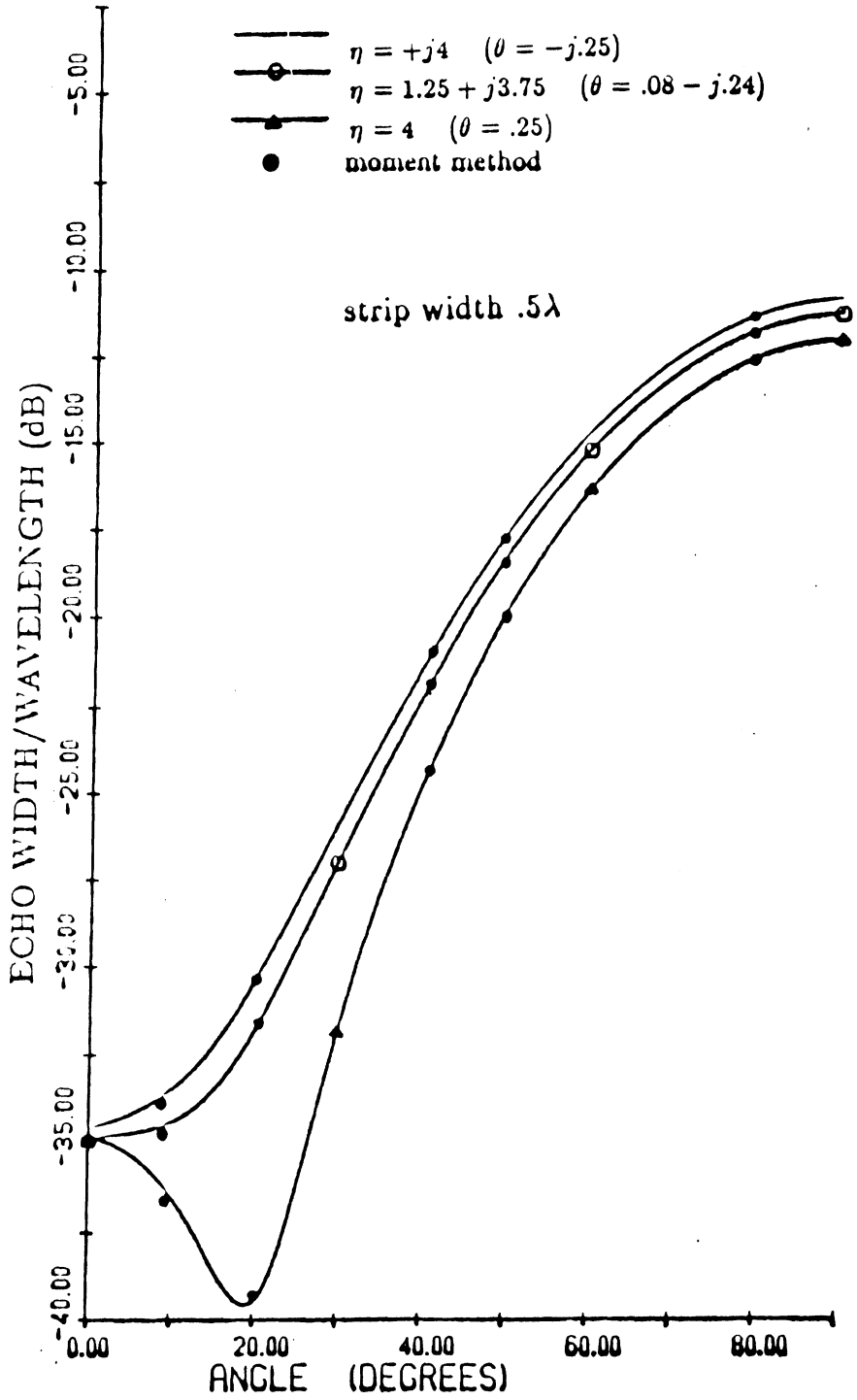


Fig. 18. Comparison of the solution for backscattering with moment method data from a .5λ wide resistive strip with $\eta = j4, 1.25 + j3.75$, and 4(constant surface wave pole magnitude ~ .25), E-polarization.

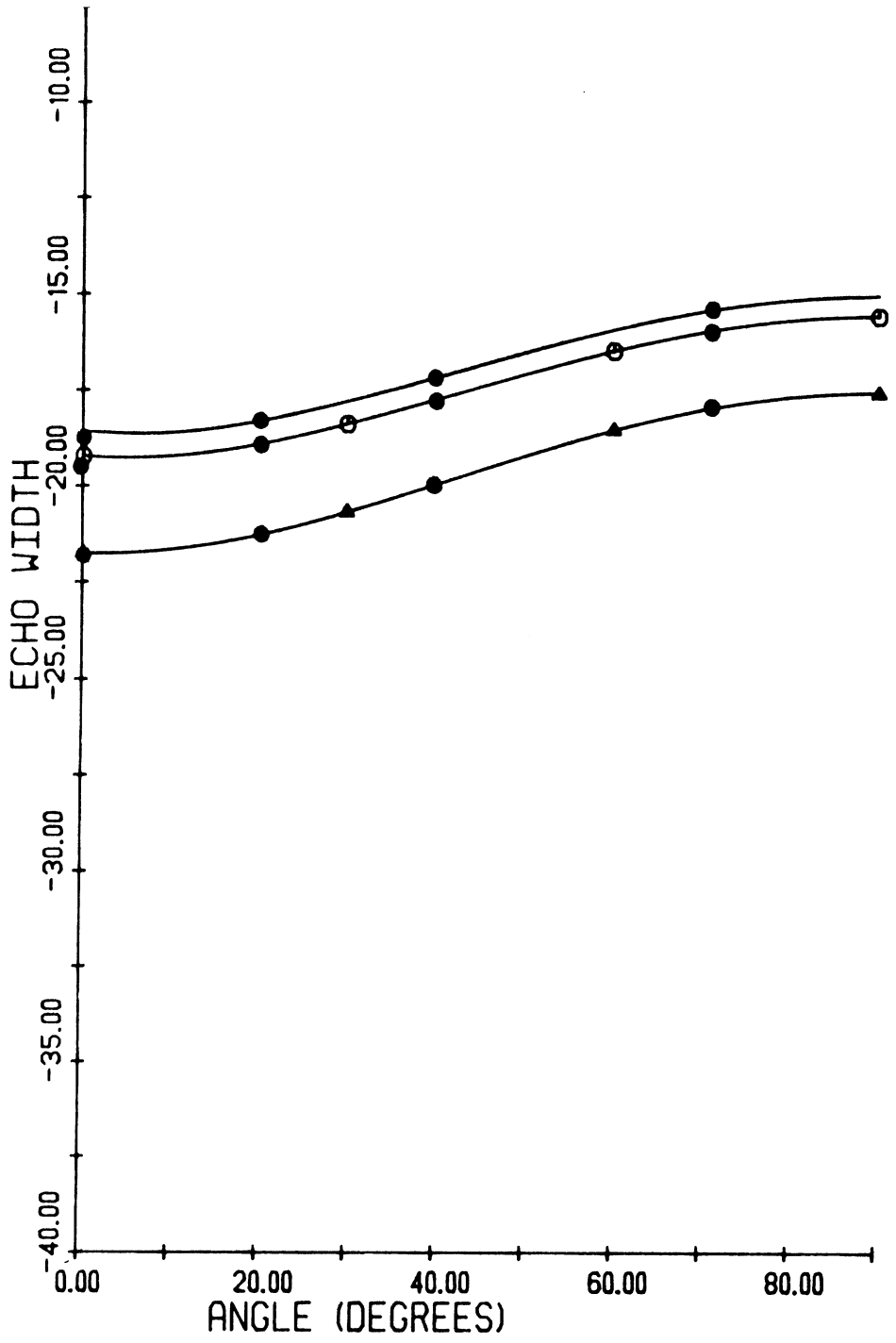


Fig. 19. Comparison of the solution for backscattering with moment method data from a .25$\lambda$ wide resistive strip with $\eta = -j4, 1.25 - j3.75$, and 4(constant surface wave pole magnitude $\sim$ .25), E-polarization.

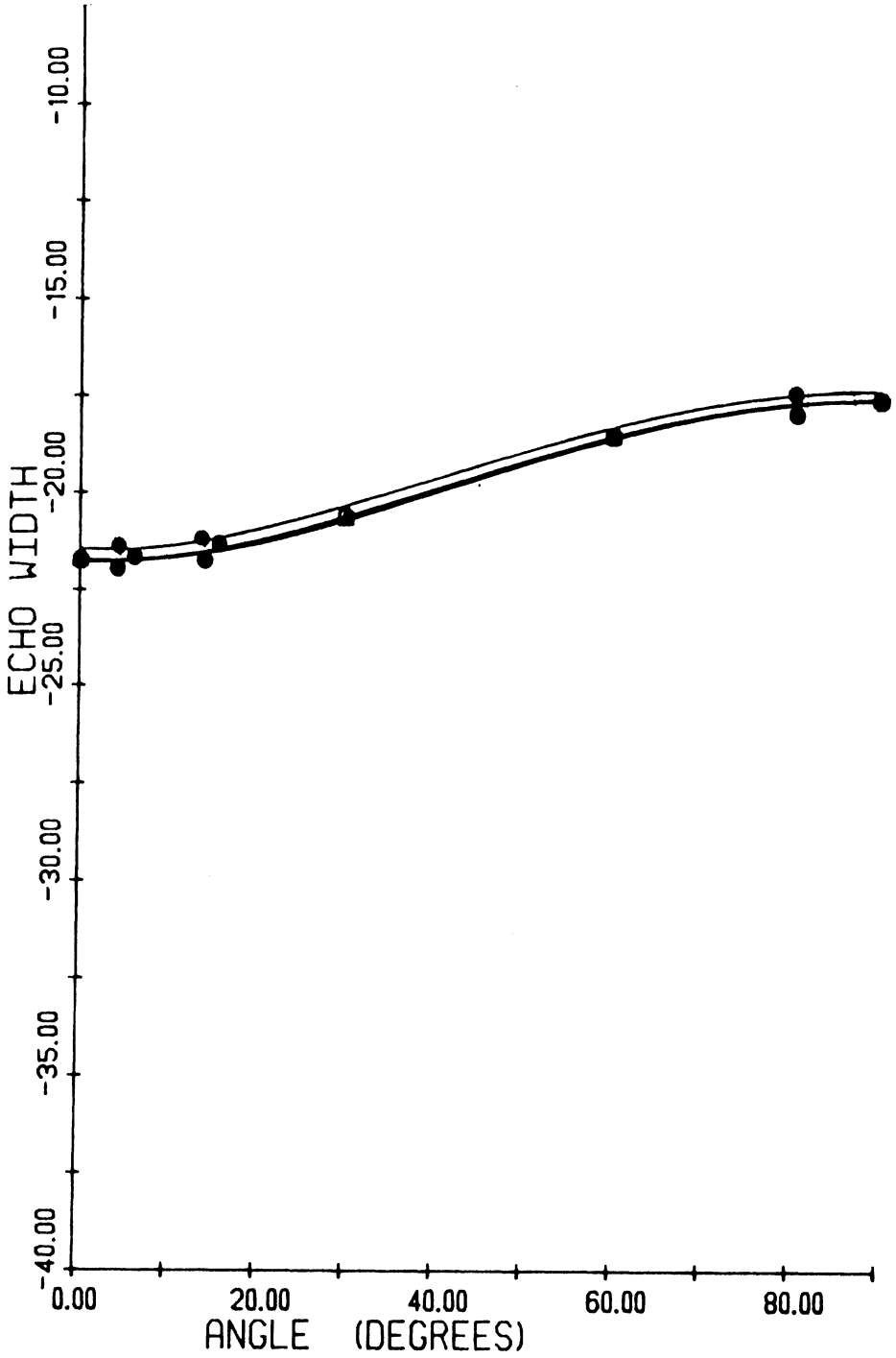


Fig. 20. Comparison of the solution for backscattering with moment method data from a .25$\lambda$ wide resistive strip with $\eta = j4, 1.25 + j3.75$, and 4(constant surface wave pole magnitude $\sim$ .25), E-polarization.

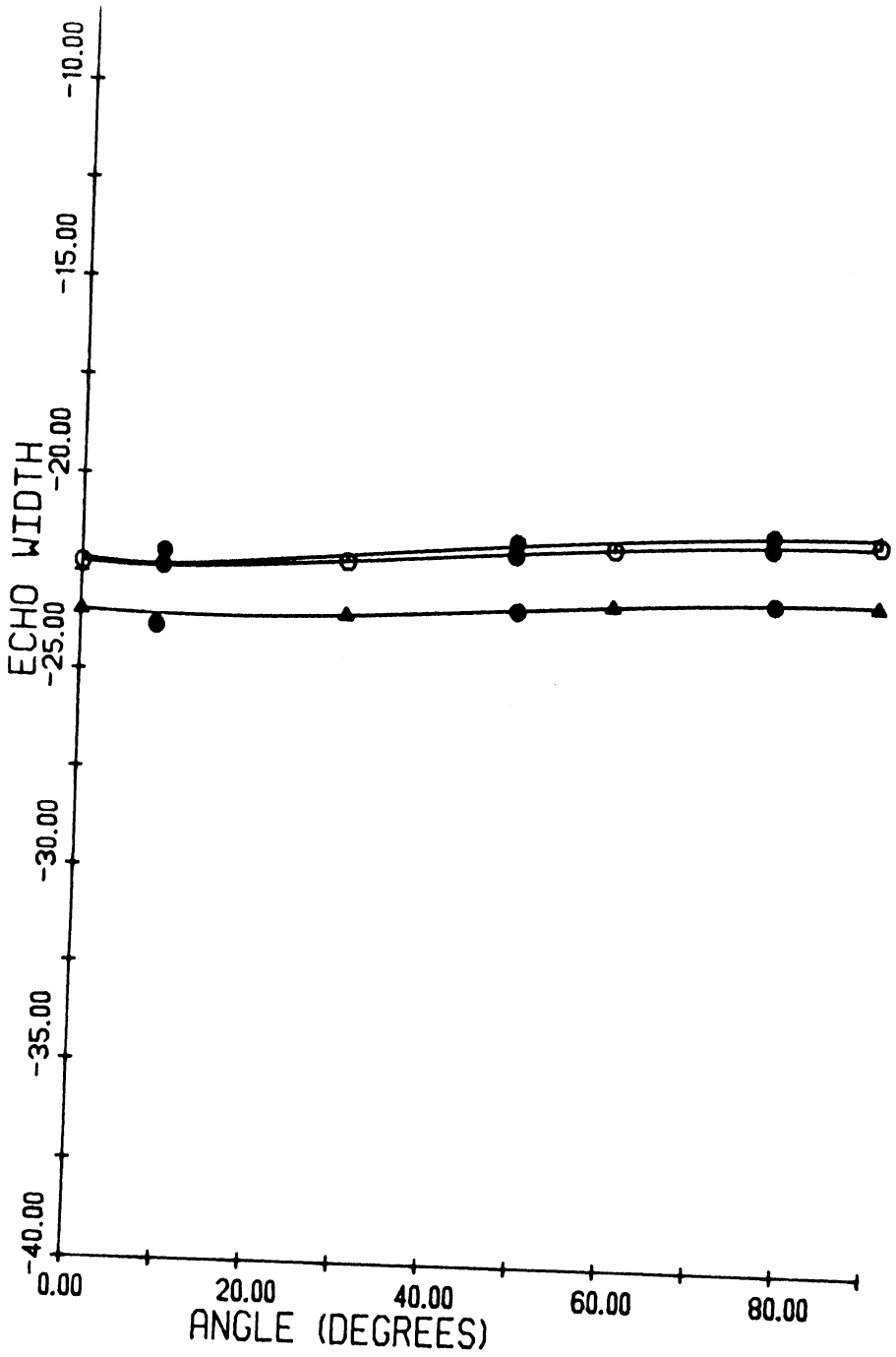


Fig. 21. Comparison of the solution for backscattering with moment method data from a .125$\lambda$ wide resistive strip with $\eta = -j4, 1.25 - j3.75$, and 4(constant surface wave pole magnitude $\sim$ .25), E-polarization.

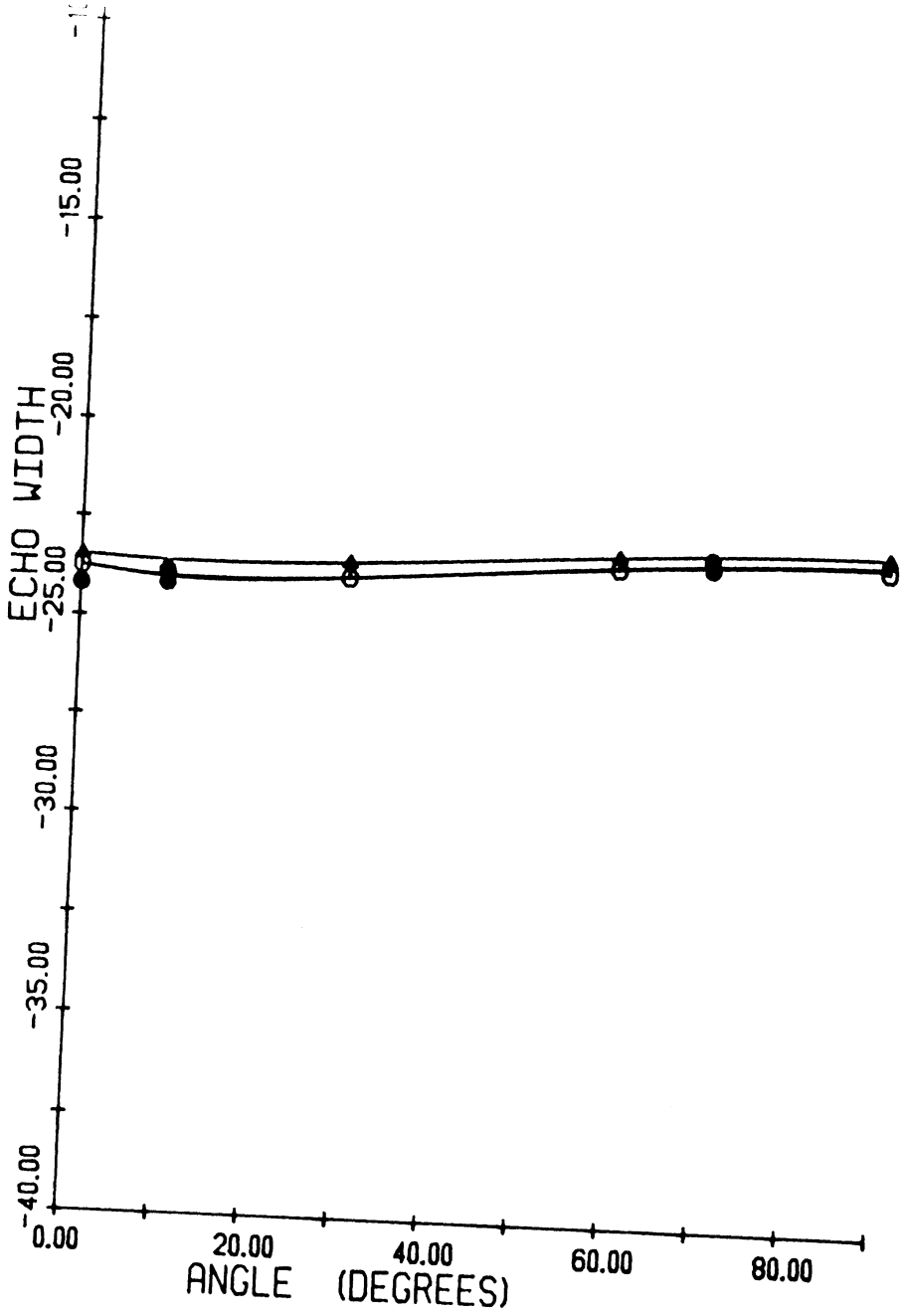


Fig. 22. Comparison of the solution for backscattering with moment method data from a .125$\lambda$ wide resistive strip with $\eta = j4, 1.25 + j3.75$, and 4(constant surface wave pole magnitude $\sim$ .25), E-polarization.

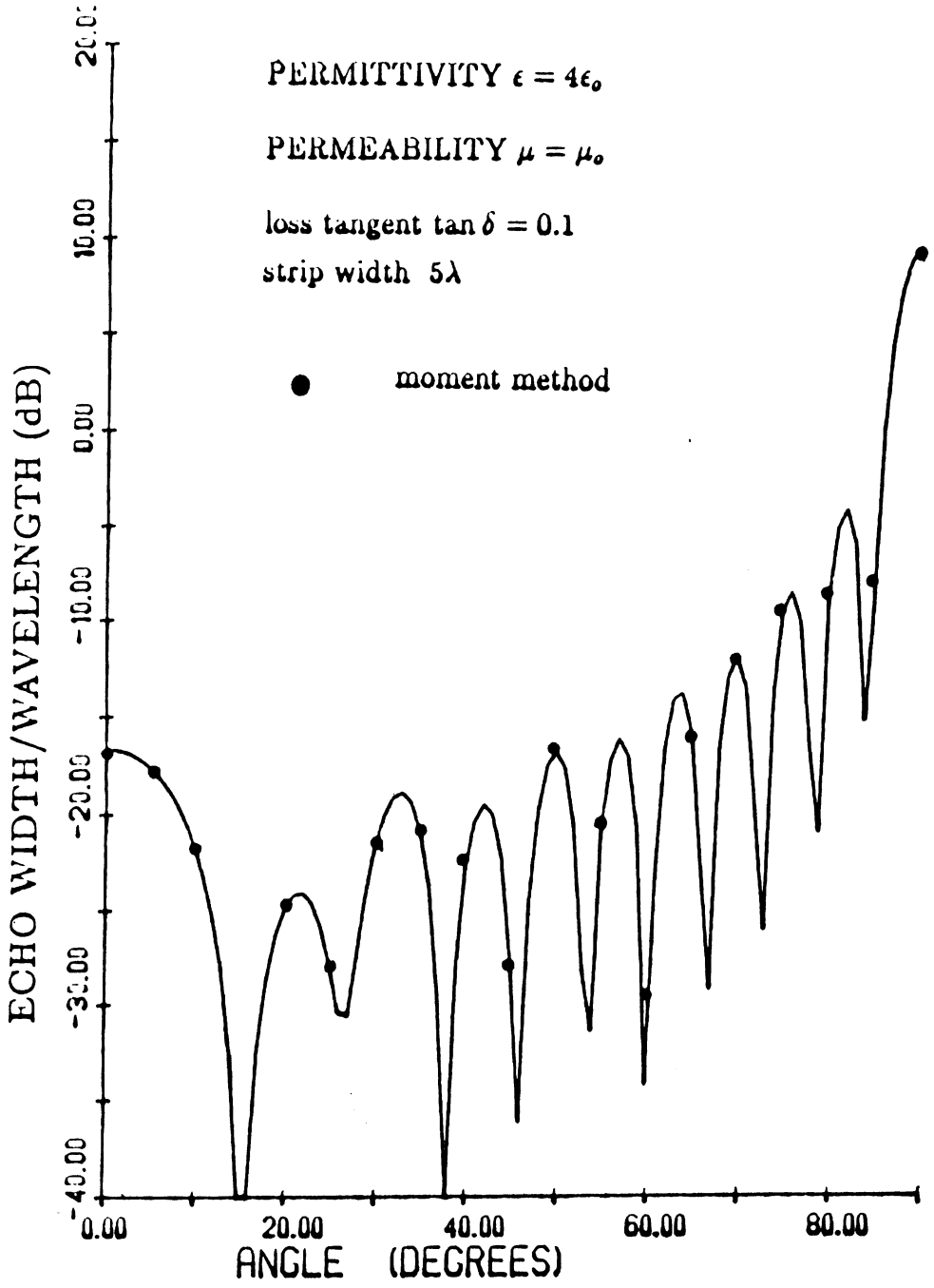


Fig. 23. Comparison of backscatter pattern with moment method for a resistive strip ($\eta = .55 - j4.2$) which models a thin dielectric slab with thickness $\lambda/40$ and $\epsilon_r = 4(1 - j.1)$, E-polarization.

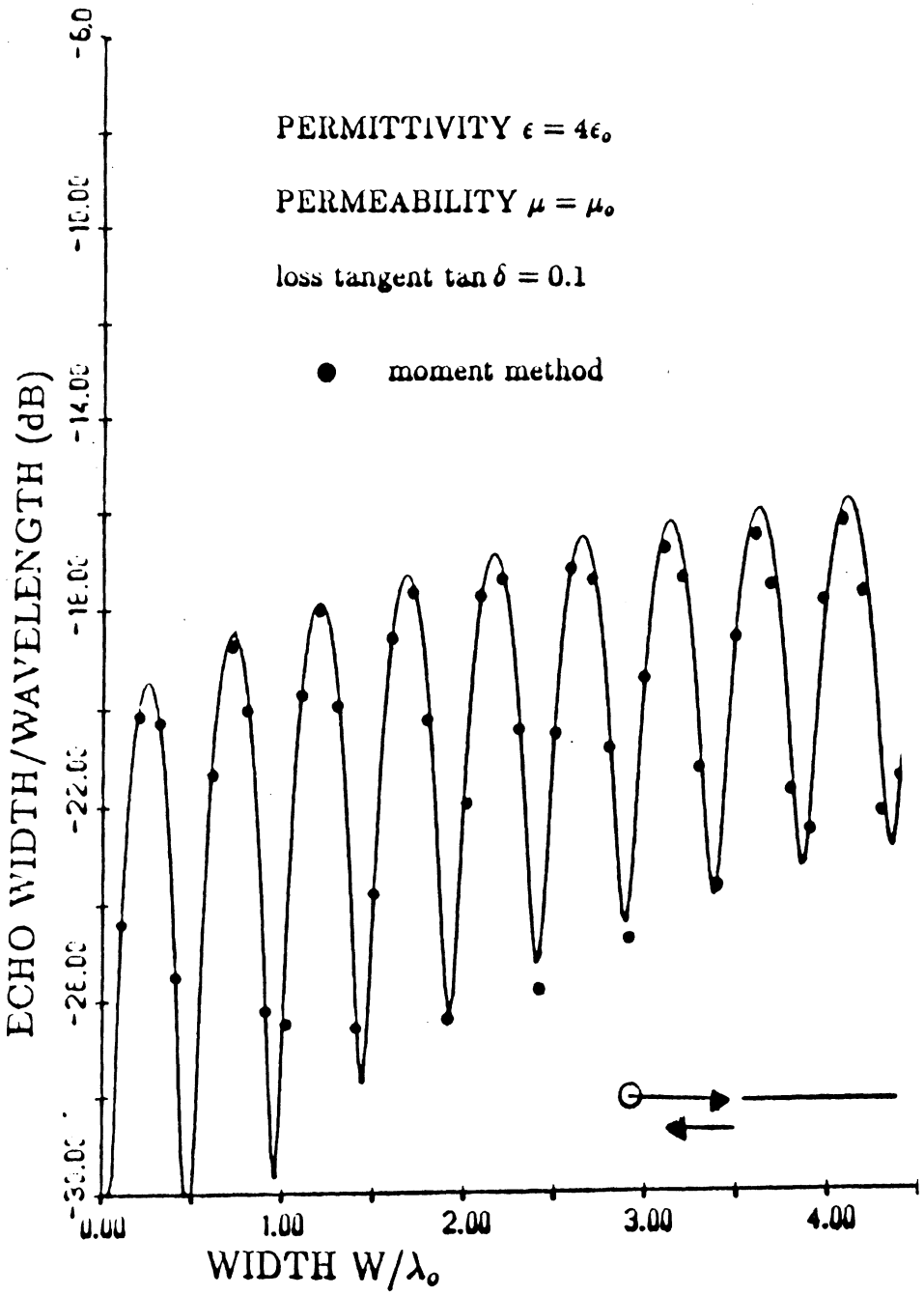


Fig. 24. Comparison of edge-on backscattering with width of a resistive strip, E-polarization.

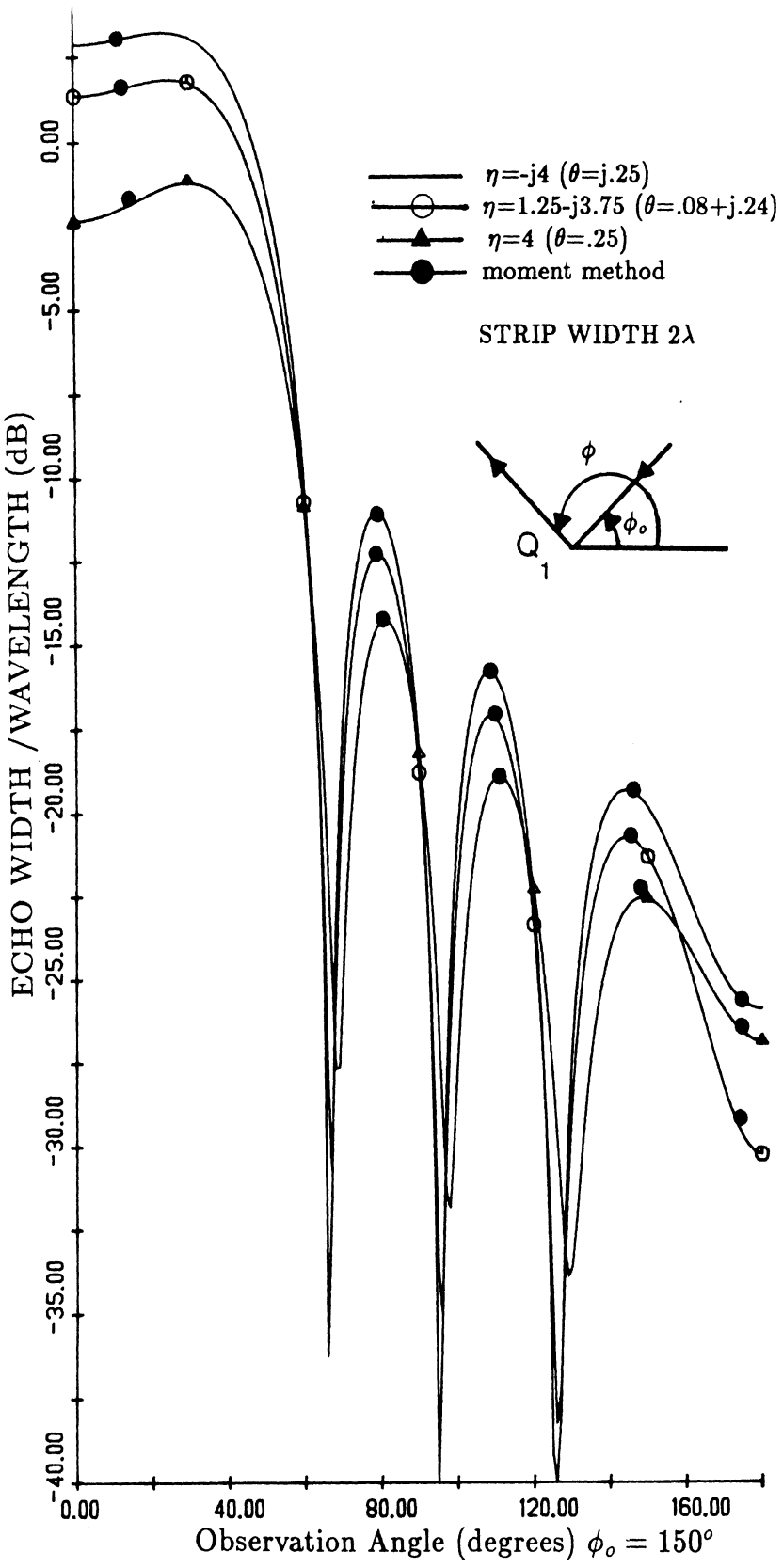


Fig. 25. Comparison of bistatic solution with moment method data for a $2\lambda$ wide resistive strip with $\eta = -j4, 1.25 - j3.75$, and 4 (constant surface wave magnitude $\sim .25$), angle of incidence=150°, E-polarization.

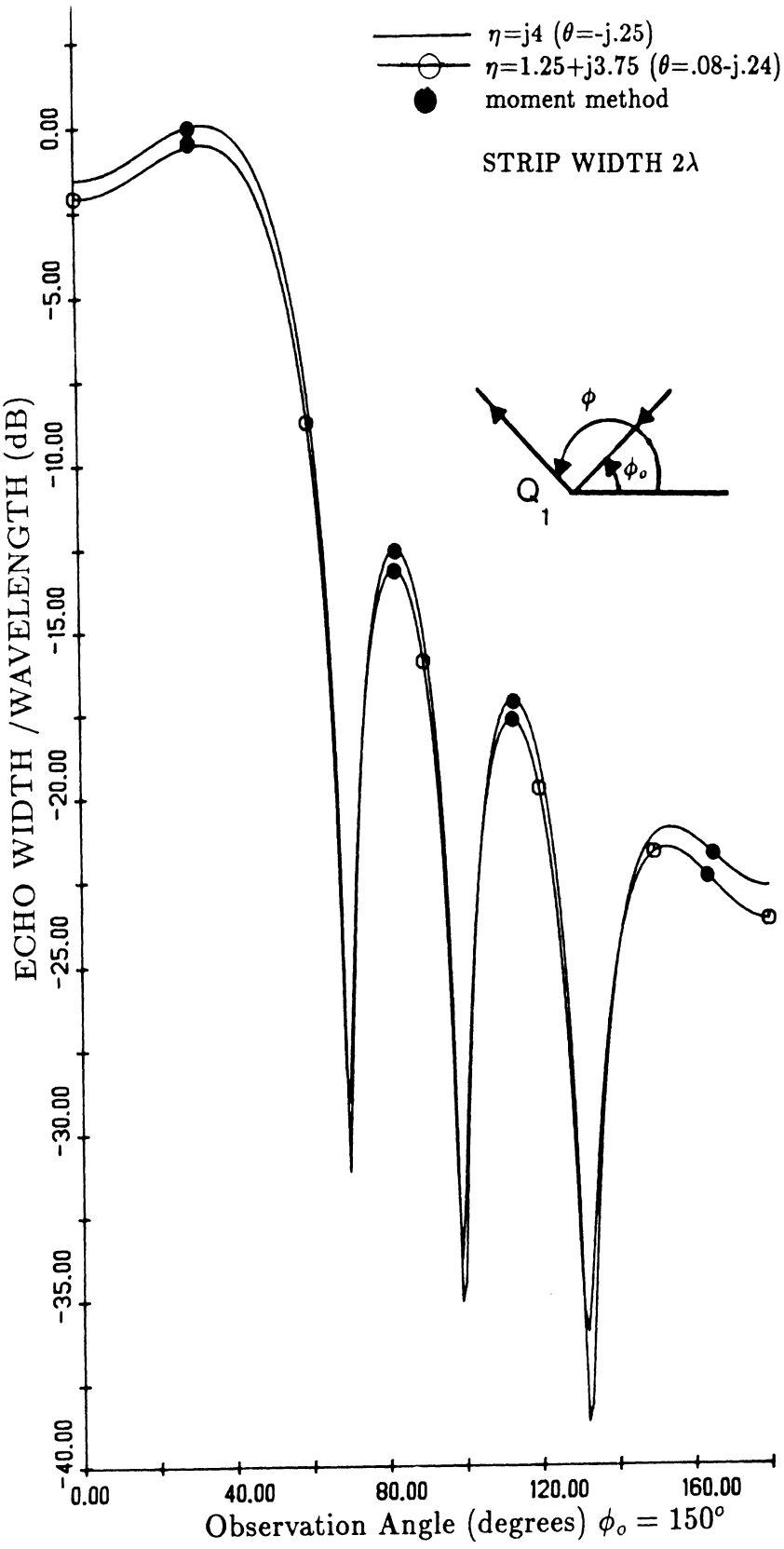


Fig. 26. Comparison of bistatic solution with moment method data for a $2\lambda$ wide resistive strip with $\eta = j4$, and 1.25+j3.75 (constant surface wave magnitude $\sim .25$), angle of incidence=150°, E-polarization.

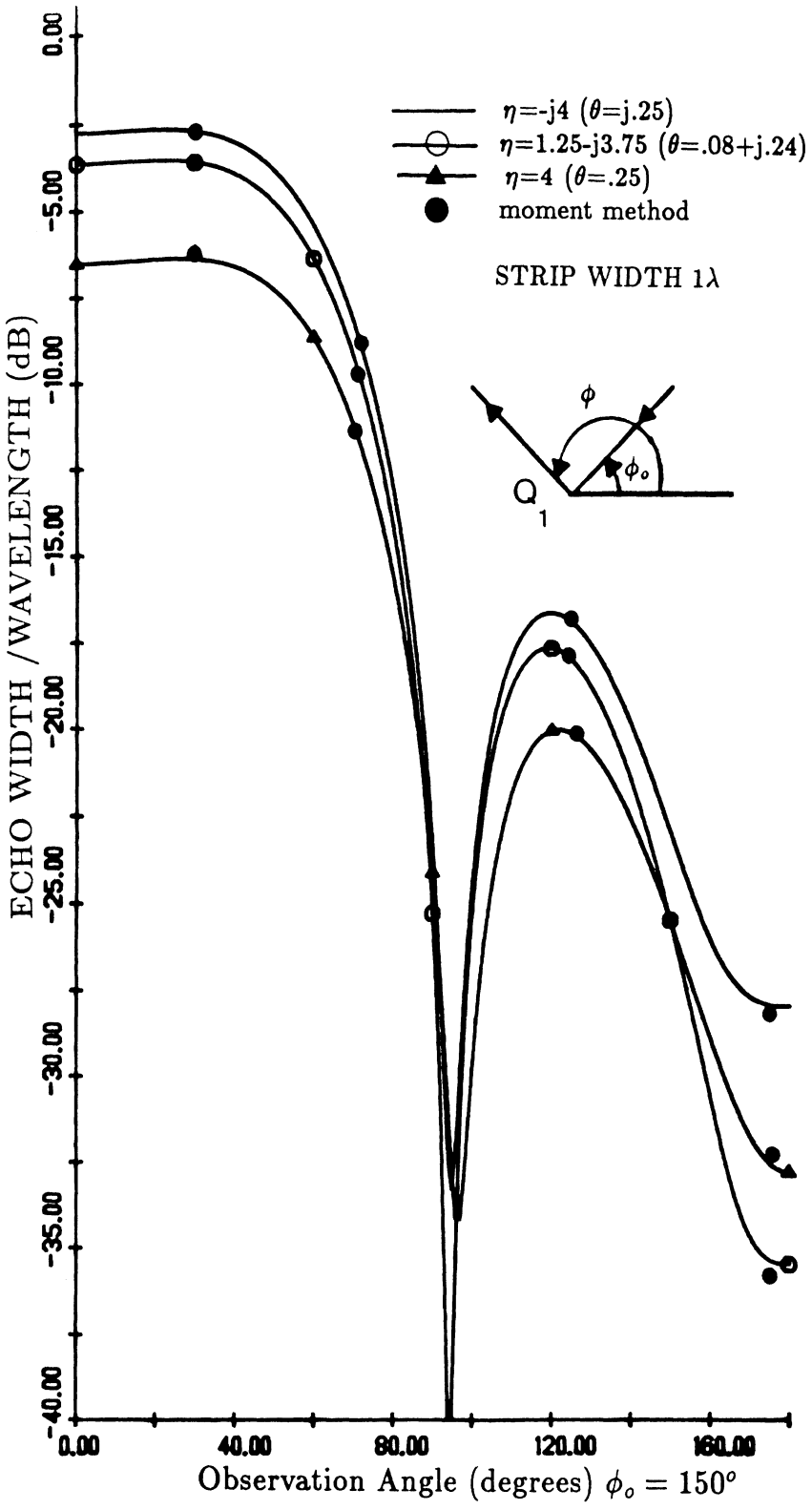


Fig. 27. Comparison of bistatic solution with moment method data for a $1\lambda$ wide resistive strip with $\eta = -j4, 1.25 - j3.75$, and 4 (constant surface wave magnitude $\sim .25$), angle of incidence=150°, E-polarization.

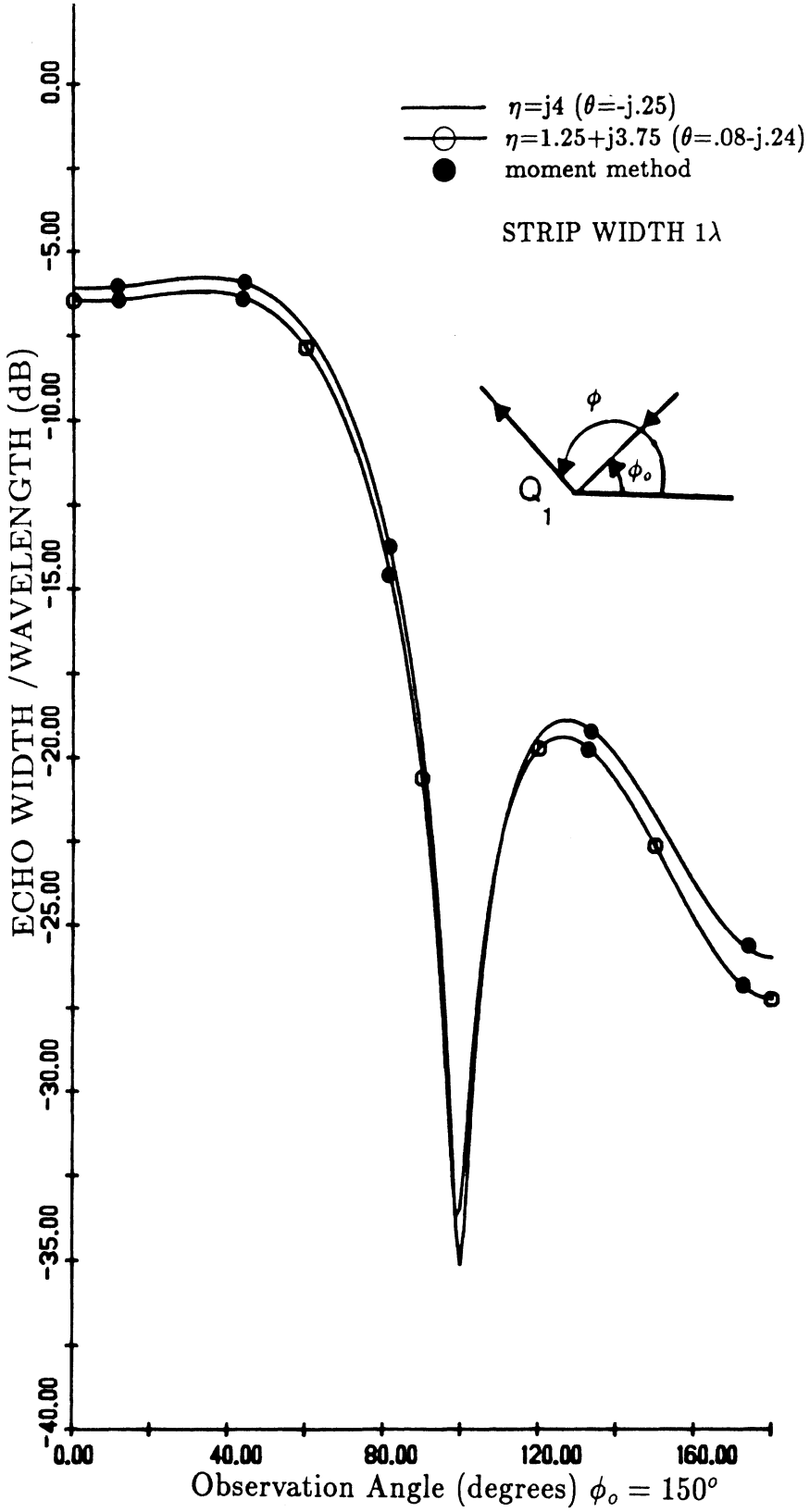


Fig. 28. Comparison of bistatic solution with moment method data for a 1λ wide resistive strip with $\eta = j4$, and 1.25+j3.75 (constant surface wave magnitude $\sim$ .25), angle of incidence=150°, E-polarization.

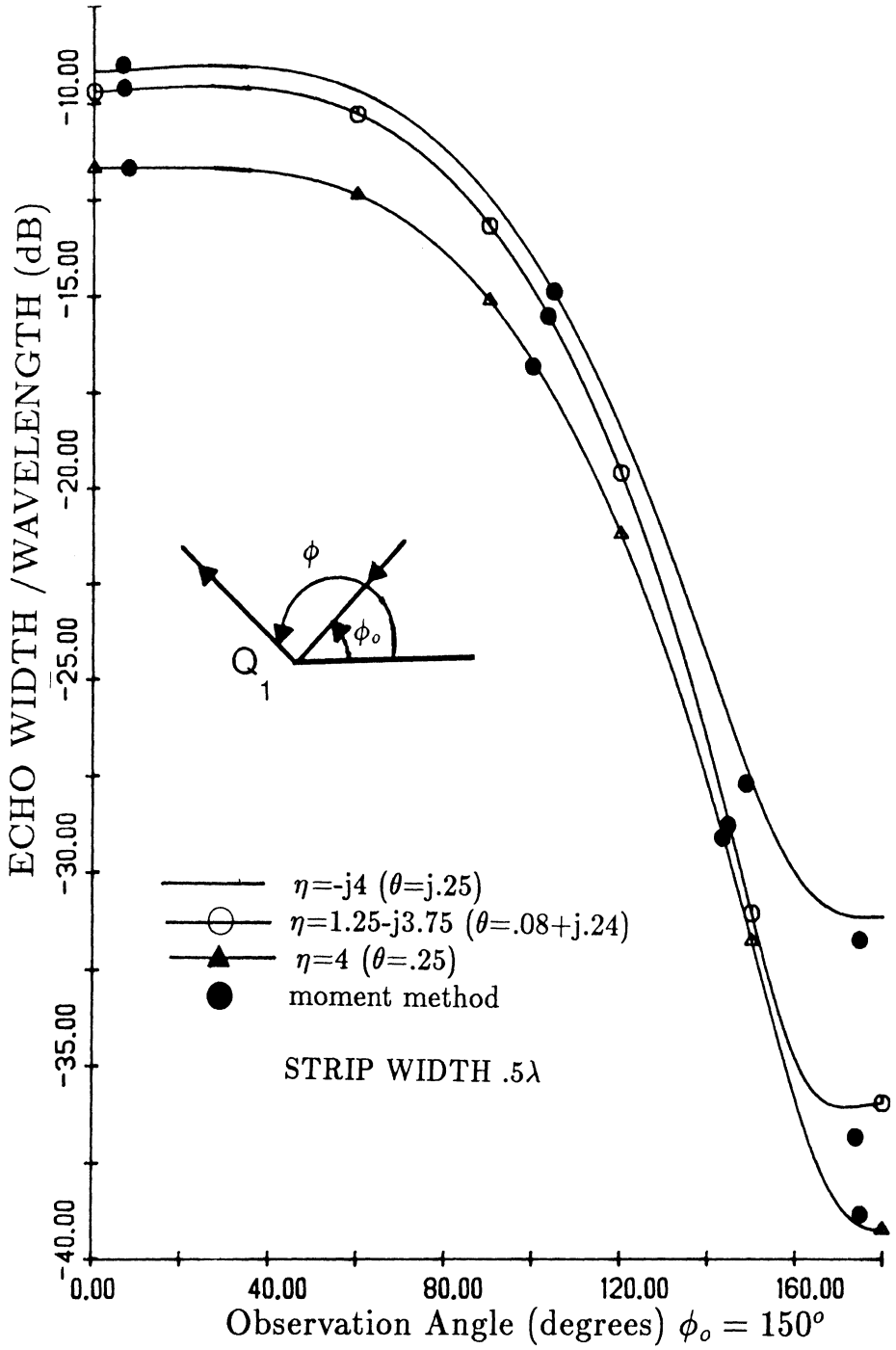


Fig. 29. Comparison of bistatic solution with moment method data for a .5$\lambda$ wide resistive strip with $\eta = -j4, 1.25 - j3.75$, and 4 (constant surface wave magnitude $\sim$ .25), angle of incidence=150°, E-polarization.

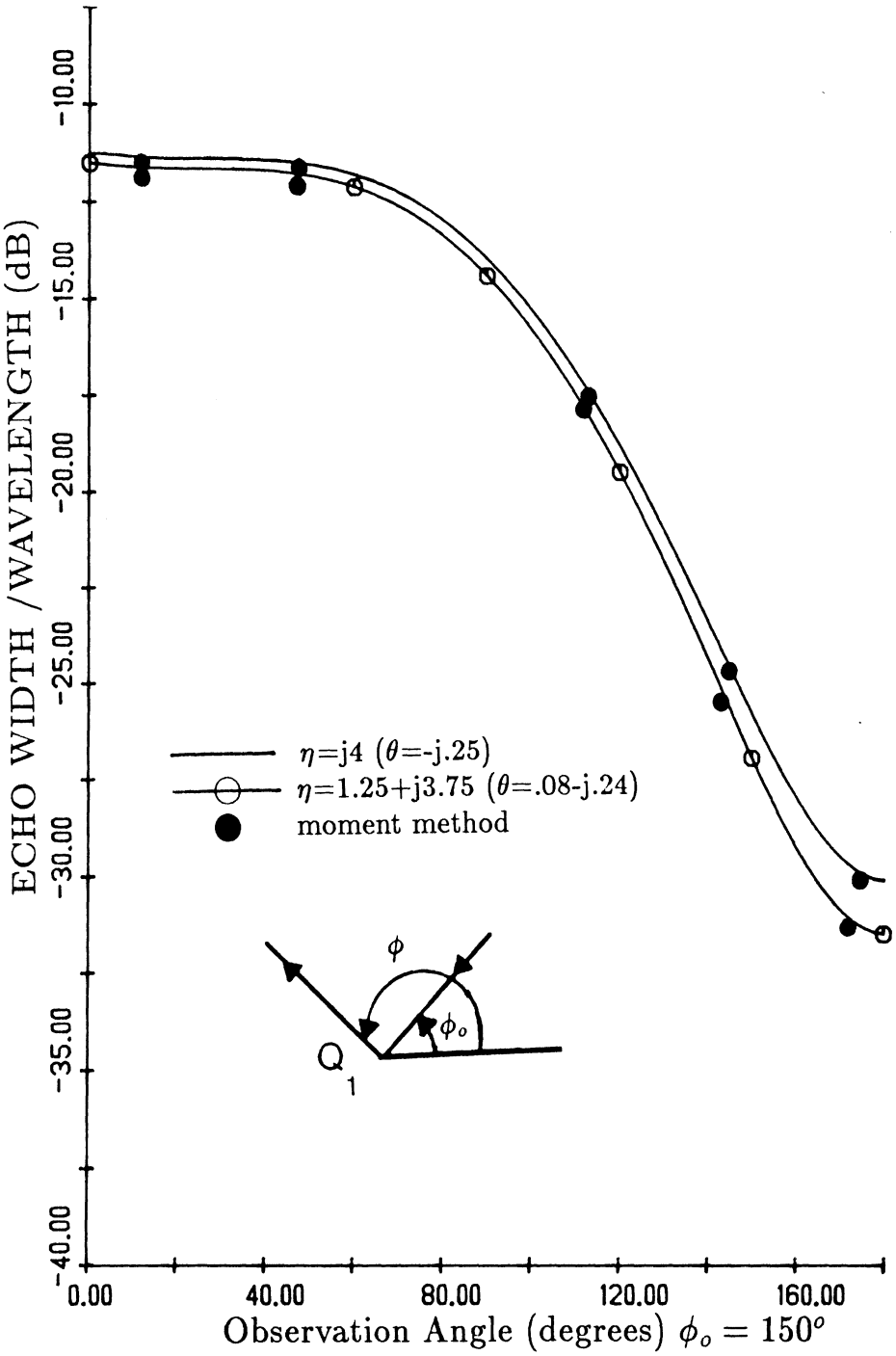


Fig. 30. Comparison of bistatic solution with moment method data for a .5$\lambda$ wide resistive strip with $\eta = j4$, and 1.25+j3.75 (constant surface wave magnitude $\sim$ .25), angle of incidence=150°, E-polarization.

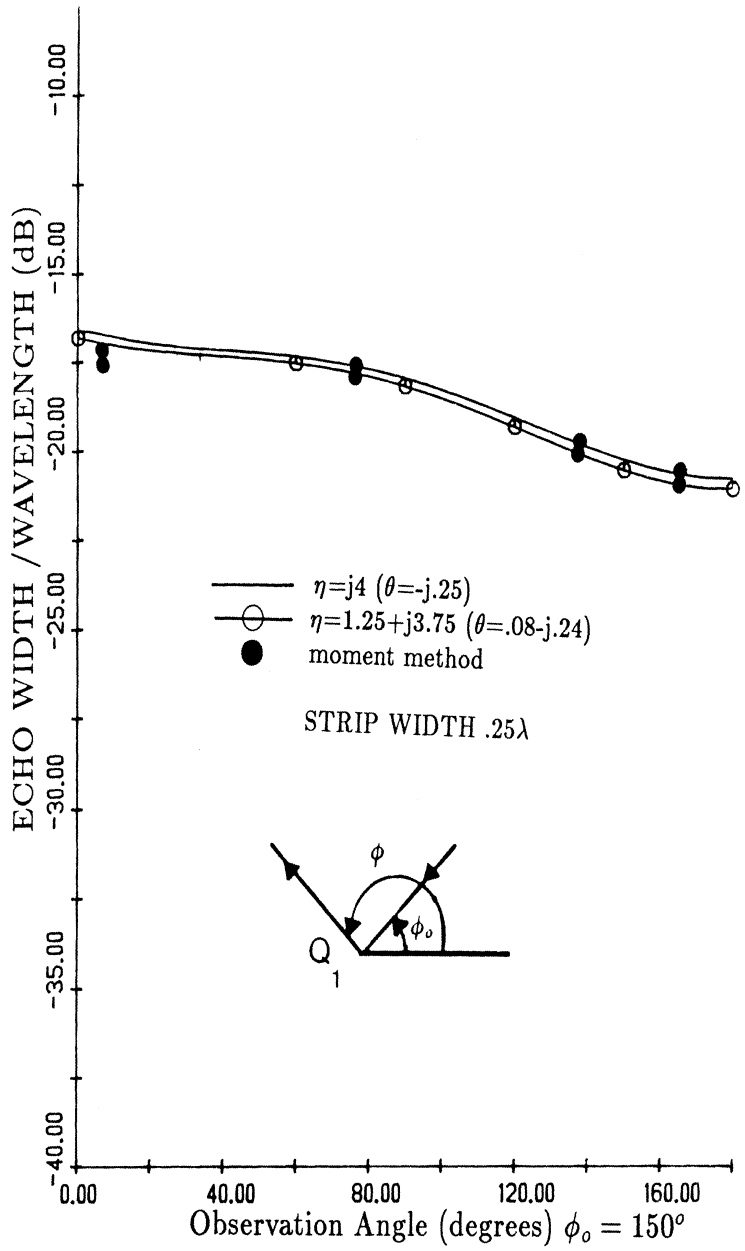


Fig. 32. Comparison of bistatic solution with moment method data for a .25$\lambda$ wide resistive strip with $\eta = j4$, and 1.25+j3.75 (constant surface wave magnitude $\sim$ .25), angle of incidence=150°, E-polarization.

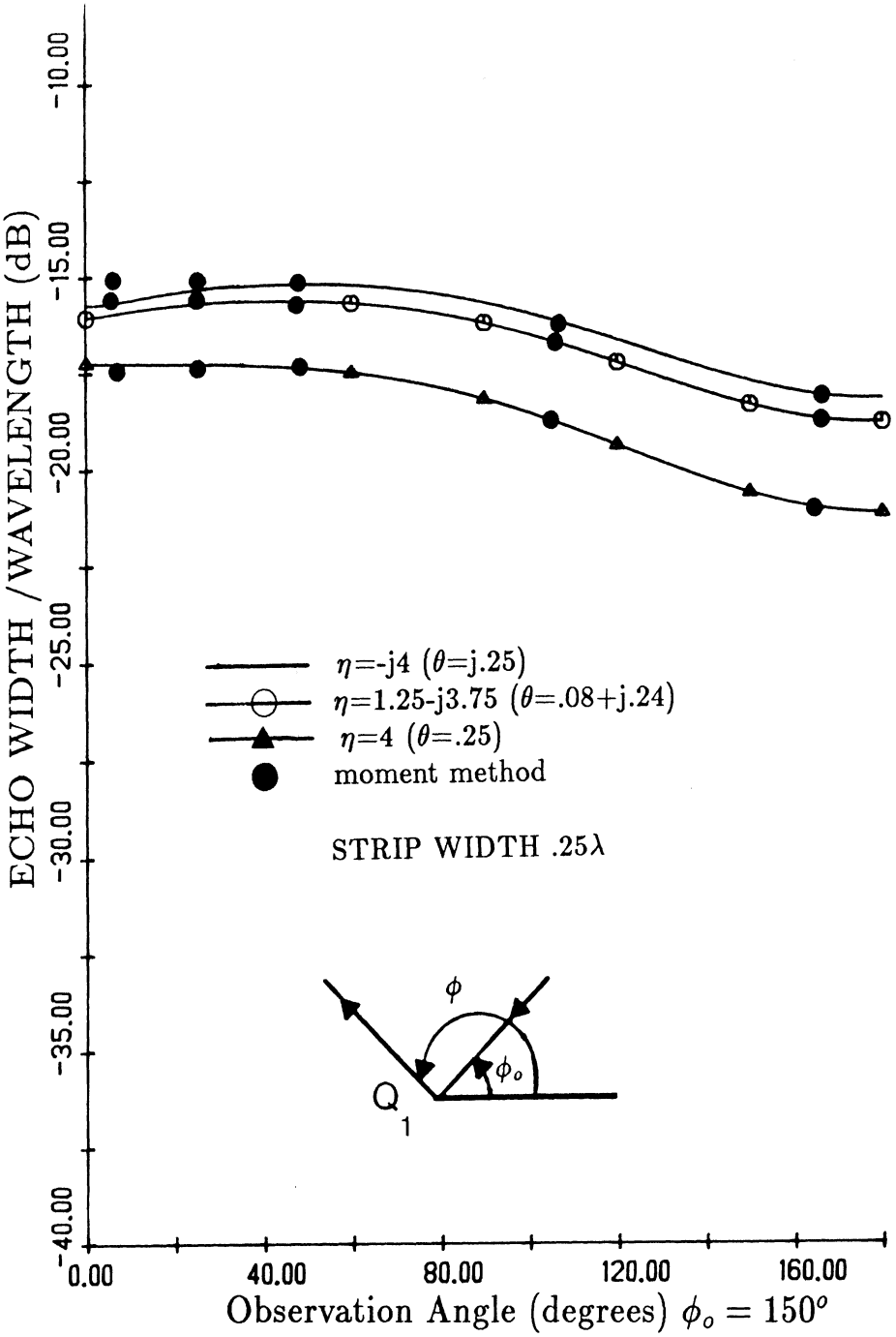


Fig. 31. Comparison of bistatic solution with moment method data for a .25$\lambda$ wide resistive strip with $\eta = -j4, 1.25 - j3.75$, and 4 (constant surface wave magnitude $\sim$ .25), angle of incidence=150°, E-polarization.

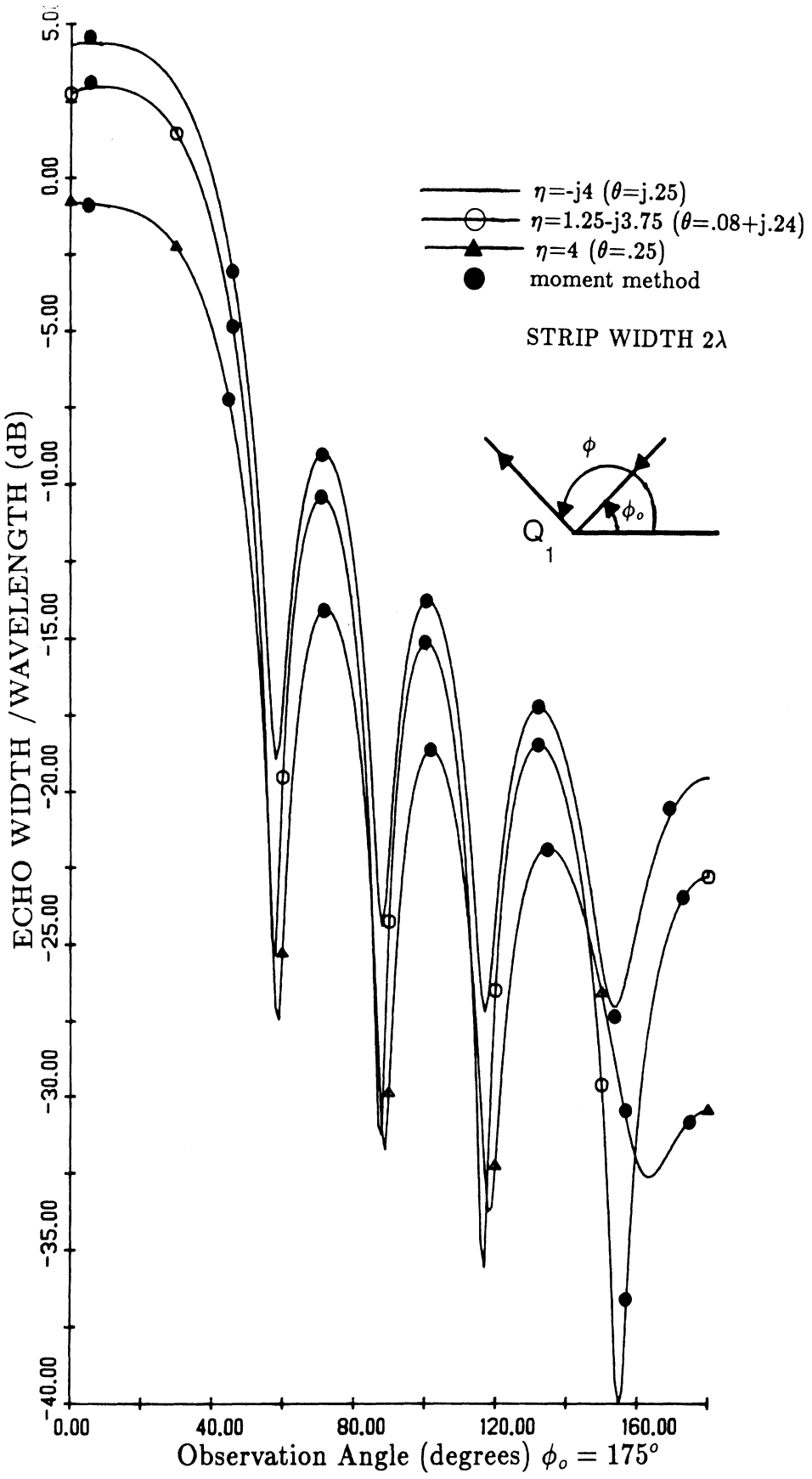


Fig. 33. Comparison of bistatic solution with moment method data for a $2\lambda$ wide resistive strip with $\eta = -j4, 1.25 - j3.75$, and 4 (constant surface wave magnitude $\sim .25$), angle of incidence=175°, E-polarization.

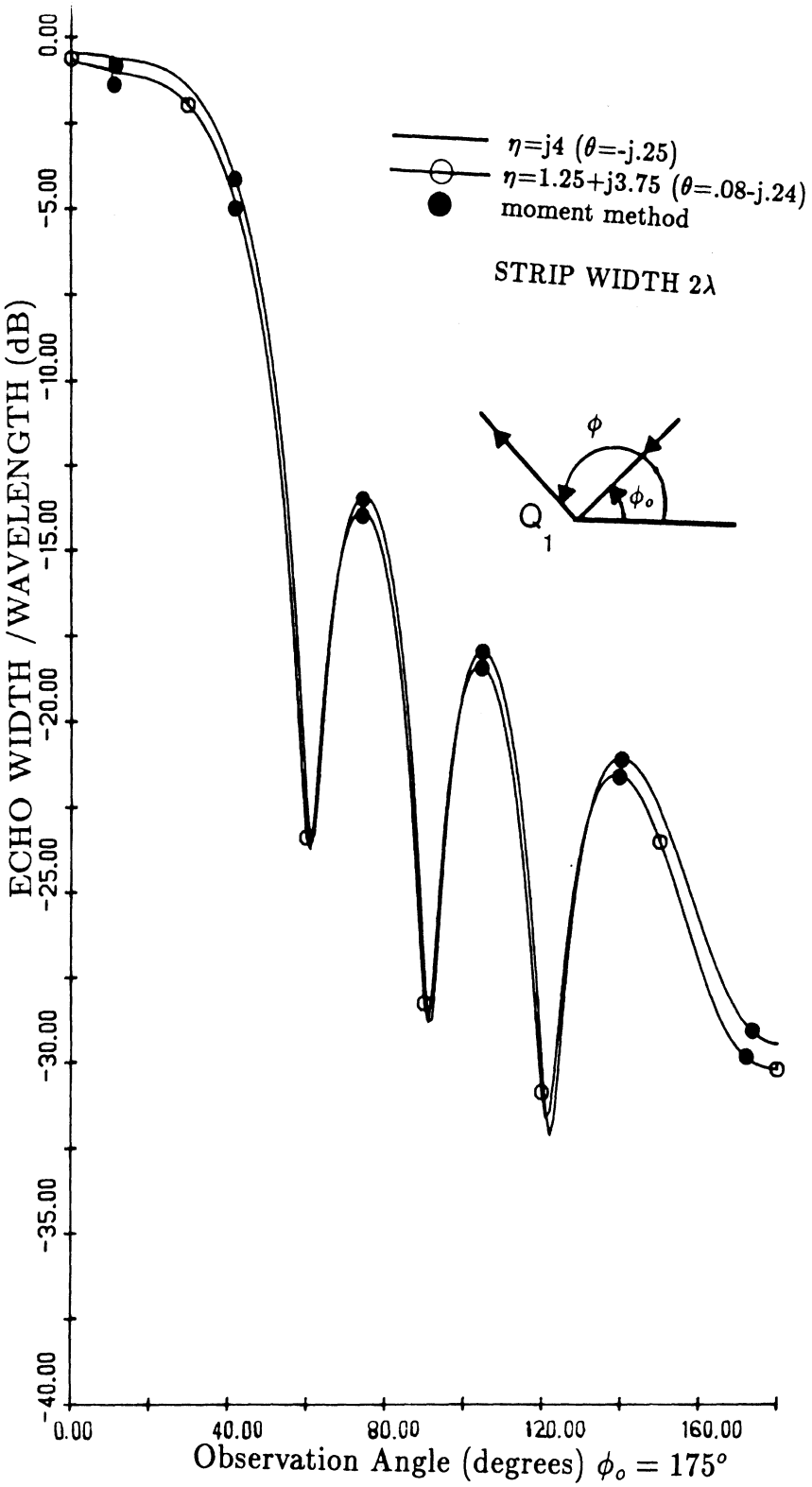


Fig. 34. Comparison of bistatic solution with moment method data for a $2\lambda$ wide resistive strip with $\eta = j4$, and 1.25+j3.75 (constant surface wave magnitude $\sim$ .25), angle of incidence=175°, E-polarization.

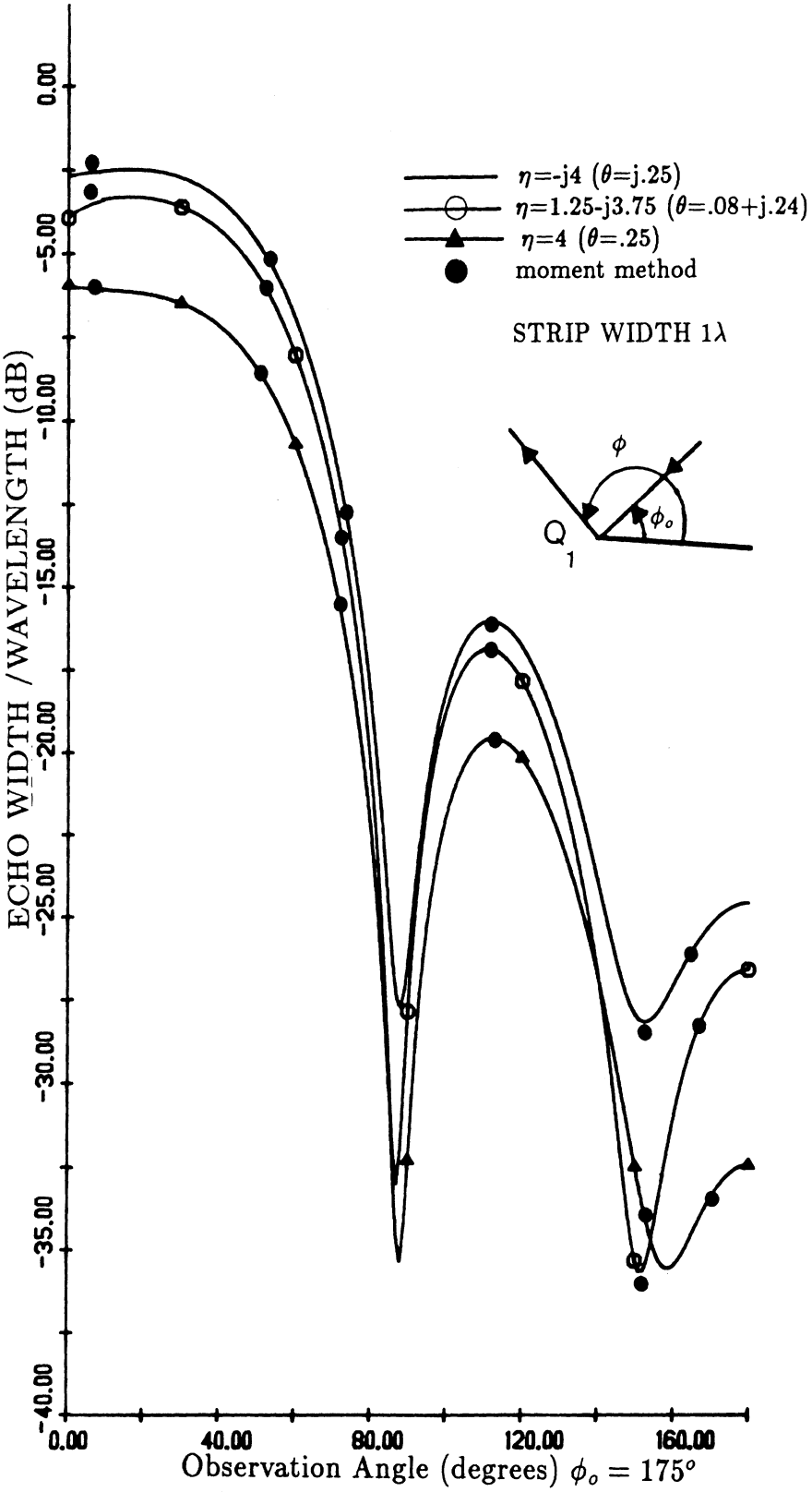


Fig. 35. Comparison of bistatic solution with moment method data for a $1\lambda$ wide resistive strip with $\eta = -j4, 1.25 - j3.75$, and 4 (constant surface wave magnitude $\sim .25$), angle of incidence=175°, E-polarization.

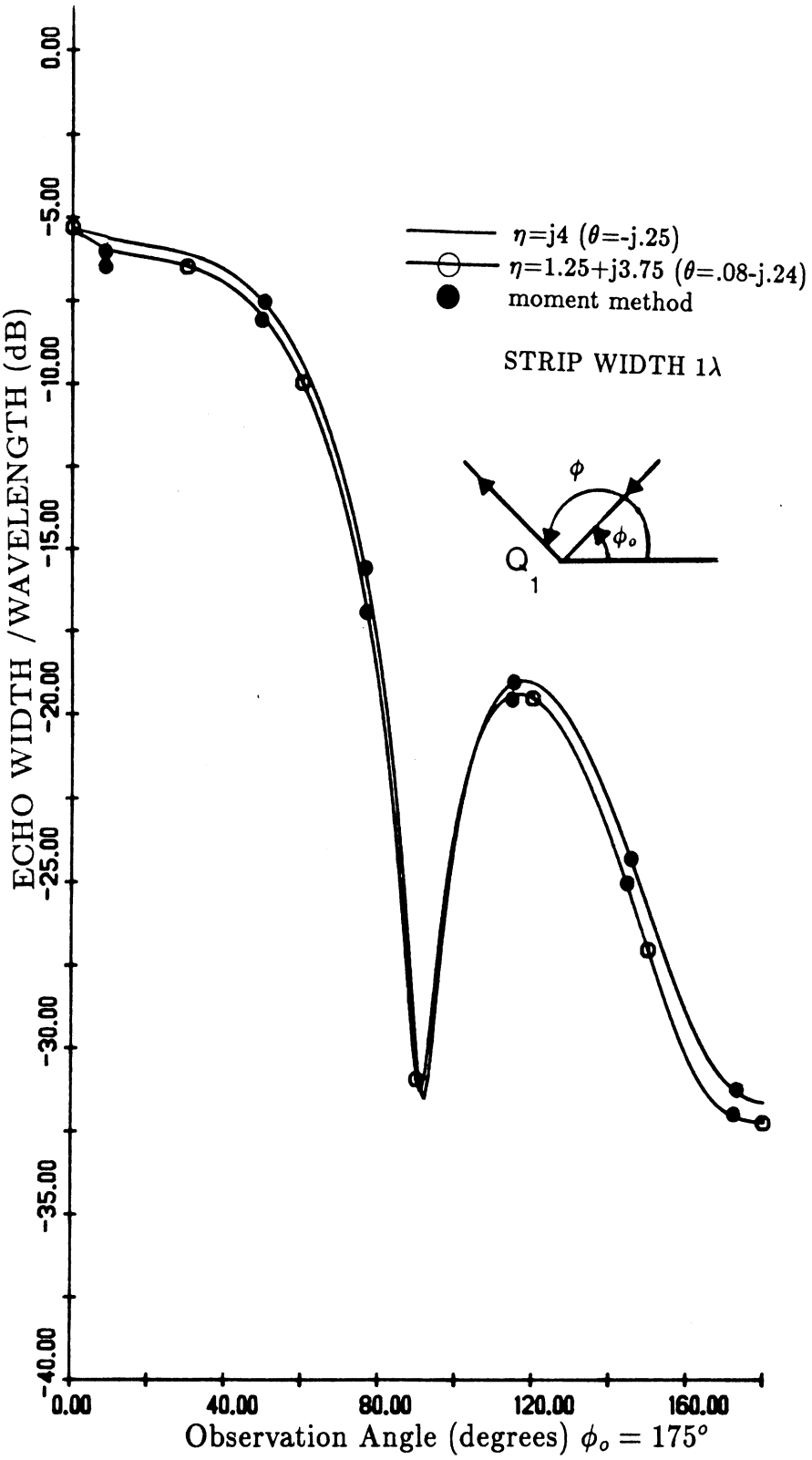


Fig. 36. Comparison of bistatic solution with moment method data for a $1\lambda$ wide resistive strip with $\eta = j4$, and 1.25+j3.75 (constant surface wave magnitude $\sim$ .25), angle of incidence=175°, E-polarization.

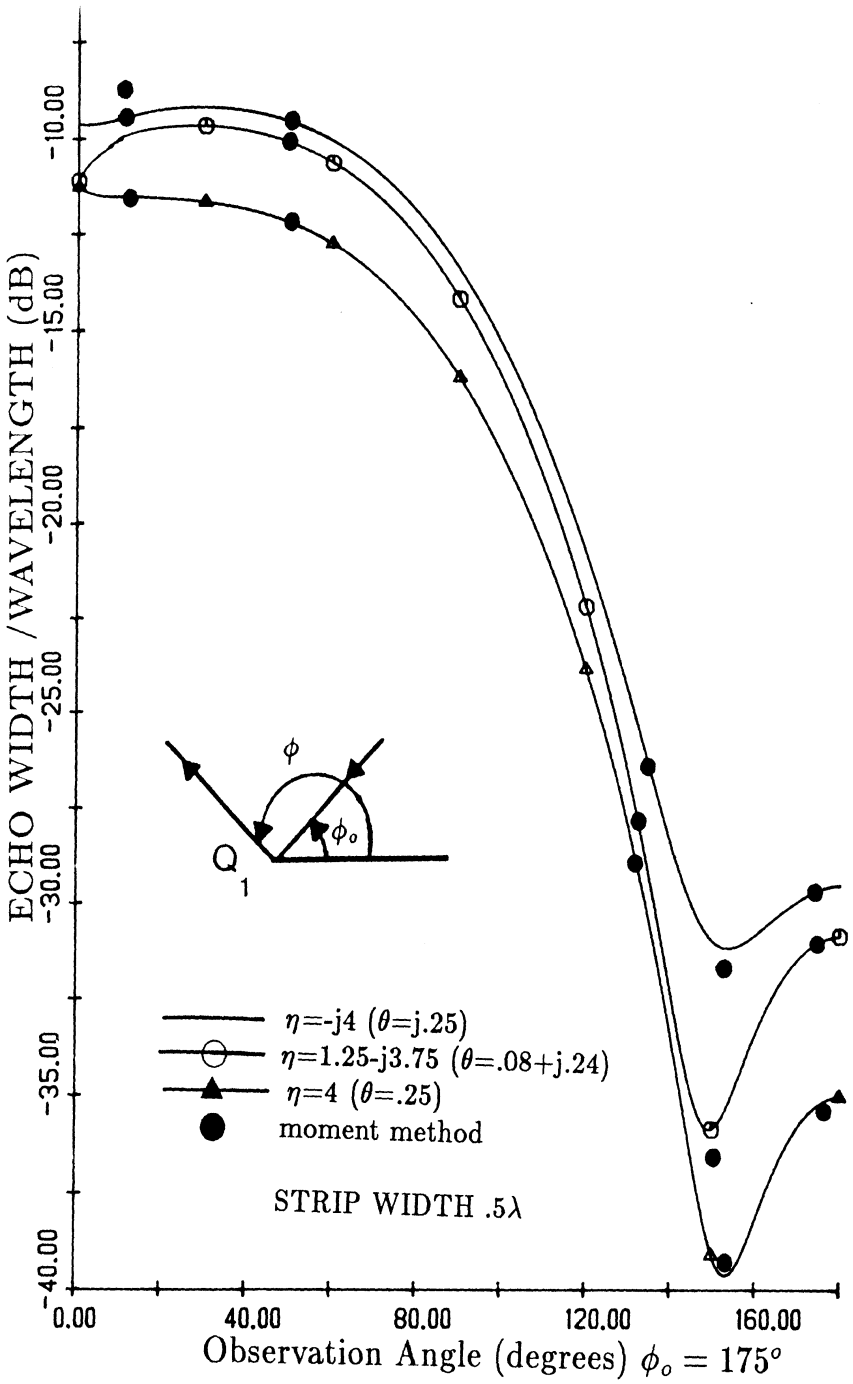


Fig. 37. Comparison of bistatic solution with moment method data for a .5$\lambda$ wide resistive strip with $\eta = -j4, 1.25 - j3.75$, and 4 (constant surface wave magnitude $\sim$ .25), angle of incidence=175°, E-polarization.

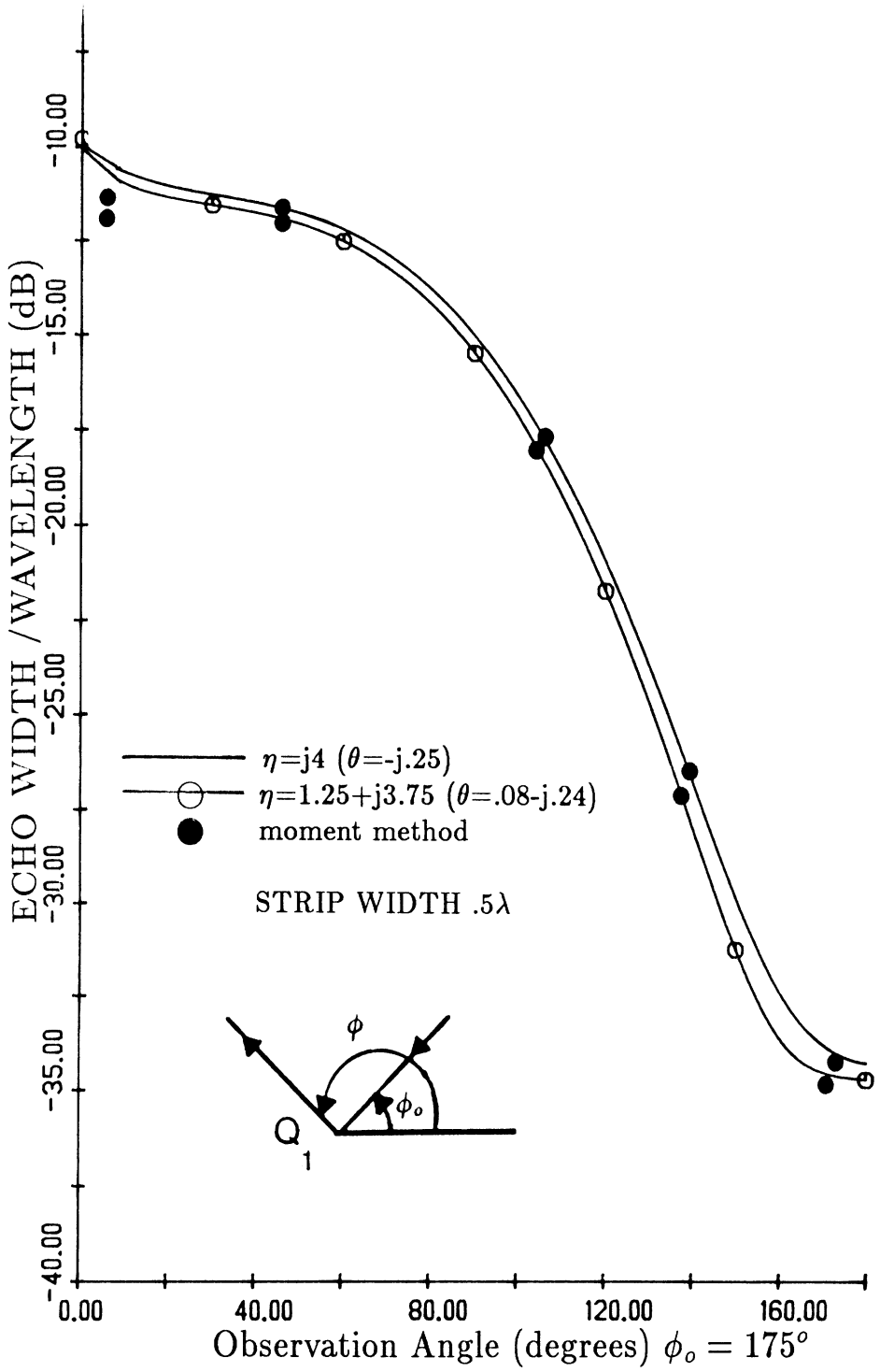


Fig. 38. Comparison of bistatic solution with moment method data for a .5$\lambda$ wide resistive strip with $\eta = j4$, and 1.25+j3.75 (constant surface wave magnitude $\sim$ .25), angle of incidence=175°, E-polarization.

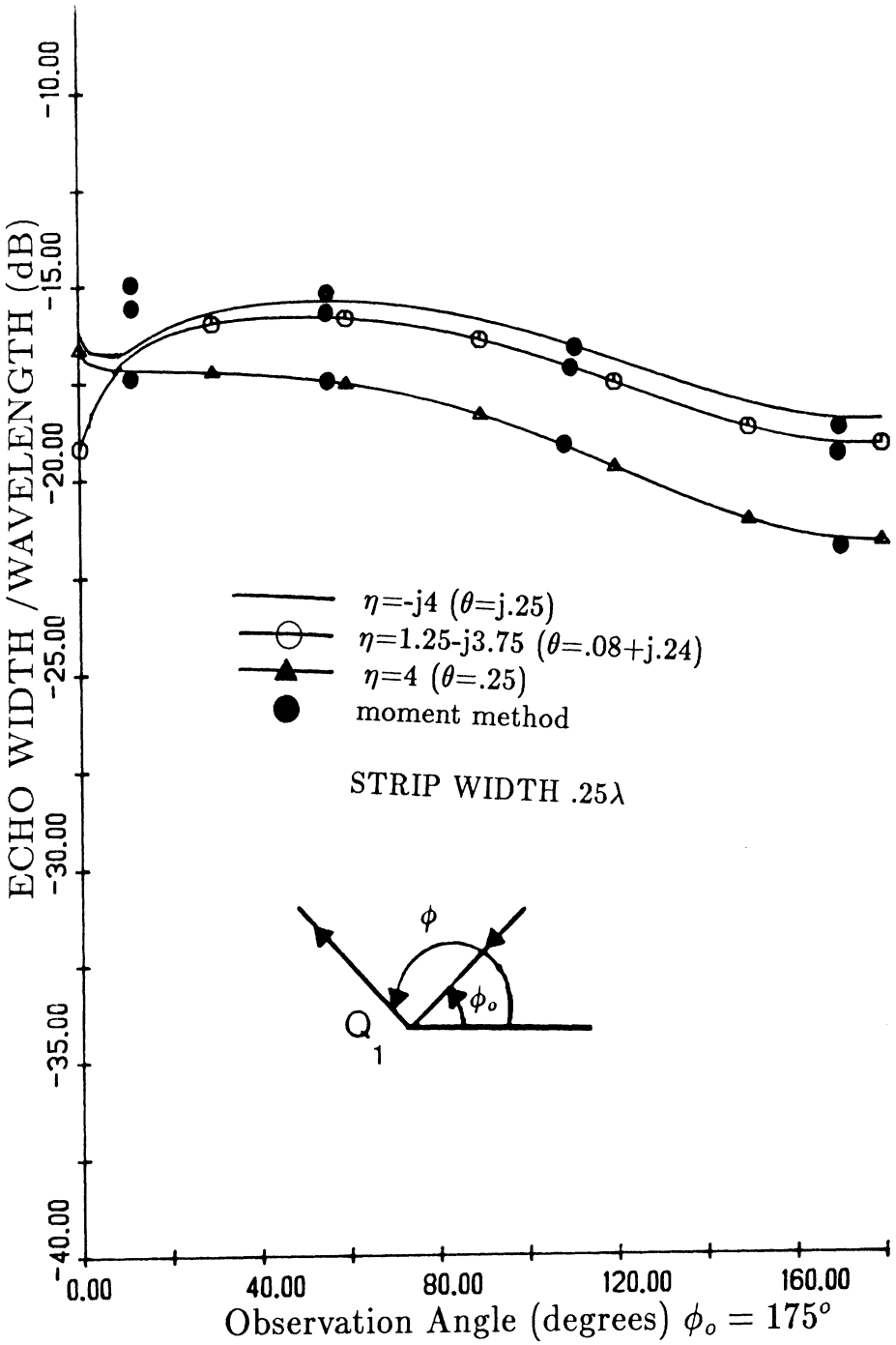


Fig. 39. Comparison of bistatic solution with moment method data for a .25$\lambda$ wide resistive strip with $\eta = -j4, 1.25 - j3.75$, and 4 (constant surface wave magnitude $\sim$ .25), angle of incidence=175°, E-polarization.

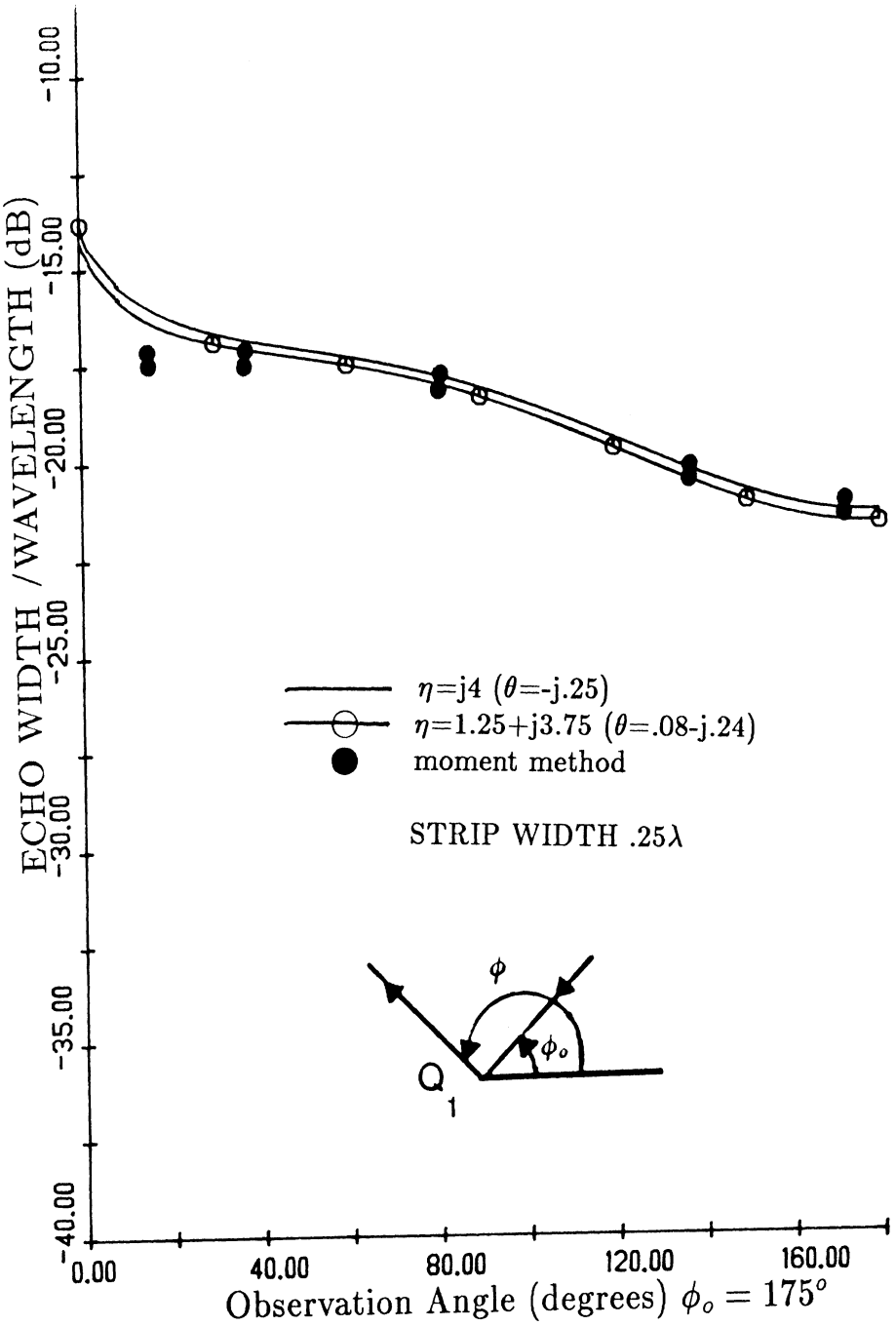


Fig. 40. Comparison of bistatic solution with moment method data for a .25$\lambda$ wide resistive strip with $\eta = j4$, and 1.25+j3.75 (constant surface wave magnitude $\sim$ .25), angle of incidence=175°, E-polarization.

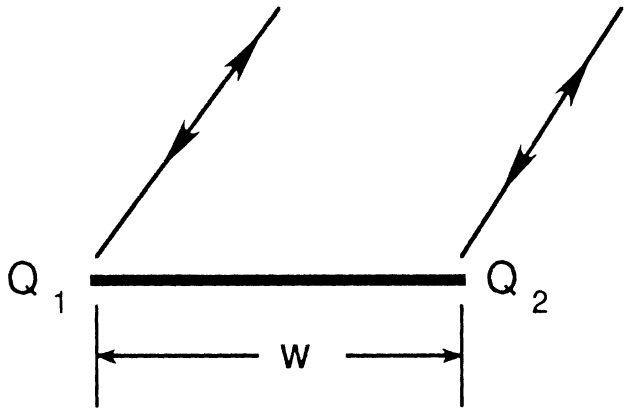


Fig. 41. Primary backscatter edge diffraction from a strip.

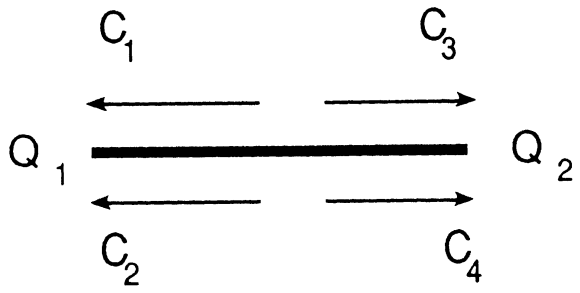


Fig. 42. Equivalent surface fields on a strip.

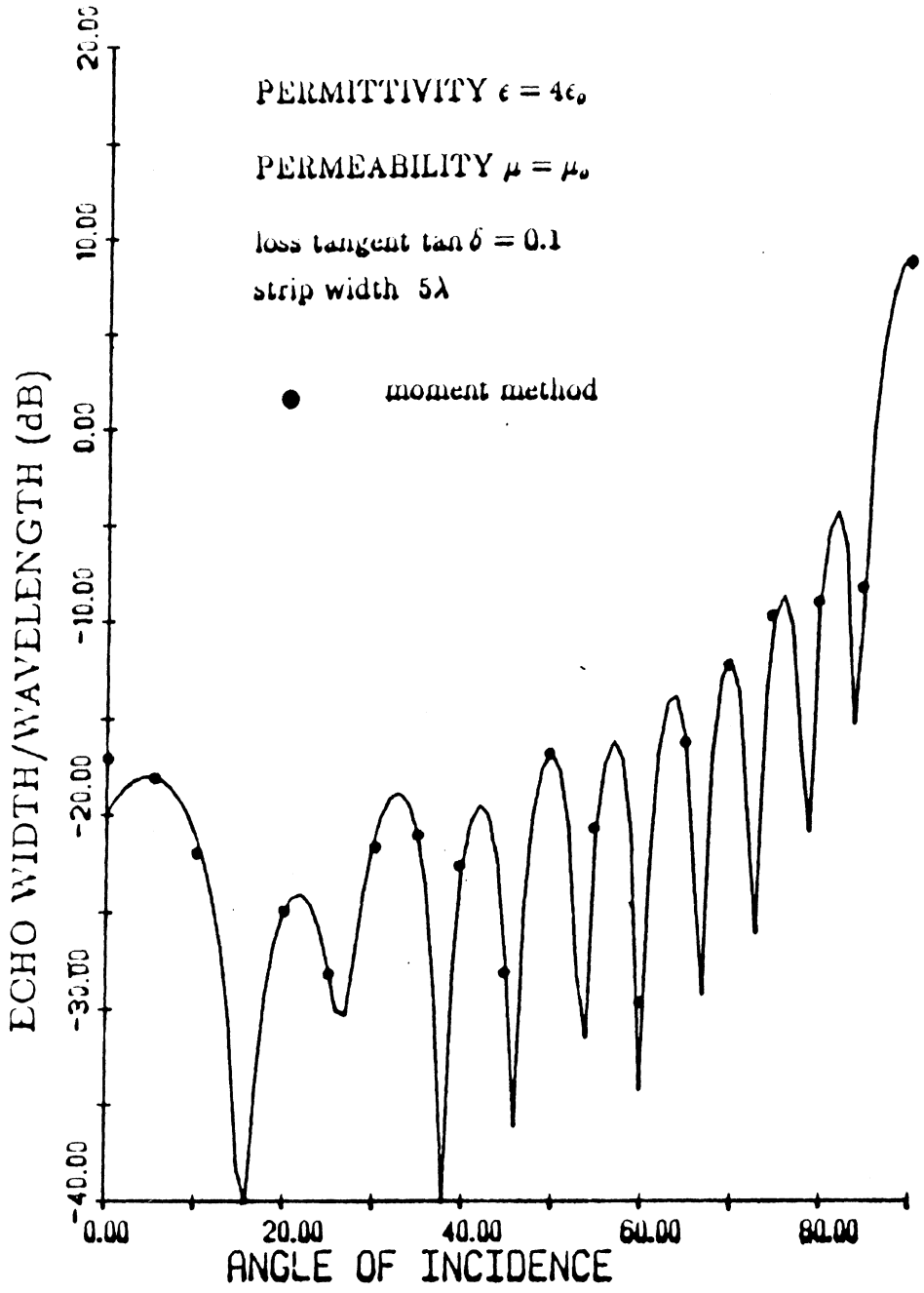


Fig. 43. Backscattering from a resistive strip using a self-consistent approach, and comparing the results to moment method results.